UCSF
UC San Francisco Electronic Theses and Dissertations

Title
Computational and experimental dissection of the response of Saccharomyces cerevisiae to inorganic phosphate starvation

Permalink
https://escholarship.org/uc/item/17w3f49q

Author
Springer, Michael,

Publication Date
2003

Peer reviewed|Thesis/dissertation

eScholarship.org Powered by the California Digital Library
University of California

Computational and Experimental Dissection of the Response of *Saccharomyces cerevisiae* to Inorganic Phosphate Starvation

by

Michael Springer

DISSERTATION

Submitted in partial satisfaction of the requirements for the degree of

DOCTOR OF PHILOSOPHY

in

Cell Biology

in the

GRADUATE DIVISION

of the

UNIVERSITY OF CALIFORNIA, SAN FRANCISCO

[redacted]

Acknowledgement:

I would like to acknowledge several people who had this thesis possible. I would like to thank Erin O'Shea, my advisor, for the intensity to beat some sense into a stubborn graduate student and her amazing ability to convert ideas into reality. I would like to thank Jonathan Weissman for his keen insight and helpful discussions. I would like to thank Sandy Johnson for his creative perspective on science, intellectual discussion, and friendship. I would like to thank the O'Shea lab for a wonderful working environment and critical input on my work. I would like to thank my baymates, Noah Dephoure, Jonathan Raser, and Meghan Byrne, for their liberal politics and supportive nature which helped to culture a positive working environment. I also would like to thank Tamara Brenner who has been extremely helpfully in compiling this thesis and whose love and support has been essential. I would like to thank my parents for making sure I would be able to pursue whatever I desired. I would finally like to thank the Public Library of Science and Journal of Molecular Biology for publishing my work.

Abstract:

Computational and Experimental Dissection of the Response of *Saccharomyces cerevisiae* to Inorganic Phosphate Starvation

By Michael Springer

Cells grow in complex and dynamic environments. In order to survive, cells must be able to adapt by bring in the proper amounts of nutrients regardless of their extracellular level and form. The response of the budding yeast *Saccharomyces cerevisiae* to inorganic phosphate starvation serves as a model system for studying this process. I used experimental *in vitro* data to simulate the rate at which Pho80-Pho85, the central kinase of the phosphate response, phosphorylates Pho4, the transcription factor which controls all phosphate responsive genes. This allowed me to form a testable model about the regulation of Pho4 by Pho80-Pho85 *in vivo*. The model predicted that three different phosphorylated forms of Pho4 should exist in vivo: a completely phosphorylated form, a completely unphosphorylated form, and a form where the predominate phosphorylation is on only one of the five potential phosphorylation sites. I predicted that changes in the levels of external phosphate concentrations should control which of these three forms of Pho4 would exist *in vivo*. I experimentally tested this model and found that in fact yeast have three distinct responses to different levels of phosphate in their environment. These three states correlate with the three different predicted phosphorylated forms of Pho4. Comparison of the phosphate response to other homeostatic responses led to a broad but simple model for the core homeostatic network. The model of this core homeostatic network predicts that homeostatic systems respond like damped harmonic oscillators with the ability to respond to any change in environment or intracellular needs without changing the steady-state level of nutrients. This model is robust but evolvable and provides an explanation for many of the additional features of the phosphate response such as an intracellular buffer and low affinity receptors. In total this combined approach of computational and experimental approaches has increased our understanding of the physiology of the response to phosphate starvation.

EKOShea

Table of Contents

Introduction 1

Chapter 1 In vitro analysis of a kinase 5

References 32

Figure Legends 37

Figures 41

Chapter 2 Partially Phosphorylated Pho4 Activates Transcription of a Subset of Phosphate-Responsive Genes 54

References 75

Figure Legends 79

Figures 83

Chapter 3 Model of Conserved Network Design Allows for Robust Homeostatic Response 91

References 113

Figure Legends 115

Figures 117

Conclusion 124

Introduction:

Cells have an amazing ability to adapt to changes in their environment. Adaptation needs to be quick and precise if an organism is to survive and outcompete other organisms. Responses also need to be plastic so that as an environment changes cell are not locked into behaviors that are no longer useful. The budding yeast, *Saccharomyces cerevisiae*, serves as a model organism for studying how cell interpret their environment.

When yeast are grown in medium devoid of extracellular inorganic phosphate they respond in three ways. They increase the level of phosphate transporters at the plasma membrane, such as Pho84, a high affinity phosphate transporter, which allows them to bring in more phosphate from the environment. They secrete phosphatases, such as Pho5, a secreted acid phosphatase, which allow them to scavenge phosphate from organic molecules in the environment. They also mobilize internal stores of phosphate stored as polyphosphate in the vacuole.

The ability of yeast to respond to their environment relies on their ability to turn on these three sets of genes: transporters, scavengers, and mobilizers. Understanding the behavior of a cell requires not just knowing if there is a response but also knowing how the magnitude of the signal, the duration of the signal, and the previous state of the cell affect the magnitude and duration of response. The goal of my research has been to better characterize the phosphate response, and to determine a molecular basis for any newly characterized behaviors.

Characterization of the phosphate response revealed a number of complex responses. I started by simply characterizing the concentration dependence of the response. When phosphate levels are high cells do not induce any of the phosphate responsive genes. As the extracellular phosphate concentration drops, there is a narrow range of change in external phosphate over which cells begin to respond. The exact concentration at which a cell responds varies from cell to cell, but individual cells respond in an ultrasensitive or switch-like manner. Surprisingly, only a subset of the genes involved in the response in medium devoid of phosphate are induced when cells respond to a low level of phosphate in their medium. More careful kinetic analysis revealed that this same subset of genes, consisting mostly the transporters and mobilizing genes, are also induced first when cells are starved for inorganic phosphate. After several hours in low phosphate medium cells completely adapt to their new environment, apparently downregulating most of their response. While the cells no longer seem to be responding as if they were starving for phosphate, they are able to maintain a higher level of phosphate transporter at their plasma membrane than they maintain at their plasma membrane in higher extracellular concentrations of phosphate. My research after this focused on computationally and experimentally understanding the mechanisms which underlie these behaviors.

Previous work had determined a number of molecular features of the phosphate response. A cyclin dependent kinase, Pho85, and its cyclin partner, Pho80, regulate the activity of Pho4, a transcription factor which controls all of the phosphate responsive genes. Pho80-Pho85 phosphorylates Pho4 on five sites, and Pho4 is phosphorylated only by Pho80-85. Pho80-Pho85 is in turn regulated by Pho81, a cyclin dependent kinase inhibitor, which is regulated by internal phosphate levels by an unknown mechanism.

Pho80-Pho85 regulates the activity of Pho4 in two ways. Phosphorylation on sites 2 and 3 increases the rate at which Pho4 is exported from the nucleus. Phosphorylation on site 4 decreases the rate at which Pho4 is imported into the nucleus. Phosphorylation on site 6 decreases the ability of Pho4 to interact with a necessary transcriptional coactivator, Pho2. Thus, one kinase, Pho80-Pho85, regulates Pho4 by controlling both its nuclear localization and its transcriptional activity in the nucleus. Therefore, under high phosphate conditions, Pho80-Pho85 is active and phosphorylates Pho4 on all four functionally relevant sites, leading to Pho4 being localized to the cytoplasm and hindered for its interaction with Pho2.

From this knowledge, it appeared that a more detailed understanding of the manner in which the central kinase Pho80-Pho85 phosphorylates Pho4 would be helpful in understanding *in vivo* behaviors.

I modeled *in vitro* kinetics of Pho80-Pho85 phosphorylating Pho4. From this I was able to obtain a model which was not only able to explain the existing data, but was able to predict the results of several experiments which we later preformed to help confirm the validity of the model. The key result of the model was that phosphorylation of the five phosphorylatable residues on Pho4 is semi-processive with a strong preference for phosphorylation of site 6. This led to the intriguing possibility that Pho4 could exist in three states *in vivo*. One state would be completely unphosphorylated, one state completely phosphorylated, and one state where the predominate phosphorylation would be on site 6.

I then examined site 6 phosphorylation *in vivo* and determined that it correlated with induction of only a subset of the phosphate responsive genes as compared to the induction profile when no sites are phosphorylated. Site 6 phosphorylation was sufficient to create a state of differential gene induction, and site 6 phosphorylation is the predominate phosphorylation in a concentration range of external phosphate which I will refer to as intermediate phosphate. Surprisingly, while sufficient, site 6 phosphorylation is not the only mechanism which contributes to creating this differential induction in intermediate phosphate, implying that a secondary mechanism is functioning that is redundant to site 6 phosphorylation. A number of experiments suggests that this differential induction might result from phosphorylation at sites 2 and 3 being in a kinetic balance with transcriptional activation, equivalent to the kinetic proofreading models for translational and transcriptional fidelity.

In attempt to connect all these results into one model I compared the response of this system to external nutrient levels with other homeostatic responses. Surprisingly, the basic mechanism of response is very similar in a large number of the homeostatic systems. A simple set of coupled differential equations can be used to describe this system and its solution suggests that the phosphate response should act like a damped harmonic oscillator. This in total helps to explain many of the behavioral responses we have observed for the phosphate responsive pathway.

Chapter 1

Multi-Site Phosphorylation of Pho4 By the Cyclin-CDK Pho80-Pho85 is Semi-Processive with Site Preference

Credits

Doug Jeffery performed all of the experiments in this paper and Mike Springer designed and carried out the computer modeling. David King synthesized and purified Pho4 peptides used in kinase assays.

As part of a nutrient responsive signaling pathway, the budding yeast cyclin-CDK complex Pho80-Pho85 phosphorylates the transcription factor Pho4 on five sites and inactivates it. Here we describe the kinetic reaction between Pho80-Pho85 and Pho4. Through experimentation and computer modeling we have determined that Pho80-Pho85 phosphorylates Pho4 in a semi-processive fashion that results from a balance between k_{cat} and k_{off}. In addition, we show that Pho80-Pho85 phosphorylates certain sites preferentially. Phosphorylation of the site with the highest preference inhibits the transcriptional activity of Pho4 when it is in the nucleus, while phosphorylation of the lowest-preference sites is required for export of Pho4 from the nucleus. This method of phosphorylation may allow Pho80-Pho85 to quickly inactivate Pho4 in the nucleus and efficiently phosphorylate Pho4 to completion.

Cyclin-dependent kinases (CDKs) are important regulators of cell growth and metabolism (Moffat *et al.*, 2000; Morgan, 1997). CDK monomers are inactive and full activity requires binding of a protein partner, called a cyclin. Some CDKs also require an activating phosphorylation on a serine or threonine residue close to the active site (Morgan, 1997).

An important problem is how cyclin-CDK complexes bind and phosphorylate their substrates. Substrate recognition occurs at two levels. First, all CDKs require a proline residue immediately following the serine or threonine phosphoacceptor site. The CDK1 family of CDKs, which are responsible for cell cycle regulation, also require a positively charged lysine or arginine at the third position from the phosphoacceptor site, with the consensus site being S/TPXK/R (Holmes & Solomon, 1996; Songyang *et al.*, 1994). Crystallography has revealed that these residues make critical contacts with residues in the active site cleft and constrain the conformation of the peptide so it can be accommodated by the kinase (Brown *et al.*, 1999). Second, efficient phosphorylation of some physiologically relevant substrates requires high-affinity binding between the cyclin subunit and regions of the protein substrate that are distinct from the phosphorylation sites (Adams *et al.*, 1999; Brown et al., 1999; Schulman *et al.*, 1998). Few physiologically relevant substrates for CDKs have been identified so, as a result, CDK activity has commonly been measured using general substrates such as histone H1 or small peptides. Specific, full-length substrates are phosphorylated with much greater efficiency than small peptides, most likely because the peptides lack these high affinity interactions.

Previously, we identified the transcription factor Pho4 as a physiologically relevant substrate of the *S. cerevisiae* cyclin-CDK pair Pho80-Pho85 (Kaffman *et al.*, 1994). Pho80-Pho85 and Pho4 are critical components of a signal transduction pathway that is required for yeast to respond to levels of inorganic phosphate in the environment (Oshima, 1997). When phosphate is abundant, Pho80-Pho85 phosphorylates and inactivates Pho4, resulting in repression of phosphate-responsive genes. When phosphate levels are low, Pho80-Pho85 is inactivated (Schneider *et al.*, 1994), Pho4 is hypo-phosphorylated and it activates transcription of a large number of phosphate-responsive genes (Ogawa *et al.*, 2000).

Several studies suggest that Pho80-Pho85 targets Pho4 through a high-affinity interaction with the cyclin Pho80. The interaction between Pho4 and Pho80-Pho85 can be detected by co-immunoprecipitation (Kaffman et al., 1994). Two-hybrid analysis has identified two regions of Pho4 that interact with Pho80 (Jayaraman *et al.*, 1994) and point mutations in Pho4 that abolish Pho4 regulation *in vivo* can be suppressed by point mutations in Pho80, suggesting that the two proteins interact directly (Okada & Toh-e, 1992). Finally, Pho85 in association with a different cyclin partner does not phosphorylate Pho4 as well as does Pho80-Pho85 (Huang *et al.*, 1998), most likely because Pho80 is better at recruiting Pho4 to the active site than a different cyclin.

Pho4 is phosphorylated on five serines by Pho80-Pho85 both *in vivo* and *in vitro*, with a consensus phosphorylation site sequence SPXI/L (O'Neill *et al.*, 1996). We refer to the five sites as SP1, SP2, SP3, SP4, and SP6. Interestingly, phosphorylation on the different SP sites inactivates Pho4 in distinct ways (Komeili & O'Shea, 1999). Phosphorylation on SP2 and SP3 inactivates Pho4 by promoting its rapid export from the nucleus. Import of Pho4 into the nucleus is blocked by phosphorylation of SP4. Finally, phosphorylation of SP6 prevents the interaction of Pho4 with its transcriptional co-activator Pho2, leading to repression of a subset of phosphate-responsive genes.

Although we know much about the effect of phosphorylation on regulation of Pho4, we do not understand the kinetics of phosphorylation of Pho4. In this study we use kinetic analysis and computer modeling to dissect the reaction between Pho4 and Pho80-Pho85.

Initial Characterization of the Kinase Reaction

We purified Pho80-Pho85 and Pho4 from *E. coli* and used standard kinetic assays to determine the specific activity of the kinase. Like Pho80-Pho85 purified from yeast (O'Neill et al., 1996), recombinant Pho80-Pho85 phosphorylated wild-type Pho4 but not Pho4 lacking phosphorylation sites SP1-SP6. This phosphorylation was dependent on Pho80, as the Pho85 monomer alone had no activity (data not shown). We used Henri-Michaelis-Menten kinetic analysis to measure the apparent k_{cat} and K_M for the phosphorylation of Pho4 because this is the standard in the field for evaluating the specific activity of an enzyme for a substrate. These are the apparent kinetic constants because there are five phosphorylation sites and this standard analysis cannot measure the true k_{cat} and K_M (see below). At physiological concentrations of ATP (900 μM), the apparent K_M expressed in terms of Pho4 monomer is 420 ± 80 nM and, since there are five sites per monomer, 2.1 μM in terms of phosphorylatable sites, while the apparent k_{cat} of the reaction is 12.8 ± 2 s^{-1} ($k_{cat}/K_M = 6.0 \times 10^6\ M^{-1}\ s^{-1}$). We also measured K_M for ATP to be 70 μM when full length Pho4 is the protein substrate. These kinetic constants are comparable to those measured for the phosphorylation of Gsy2, a physiological substrate of Pho85, when Pho85 is activated by a different cyclin, Pcl10 ($k_{cat}/K_M = 10.7\ s^{-1}/3.0\ \mu M = 2.6 \times 10^6\ M^{-1}\ s^{-1}$) (Wilson *et al.*, 1999), and for human cyclin E-CDK2 phosphorylation of a specific substrate, the Retinoblastoma gene product (pRB) ($k_{cat}/K_M = 5.3\ s^{-1}/2.2\ \mu M = 2.4 \times 10^6\ M^{-1}\ s^{-1}$) (Xu *et al.*, 1999). In contrast, phosphorylation of non-specific substrates, such as histone H1, by human cyclin A-CDK2 (Kaldis *et al.*, 2000), or peptide phosphorylation by Pcl10-Pho85 (Wilson et al., 1999), occurs with a k_{cat}/K_M ratio at least 1000-fold lower. We see similarly lower levels of Pho80-Pho85 specific activity toward peptide substrates (see below) and towards casein, a non-specific substrate (data not shown). Thus, the purified recombinant Pho80-Pho85 has a high specific activity towards Pho4 that is similar to the activities of other purified cyclin-CDK complexes.

Kinetic Model of Pho4 Phosphorylation

Analysis of Pho4 phosphorylation using SDS-PAGE gels and Henri-Michaelis-Menten kinetics cannot provide enough information to dissect the complicated reaction between Pho80-Pho85 and Pho4. Partially phosphorylated intermediates may accumulate during the kinase reaction, but these would all be measured as a single band on SDS-PAGE gels. In fact, there could be 32 different phosphorylated species of Pho4 that may follow 120 different paths when going from unphosphorylated to completely phosphorylated (Fig. 1a). Throughout the paper we shall call Pho4 that is phosphorylated once phosphoform 1, Pho4 that is phosphorylated twice phosphoform 2, etc., without regard to which sites are phosphorylated. It should be noted that there are actually five different species of phosphoforms 1 and 4, and ten different species of phosphoforms 2 and 3 (Fig. 1a). A simple kinetic equation can be used to describe the reaction between Pho80-Pho85 and each of the 32 species of Pho4 (Fig. 1b). This means there are 32 potentially different k_{on} and k_{off} reaction constants and 80 different k_{cat} constants that describe the complete reaction. The apparent k_{cat} and K_M measured in the previous section are actually composites of the subset of the 144 total constants that govern the initial rate of the reaction.

Phosphorylation of Pho4 is Semi-Processive

As a first step toward dissecting the reaction between Pho4 and Pho80-Pho85 we used one-dimensional isoelectric focusing (IEF) to separate the different phosphoforms of Pho4 generated during a kinase reaction. Using mutant Pho4 proteins lacking specific phosphorylation sites, we demonstrated that it was possible to separate phosphoforms 1 through 5 (Fig. 2a). We used Pho4 mutants that lacked other specific sites to show that the phosphoforms migrate consistently to the same place in the IEF gel independently of which specific sites are phosphorylated (data not shown).

We quantitated the rate of formation of the phosphoforms as the kinase reaction proceeded to completion (Fig. 2b and see Fig. 5a for quantitation). To obtain the relative molar amounts of each phosphoform we divided the amount of radioactivity in each band by the number of times the phosphoform had been phosphorylated. At early time points phosphoform 1 and phosphoform 2 predominated, and as the reaction proceeded, the amounts of phosphoforms 1, 2, and 3 rose and fell until at the end of the reaction the majority of Pho4 was in phosphoforms 4 and 5 (Fig. 2b and Fig. 5a).

We next investigated whether phosphorylation of Pho4 by Pho80-Pho85 is processive or distributive. If the kinase is completely processive it will phosphorylate Pho4 on all five sites every time it is bound, and the concentrations of phosphoforms 1-4 should never be higher than the concentration of kinase in the reaction. The concentration of phosphoform 1 reached a level of 400 nM in a reaction with only 2 nM Pho80-Pho85 (Fig. 5a). Therefore, Pho80-Pho85 does not phosphorylate Pho4 in a completely processive manner. In contrast, if the kinase is distributive it will phosphorylate Pho4 on only one site every time it is bound. Increasing the molar ratio of Pho4 to Pho80-Pho85 should lead to an increase in the amount of phosphoform 1 relative to phosphoform 2 and the other phosphoforms. In a distributive reaction, phosphoform 2 is only generated by phosphorylation of phosphoform 1, and an excess of unphosphorylated Pho4 will prevent Pho80-Pho85 from phosphorylating phosphoform 1. When we varied the Pho4 to Pho80-Pho85 ratio over a 100-fold range and stopped the reaction at an early time point we saw no significant change in the relative amounts of the different phosphoforms (Fig. 2c). These data strongly suggest that phosphorylation of Pho4 by Pho80-Pho85 is not completely distributive. We calculated an average of 2.1 phosphorylation events per binding event by multiplying the percentage of each phosphoform by the number of times it was phosphorylated. These data demonstrate that the phosphorylation of Pho4 occurs through semi-processive activity of Pho80-Pho85. While Pho80-Pho85 is bound to Pho4 it can phosphorylate more than one site but it does not phosphorylate all five sites every time.

Pho80-Pho85 Exhibits Site Preference

To determine if there was an order in which the sites were phosphorylated we did tryptic phosphopeptide mapping on each phosphoform purified from IEF gels. Using mutants defective for specific phosphorylation sites, we showed that we could separate the SP2-SP3, SP4, and SP6 phosphopeptides from each other (data not shown) (O'Neill et al., 1996).

Surprisingly, when we quantitated which phosphopeptides were phosphorylated in phosphoform 1 we found a marked preference for phosphorylation of SP6. 60% of the radioactive signal was in the SP6 phosphopeptide versus 16% in the SP4 and 24% in the SP2-SP3 phosphopeptides (Fig. 3b and 3g). As Pho4 was converted to phosphoforms 2, 3, and 4 the SP6 phosphopeptide predominated less and less until all 4 phosphopeptides were represented fairly equally in phosphoform 5 (Fig. 3c-3g). Thus, SP6 has the highest probability of being phosphorylated first, followed by SP4, and SP2 and SP3 are most likely to be phosphorylated last.

We tested if site preference could be explained by the local amino acid sequence around the phosphorylation sites by synthesizing peptides that contained SP2, SP4, and SP6 and measuring how efficiently they were phosphorylated by Pho80-Pho85. We found little difference in the specific activity of Pho80-Pho85 towards these peptides. The k_{cat}/K_M ratios were; SP2 - 14.8 s^{-1} / 4.8 mM = 3080 M^{-1} s^{-1}; SP4 - 18.4 s^{-1} / 8.0 mM = 2300 M^{-1} s^{-1}; SP6 - 18.1 s^{-1} / 5.3 mM = 3420 M^{-1} s^{-1}. Since Pho80-Pho85 has similar activity towards the SP2 and SP6 peptides site preference is not determined simply by the local amino acid sequence around the phosphorylation site. The fact that these peptides are phosphorylated with a higher k_{cat} and 1000-fold lower K_M suggests that the low apparent K_M measured for the phosphorylation of full length Pho4 is due to high affinity binding between Pho4 and Pho80-Pho85.

Computer Modeling of the Kinase Reaction

Due to the complexity of the system, we turned to computer modeling to obtain numerical values for the kinetic constants that describe the reaction and to make it possible to dissect the overall reaction. There are 65 different species in the complete reaction: 32 species of Pho4 that can each be free or associated with Pho80-Pho85, and free kinase (Fig. 1a, b). We generated differential equations to describe the rate of change of the concentrations of all 65 species during the course of the reaction (Fig. 4a and Methods).

To better describe binding and phosphorylation of Pho4 by Pho80-Pho85, we made specific definitions for the kinetic constants that govern the reaction. The association and dissociation rate constants, k_{on} and k_{off}, govern the high affinity interaction between Pho4 and Pho80-Pho85. The rate constant governing phosphorylation of Pho4 on a specific site is k_{cat}. The total k_{cat}, $k_{cat\text{-}Tot}$, for a Pho4-Pho80-Pho85 complex governs the rate at which Pho4 is phosphorylated on any site, and is equal to k_{cat} times the sum of the probabilities of being phosphorylated on the remaining sites (Fig. 4a and Methods).

To help constrain the system, we made several simplifying assumptions about the way that the reaction proceeds (Methods). Our first assumption was that phosphorylation can affect the kinetic constants. Two models tested whether phosphorylation of a single site could affect k_{on}, k_{off}, and k_{cat} for subsequent phosphorylation of other sites. This effect of phosphorylation on the kinetic constants could obey many mathematical relationships, but if one assumes phosphorylation affects the free energy of the reaction, the effect should be multiplicative (Fig. 4b, Synergistic model). We also tested whether the effect could be additive (Fig. 4b, Additive model). In these two models, referred to as the Synergistic k_{all} and Additive k_{all} models, all three constants, k_{on}, k_{off}, and k_{cat} are allowed to change when a specific site is phosphorylated.

Our second assumption tested what the rate-limiting step in phosphorylation was once Pho4 was stably bound to Pho80-Pho85. If the rate-limiting step is locating a phosphorylatable site, $k_{cat\text{-}Tot}$ for phosphorylation of Pho4 should decrease once Pho4 is phosphorylated and locating an unphosphorylated site is more difficult. This model also assumes that phosphorylation of one site does not affect the site preference of another site. If the rate-limiting step in catalysis is one of the other events that contribute to k_{cat}, such as binding of ATP, release of ADP, or transfer of phosphate to a site when it is in the catalytic cleft, then $k_{cat\text{-}Tot}$ should remain constant since the concentration of kinase is constant and the concentration of ATP is saturating and constant throughout the reaction. We called these two models the Decreasing k_{cat} and Constant k_{cat} models (Fig. 4b).

Using a searching algorithm and least squared analysis, we fit all four models to the rate of phosphoform production data (Fig. 2b, Fig. 5a) and the site preference data in phosphoform 1 (Fig. 3g). We then asked how well the fit of that data predicted the outcome of two other sets of experimental data: the apparent k_{cat}/K_M data from the initial characterization of the kinase reaction; and the site preference in phosphoforms 2, 3, and 4, as well as the site preference in phosphoform 1 produced from a reaction containing a sub-saturating concentration of ATP. In a reaction with a low concentration of ATP, only phosphoform 1 is produced and the site preference approximates the true site preference of the kinase (data not shown).

We found that three of the four models could fit the rate of phosphoform production and the site preference data in phosphoform 1 (Table 1, columns 1 and 2). Only one model then predicted the outcome of the other data sets to a statistically significant degree (Table 1, columns 3 and 4). This model is a combination of the Synergistic k_{all} and Decreasing k_{cat} models.

To further refine the Synergistic k_{all} and Decreasing k_{cat} model, we fit the data allowing only one of the kinetic constants to be affected by phosphorylation while the other two remained unaffected (Table 1, bottom section). The Synergistic k_{cat} model fit some of the data although it did not predict the site preference data very well, and the Synergistic k_{on} model did not fit any of the data. The Synergistic k_{off} model predicted all our data as well as the Synergistic k_{all} model, suggesting that phosphorylation only affects k_{off}.

Kinetic Constants for the Kinase Reaction

The fit of the Synergistic k_{off} and Decreasing k_{cat} model to the experimental data and the predicted ranges for the kinetic constants are shown (Fig 5a-5c and Table 2). Rather than show the kinetic constants for all 32 species of Pho4 we calculated the average constants for the five phosphoforms. This is justified because only one or two species predominate in each phosphoform due to the site preference. The model predicts a $k_{cat\text{-}Tot}$ of 24.7 - 26.5 s^{-1} for phosphorylation of unphosphorylated Pho4 by Pho80-Pho85, and, when we simulated the Henri-Michaelis-Menten analysis it predicted an apparent k_{cat} of 12 - 14.1 s^{-1}, compared with an experimentally measured value of 10.8 - 14.8 s^{-1} (Fig. 5b). The apparent k_{cat} is smaller than the predicted $k_{cat\text{-}Tot}$ because the apparent k_{cat} is limited by k_{off} in the experimental reaction.

The $k_{cat\text{-}Tot}/k_{off}$ ratio predicts that Pho4 is phosphorylated at least once in two-thirds of all binding events, and, when it does get phosphorylated, is phosphorylated an average of two times. This prediction agrees with our experimental data showing that Pho80-Pho85 phosphorylates Pho4 in a semi-processive fashion with an average of 2.1 phosphorylation events per binding event (Fig. 2). This means that when Pho4 is bound to Pho80-Pho85 there is a chance that the complex will fall apart and a chance that Pho4 will get phosphorylated. The probability of either event occurring before the other is determined by the $k_{cat\text{-}Tot}/k_{off}$ ratio. Phosphorylation of specific sites on Pho4 leads to a slight decrease in k_{off} of the kinase reaction and in K_D for binding of Pho4 to Pho80-Pho85.

Finally, $k_{cat\text{-}Tot}$ of the reaction decreases as Pho4 becomes more phosphorylated and finding an unphosphorylated site is more difficult. $k_{cat\text{-}Tot}$ for any species of Pho4 can be calculated by multiplying the $k_{cat\text{-}Tot}$ of unphosphorylated Pho4 (24.7 - 26.5 s^{-1}) by the sum of the site preferences of the remaining unphosphorylated sites. This suggests that there is no direct effect of phosphorylation of one site on phosphorylation of another. Instead, the chance of finding any particular site is always the same and is determined by the site preference. The predicted site preferences are similar to what we measured experimentally, except for SP1, which we can't detect, but is only predicted to account for 4-5% of the total phosphorylation (Fig. 4c). It has been shown previously that phosphorylation of SP1 is less efficient than phosphorylation of SP2-SP6, perhaps because the sequence of the site does not conform to the consensus sequence of the other sites (SPXT vs. SPXI/L) (O'Neill et al., 1996).

In summary, the computer modeling of the experimentally determined rate of phosphoform production and site preference allowed us to determine numerical values for the kinetic constants that describe the reaction between Pho4 and Pho80-Pho85. Importantly, the best-fitting model accurately predicts the results of other experiments we performed. These results give us a more detailed view of the reaction than we could have obtained from just experimentation.

Discussion

We have shown that phosphorylation of Pho4 by Pho80-Pho85 is semi-processive due to a balance between the values of k_{off} and $k_{cat\text{-}Tot}$ (Fig 2 and Table 2). This suggests that Pho4 remains bound to Pho80-Pho85 while multiple phosphorylation site peptides are phosphorylated in the catalytic cleft. It seems likely that high-affinity interaction between Pho80 and Pho4 allows phosphorylation to proceed in this way. Another example of processive substrate phosphorylation involves kinases that contain Src homology 2 (SH2) domains. These SH2 domains are required for the kinases to bind substrates that contain

phosphotyrosine and to carry out processive phosphorylation on multiple sites (Duyster *et al.*, 1995; Lewis *et al.*, 1997; Mayer *et al.*, 1995). This reaction may be similar to the reaction between Pho4 and Pho80-Pho85 where tight binding between the kinase and the substrate in regions that are distinct from the catalytic cleft and the phosphorylation sites allows for processive activity. In contrast, phosphorylation of two sites on MAPK, Tyr^{185} and Thr^{183}, occurs through distributive activity of MAPKK (Burack & Sturgill, 1997; Ferrell & Bhatt, 1997). In this reaction there may be a requisite release of the entire substrate before ADP and ATP can exchange. Experiments using a peptide derived from pRB and human cyclin D-CDK4 showed that the phosphorylated substrate is released before the exchange of ADP for ATP (Konstantinidis *et al.*, 1998). It is possible that the interaction between MAPK and MAPKK is mediated in large part through residues that are near to or part of the phosphorylation site and the catalytic cleft of the kinase. Release of the phosphorylated residue, a prerequisite for ADP and ATP exchange, would lead to release of the entire substrate and force the reaction to be distributive.

Our data indicate that Pho80-Pho85 exhibits site preference when it phosphorylates Pho4 (Fig. 3). This site preference has interesting consequences for the regulation of Pho4 activity *in vivo*. Phosphorylation of Pho4 by Pho80-Pho85 takes place in the nucleus (Kaffman *et al.*, 1998) where partially phosphorylated species of Pho4 may accumulate. Nuclear Pho4 will be rapidly inactivated by phosphorylating SP6 first, resulting in immediate repression of Pho4-Pho2 dependent genes (Komeili & O'Shea, 1999). Phosphorylation of both

SP2 and SP3 is required for export of Pho4 from the nucleus (Kaffman et al., 1998). Computer modeling predicts that 87-92% of the Pho4 molecules which are phosphorylated on both SP2 and SP3 will also be phosphorylated on SP4 and SP6, assuring that Pho4 is almost always completely phosphorylated on the critical sites before it is exported. This helps to prevent a futile cycle where Pho4 that is not phosphorylated on SP4 is exported into the cytoplasm and then quickly re-imported into the nucleus.

MAPKK also exhibits site preference, phosphorylating Tyr^{185} before Thr^{183} in MAPK (Ferrell & Bhatt, 1997; Haystead *et al.*, 1992; Robbins & Cobb, 1992), but it is not clear how this preference is achieved. It seems unlikely that site preference exhibited by Pho80-Pho85 is due simply to the local sequence surrounding the phosphorylation site since Pho80-Pho85 phosphorylates SP2 and SP6 containing peptides with equal efficiency. The Decreasing k_{cat} computer model predicts that as Pho4 is phosphorylated the chance of another phosphorylation event occurring decreases (Table 2), and that the decrease is proportional to the site preference of the site that was phosphorylated. This leads us to propose that when Pho4 is bound stably to Pho80-Pho85, the ability of the kinase to locate, bind, and orient an SP site in the catalytic cleft is the rate-limiting step in catalysis. The chance of finding and phosphorylating any particular site is reflected in the site preference data - SP6 > SP4 > SP3, SP2 > SP1. The preference for SP6 could be due to the fact that SP6 is an easier site to find, perhaps because it is closer to the site of catalysis or is in a region of secondary or tertiary structure that allows for more efficient phosphorylation than the other sites.

Our results provide an important step toward complete understanding of how yeast respond to changing levels of phosphate in the environment and could serve as a model for the investigation of other kinase-substrate interactions. Several interesting issues remain to be addressed. Pho80-Pho85 is bound to the CDK inhibitor Pho81 at all times in the cell (Schneider et al., 1994) and it will be interesting to understand how Pho81 inhibits Pho80-Pho85 activity. We currently do not have a source of Pho81 to study its effect on Pho80-Pho85 activity *in vitro*. It has been shown that binding of Pho81 to Pho80-Pho85 in high phosphate, when Pho81 is not an active inhibitor, does not cause a significant decrease in kinase activity *in vitro* (Schneider et al., 1994). For this reason, we believe that the activity of the recombinant Pho80-Pho85 that we are studying is reflective of the activity of the endogenous kinase when cells are grown in high phosphate. Additionally, the reaction of Pho4 with Pho80-Pho85 inside the cell is much more dynamic than in the test tube. Pho4 is being transported in and out of the nucleus, becoming dephosphorylated, and binding to other proteins and DNA. Further investigation into these issues will lead to a more detailed understanding of the complex regulation of signal transduction *in vivo*.

Acknowledgements - We thank J. Weissman, D. Morgan, and members of the O'Shea lab for critical reading of the manuscript. This work was supported by grants from the N.I.H. (GM51377), The Lucile and David Packard Foundation

Methods

Protein and Peptide Purification - Expression and purification of Pho4 wild-type and mutant proteins was as described (Kaffman et al., 1994). Co-expression of Pho85-His$_6$ in pQE-60 (EB1164) (Qiagen) and Pho80 in pSBETA (EB1076) (Schenk *et al.*, 1995) was done in BL21 (DE3) cells. Competent cells were co-transformed with plasmids EB1164 and EB1076 and transformants were plated on LB plates with 50 µg ml^{-1} carbenecillin and 70 µg ml^{-1} kanamycin. 50-200 freshly transformed colonies were inoculated into 1 liter of LB containing 50 µg ml^{-1} carbenecillin and 70 µg ml^{-1} kanamycin, and grown at 37° C. Cells were grown to an optical density 0.5-0.6 at 600 nm and induced with 200 µM isopropyl-β-D-thiogalactopyraniside and allowed to grow for 6.5 hours at 24° C. Cells were harvested at 4° C and pellets were stored at –20°C for up to one month.

Purification of the Pho80-Pho85 complex was as follows: Cells were resuspended in 20 ml of lysis buffer (10% (v/v) glycerol, 50 mM Tris-HCl pH 8.0, 0.25 M NaCl, 0.1% NP-40, 1 mM β-mercaptoethanol, 60 mM imidazole, 1 mM phenylmethylsulfonyl fluoride (PMSF), 2 mM benzamidine) per one liter of induced culture. Lysozyme was added to 0.5-1.0 mg ml^{-1} and the cell suspension was incubated for 5 minutes at 4° C with rotation. Cells were lysed by placing the tube in an ice/salt/water bath and sonicating with a Branson sonicator micro-tip on setting 4 for 3 x 60 seconds with 60 seconds in between pulses. DNase I was added to 5 µg ml^{-1}, RNase A was added to 10 µg ml^{-1} and the lysate was clarified by spinning in an SS34 rotor (Beckman) at 16,000 RPM for 20 minutes at 4° C. The clarified lysate was filtered using a 0.2 µm syringe filter and loaded onto a 1 ml Hi-Trap Chelating column (Pharmacia) loaded with $NiSO_4$, equilibrated in lysis buffer and attached to a Biologic FPLC (Bio-Rad). After the lysate was loaded, the column was washed with 6-8 ml of lysis buffer and 6-8 ml of low imidazole buffer (same as lysis buffer except without NP-40 and benzamidine). The protein was eluted with a 20 ml linear gradient from low imidazole buffer to high imidazole buffer (same as low imidazole buffer except with 750 mM imidazole). Fractions containing purified Pho80-Pho85 were pooled. Purified kinase was either desalted with a 5 ml Hi-Trap desalting column (Pharamacia) or dialyzed overnight into storage buffer (10% (v/v) glycerol, 50 mM Tris-HCl pH 7.5, 0.15 M NaCl, 1 mM β-mercaptoethanol, 1 mM PMSF).

Protein and peptide concentrations were measured using the absorbance at 280 nm in 6 M GuHCl at pH 6.5 (Edelhoch, 1967). The purity of the Pho4 protein preparations and the Pho80-Pho85 complex was estimated to be >95% by Coomassie staining and size exclusion chromatography. We used four different preparations each of Pho80-Pho85 and Pho4 to do the experiments in this paper and did not observe significant batch to batch variation.

Peptides were synthesized by FMOC (9-fluoroenylmethoxycarbonyl) chemistry and were purified to >96% by reversed-phase HPLC. Sequences are: SP2 peptide - TATIKPRLLYSPLIHTQSAVPVTR, SP4 peptide - SANKVTKNKSNSSPYLNKRKGKPGPDSATSLF, SP6 peptide - SAEGVVVASESPVIAPHGSTHARSY.

Kinase Assays - All kinase assays were carried out at 30°C in kinase buffer (10% (v/v) glycerol, 50 mM Tris-HCl pH 7.5, 0.15 M NaCl, 0.01% (v/v) NP-40, 1 mM dithiothreitol, 1 mM PMSF, 10 mM $MgCl_2$, 0.1 mg ml^{-1} human insulin (Boehringer Mannheim), 170 nM [γ-^{32}P]ATP (Amersham, 6000 Ci $mMol^{-1}$)). Kinase reactions to measure the apparent k_{cat} and K_M were done with 0.1 nM Pho80-Pho85, 900 µM ATP, different concentrations of Pho4 and were electrophoresed on 12% SDS polyacrylamide gels. We used 50 nM Pho80-Pho85 in the peptide kinase reactions which were quantitated by spotting on P81 paper (Whatman), washing with 75 mM phosphoric acid and scintillation counting. Reactions were stopped by the addition of an equal volume of 2x SDS-PAGE sample buffer (full length Pho4) or the addition of ethylenediamine-tetraacetic acid to 50 mM (peptide reactions). Kinase reactions to measure phosphoform production and to do tryptic phosphopeptide mapping contained 2 nM Pho80-Pho85, 3 µM Pho4, 900 and 450 µM ATP, respectively. The tryptic phosphopeptide mapping was done from a 5′ reaction. Reactions to be run on IEF gels were stopped by the addition of EDTA to 50 mM and immediate freezing in liquid nitrogen. Reactions where phosphorylation of Pho4 was completely distributive contained 2 nM Pho80-Pho85, 6 µM Pho4, 7 µM ATP. All quantitation was done using a PhosphorImager (Molecular Dynamics). Apparent k_{cat} and K_M measurements were made by plotting the initial rate of phosphorylation data and the concentration of Pho4 or peptide on a Lineweaver-Burk plot. For phosphorylation of Pho4 and Gsy2 we calculated k_{cat} from V_{MAX} assuming that 100% of the enzyme was active. Pho4 is a homo-dimer *in vitro* (our unpublished results) (Shao *et al.*, 1998), but throughout this paper we assume that each half-dimer independently binds to and is phosphorylated by one heterodimer of Pho80-Pho85 (Jayaraman et al., 1994).

Protein Gels - Isoelectric focusing (IEF) was carried out using a Hoefer SE250 mini-gel system cooled to 12° C using a circulating bath. IEF gels contained 3.15% (w/v) acrylamide, 0.19 % (w/v) bis-acrylamide, 2% (w/v) BIG CHAP (CalBiochem), 1% (w/v) Ampholine 3.5-10 ampholytes (Pharmacia), 1% (w/v) Bio-Lyte 6/8 ampholytes (Bio-Rad), and 9.1 M urea. Samples were diluted in loading buffer so that the final concentration of components was 4-6 M urea, 2 % BIG CHAP, 2 % Ampholine 3.5-10 ampholytes, 50 mM DTT. Overlay buffer was the same except it contained 2.3 M urea and bromophenol blue. 10-20 µl of sample containing 400-800 ng Pho4 was loaded into each well, overlaid with 5 µl of overlay solution, and cold (10-12°C) upper buffer was layered over the top. Upper buffer was 10 mM NaOH and lower buffer was 10 mM phosphoric acid. Gels were electrophoresed at 200 volts at the start and limited at 500 volts. Focusing was carried out for 2-3 hours. After electrophoresis, the gels were soaked for 15 minutes in three changes of SDS-PAGE gel running buffer (for tryptic phosphopeptide mapping) or 20% (w/v) tricholoroacetic acid (for quantitation) and dried.

Tryptic Phosphopeptide Mapping - Tryptic phosphopeptide mapping was carried out according to manufacturer's directions using an HTLE-7002 system

(CBS Scientific) and exactly as described (Kaffman et al., 1994). The fact that all of the phosphopeptide spots are equally represented in phosphoform 5 indicates that there are no solubility differences between the phosphopeptides under these conditions, except for phosphopeptides containing SP1 which we have never been able to detect possibly because they are insoluble. Quantitation was done using the PhosphorImager.

Computer Modeling - MacPerl 5 was used to write all sets of differential equations. These were imported into Mathematica 4.0 (Wolfram Research, Inc.) and solved using numeric integration. The entire code for both the MacPerl and Mathematica simulations can be accessed at pho.ucsf.edu/intranet/jmb.html. User name and password are "reviewer".

The events included in k_{cat} and $k_{cat\text{-}Tot}$ include: binding of Mg^{2++} and ATP in the catalytic cleft of Pho85; locating, orienting, and binding a phosphorylation site in the catalytic cleft; transfer of the gamma phosphate of ATP to the serine of the phosphorylation site; and release of both the phosphorylated site and ADP from the catalytic cleft. These definitions of k_{cat} and $k_{cat\text{-}Tot}$ are justified because phosphorylation of Pho4 is semi-processive. The enzyme can bind and release a phosphorylated residue from the catalytic cleft without requiring disassociation of the substrate-enzyme complex. It seems unlikely that binding of the phosphorylation site in the catalytic cleft contributes significantly to k_{on} and k_{off} because of the weak binding of the peptides to the kinase (see above). The rate of turnover of the enzyme is not dependent simply on transfer of phosphate to the phosphorylation site in the catalytic cleft, but also on the ability of the enzyme to locate and bind that site in the first place.

The simplifying assumptions allowed us to test different effects of phosphorylation on the reaction and reduced the number of variables in the rate equations so we could statistically evaluate the fit of the models to the experimental data. The Additive k_{all} and Synergistic k_{all} models contain 19 variables - k_{on}, k_{off}, and k_{cat} for the reaction with unphosphorylated Pho4, the separate effects of phosphorylating SP1, SP2, SP3, SP4, and SP6 on k_{on}, k_{off}, and k_{cat}, and a variable for the total concentration of kinase in the reaction. The Decreasing k_{cat} model adds five variables for the site preferences of SP1-SP6 while the Constant k_{cat} model does not add any variables. The Synergistic k_{off} and Decreasing k_{cat} model, which fits the data the best, has 14 variables.

In our models we assumed the effect of phosphorylation was determined by which combination of sites is phosphorylated. It is also possible that the total number of sites phosphorylated affects the rate constants. Because of the strong site preference for site 6 these two models turn out to be very similar. We ignored the potential effect of phosphorylation on site preference because we did not have enough data to constrain models that included such an effect. Our model fits without having to invoke an effect, suggesting that the effect is minor at best.

Models were compared to the experimental data by reduced chi-squared analysis (Press, 1992). The variables were fit by taking a random step of random length in variable space and comparing the chi-squared values (Bevington &

Robinson, 1992). If the new chi-squared value was lower, the new set of variables was used as a new starting point for future steps. When this search became inefficient (this only occurred with the models that did not fit well) a standard grid search (Bevington & Robinson, 1992) of variable space was performed until each variable was at a minimum (minimum step size of .1% of each variable).

Predictions of composite k_{cat}/K_M and site preference in phosphoforms 2, 3, and 4 and phosphoform 1 phosphorylated at a sub-saturating concentration of ATP were done by chi-squared analysis from the subset of variables which should be indistinguishable statistically from the rate of phosphoform production and site preference in phosphoform 1 data at least 99% of the time.

Refernces

Adams, P. D., Li, X., Sellers, W. R., Baker, K. B., Leng, X., Harper, J. W., Taya, Y. & Kaelin, W. G., Jr. (1999). Retinoblastoma protein contains a C-terminal motif that targets it for phosphorylation by cyclin-cdk complexes. *Mol Cell Biol* **19**(2), 1068-80.

Bevington, P. R. & Robinson, D. K. (1992). In *Data reduction and error analysis for the physical sciences*. pp.141-167, 258-259, 2nd edit, McGraw-Hill, New York.

Brown, N. R., Noble, M. E., Endicott, J. A. & Johnson, L. N. (1999). The structural basis for specificity of substrate and recruitment peptides for cyclin-dependent kinases. *Nat Cell Biol* **1**(7), 438-443.

Burack, W. R. & Sturgill, T. W. (1997). The activating dual phosphorylation of MAPK by MEK is nonprocessive. *Biochemistry* **36**(20), 5929-33.

Duyster, J., Baskaran, R. & Wang, J. Y. (1995). Src homology 2 domain as a specificity determinant in the c-Abl-mediated tyrosine phosphorylation of the RNA polymerase II carboxyl-terminal repeated domain. *Proc Natl Acad Sci U S A* **92**(5), 1555-9.

Edelhoch, H. (1967). Spectroscopic determination of tryptophan and tyrosine in proteins. *Biochemistry* **6**(7), 1948-54.

Ferrell, J. E., Jr. & Bhatt, R. R. (1997). Mechanistic studies of the dual phosphorylation of mitogen-activated protein kinase. *J Biol Chem* **272**(30), 19008-16.

Haystead, T. A., Dent, P., Wu, J., Haystead, C. M. & Sturgill, T. W. (1992). Ordered phosphorylation of p42mapk by MAP kinase kinase. *FEBS Lett* **306**(1), 17-22.

Holmes, J. K. & Solomon, M. J. (1996). A predictive scale for evaluating cyclin-dependent kinase substrates. A comparison of p34cdc2 and p33cdk2. *J Biol Chem* **271**(41), 25240-6.

Huang, D., Moffat, J., Wilson, W. A., Moore, L., Cheng, C., Roach, P. J. & Andrews, B. (1998). Cyclin partners determine Pho85 protein kinase substrate specificity in vitro and in vivo: control of glycogen biosynthesis by Pcl8 and Pcl10. *Mol Cell Biol* **18**(6), 3289-99.

Jayaraman, P. S., Hirst, K. & Goding, C. R. (1994). The activation domain of a basic helix-loop-helix protein is masked by repressor interaction with domains distinct from that required for transcription regulation. *Embo J* **13**(9), 2192-9.

Kaffman, A., Herskowitz, I., Tjian, R. & O'Shea, E. K. (1994). Phosphorylation of the transcription factor PHO4 by a cyclin-CDK complex, PHO80-PHO85. *Science* **263**(5150), 1153-6.

Kaffman, A., Rank, N. M., O'Neill, E. M., Huang, L. S. & O'Shea, E. K. (1998). The receptor Msn5 exports the phosphorylated transcription factor Pho4 out of the nucleus. *Nature* **396**(6710), 482-6.

Kaldis, P., Cheng, A. & Solomon, M. J. (2000). The effects of changing the site of activating phosphorylation in cdk2 from threonine to serine. *J Biol Chem*.

Komeili, A. & O'Shea, E. K. (1999). Roles of phosphorylation sites in regulating activity of the transcription factor Pho4. *Science* **284**(5416), 977-80.

Konstantinidis, A. K., Radhakrishnan, R., Gu, F., Rao, R. N. & Yeh, W. K. (1998). Purification, characterization, and kinetic mechanism of cyclin D1. CDK4, a major target for cell cycle regulation. *J Biol Chem* **273**(41), 26506-15.

Lewis, L. A., Chung, C. D., Chen, J., Parnes, J. R., Moran, M., Patel, V. P. & Miceli, M. C. (1997). The Lck SH2 phosphotyrosine binding site is critical for efficient TCR-induced processive tyrosine phosphorylation of the zeta-chain and IL-2 production. *J Immunol* **159**(5), 2292-300.

Mayer, B. J., Hirai, H. & Sakai, R. (1995). Evidence that SH2 domains promote processive phosphorylation by protein-tyrosine kinases. *Curr Biol* **5**(3), 296-305.

Moffat, J., Huang, D. & Andrews, B. (2000). Functions of Pho85 cyclin-dependent kinases in budding yeast. *Prog Cell Cycle Res* **4**, 97-106.

Morgan, D. O. (1997). Cyclin-dependent kinases: engines, clocks, and microprocessors. *Annu Rev Cell Dev Biol* **13**, 261-91.

O'Neill, E. M., Kaffman, A., Jolly, E. R. & O'Shea, E. K. (1996). Regulation of PHO4 nuclear localization by the PHO80-PHO85 cyclin-CDK complex. *Science* **271**(5246), 209-12.

Ogawa, N., DeRisi, J. & Brown, P. O. (2000). New components of a system for phosphate accumulation and polyphosphate metabolism in Saccharomyces cerevisiae revealed by genomic expression analysis. *Mol Biol Cell* **In Press**.

Okada, H. & Toh-e, A. (1992). A novel mutation occurring in the PHO80 gene suppresses the PHO4c mutations of Saccharomyces cerevisiae. *Curr Genet* **21**(2), 95-9.

Oshima, Y. (1997). The phosphatase system in Saccharomyces cerevisiae. *Genes Genet Syst* **72**(6), 323-34.

Press, W. H. (1992). In *Numerical recipes in C : the art of scientific computing*. pp 656-706, 2nd edit, Cambridge University Press, Cambridge ; New York.

Robbins, D. J. & Cobb, M. H. (1992). Extracellular signal-regulated kinases 2 autophosphorylates on a subset of peptides phosphorylated in intact cells in response to insulin and nerve growth factor: analysis by peptide mapping. *Mol Biol Cell* **3**(3), 299-308.

Schenk, P. M., Baumann, S., Mattes, R. & Steinbiss, H. H. (1995). Improved high-level expression system for eukaryotic genes in Escherichia coli using T7 RNA polymerase and rare ArgtRNAs. *Biotechniques* **19**(2), 196-8, 200.

Schneider, K. R., Smith, R. L. & O'Shea, E. K. (1994). Phosphate-regulated inactivation of the kinase PHO80-PHO85 by the CDK inhibitor PHO81. *Science* **266**(5182), 122-6.

Schulman, B. A., Lindstrom, D. L. & Harlow, E. (1998). Substrate recruitment to cyclin-dependent kinase 2 by a multipurpose docking site on cyclin A. *Proc Natl Acad Sci U S A* **95**(18), 10453-8.

Shao, D., Creasy, C. L. & Bergman, L. W. (1998). A cysteine residue in helixII of the bHLH domain is essential for homodimerization of the yeast transcription factor Pho4p. *Nucleic Acids Res* **26**(3), 710-4.

Songyang, Z., Blechner, S., Hoagland, N., Hoekstra, M. F., Piwnica-Worms, H. & Cantley, L. C. (1994). Use of an oriented peptide library to determine the optimal substrates of protein kinases. *Curr Biol* **4**(11), 973-82.

Wilson, W. A., Mahrenholz, A. M. & Roach, P. J. (1999). Substrate targeting of the yeast cyclin-dependent kinase Pho85p by the cyclin Pcl10p. *Mol Cell Biol* **19**(10), 7020-30.

Xu, X., Nakano, T., Wick, S., Dubay, M. & Brizuela, L. (1999). Mechanism of Cdk2/Cyclin E inhibition by p27 and p27 phosphorylation. *Biochemistry* **38**(27), 8713-22.

Figure Legends

Fig. 1 – Kinetic model of Pho4 phosphorylation. ***a,*** Representation of the 120 different paths Pho4 can take when going from unphosphorylated to completely phosphorylated. The large black circle represents Pho4, and a ball and stick projecting from Pho4 represents each of the phosphorylation sites. A filled circle indicates the site is phosphorylated. Each of the 80 dashed lines between species depicts a specific catalytic event. The dark black line is the path taken for the detailed reaction in ***b***. ***b,*** Kinetic equations showing one way in which Pho4 can become completely phosphorylated. Phosphorylation sites are represented as in ***a*** except that the number inside the darkened ball indicates which SP site has been phosphorylated. The superscript ball and stick icons next to the kinetic constants are to denote that each constant could have a different value because it describes the reaction between Pho80-Pho85 and different species of Pho4. The subscripts next to the k_{cat} constants indicate which SP site is being phosphorylated.

Fig. 2 - Separation of Pho4 phosphoforms on IEF gels. ***a,*** Pho4 mutant proteins containing serine to alanine mutations at the sites of phosphorylation were phosphorylated to 50-100% of completion and run on an IEF gel to show where the different Pho4 phosphoforms migrate: Lane 1 - SA1234; Lane 2 - SA146; Lane 3 - SA13; Lane 4 - SA1; Lane 5 - WT. The asterisks mark the completely phosphorylated species in each lane. ***b,*** Time course of Pho4 phosphoform

production electrophoresed on an IEF gel. ***c***, The molar ratio of Pho4:Pho80-Pho85 was varied over a 100-fold range and the amount of each phosphoform as a percentage of the total phosphorylated Pho4 was quantitated. Reaction components and time for different Pho4:Pho80-Pho85 ratios: 6 x 10^4:1 - 6 μM Pho4, 100 pM Pho80-Pho85, 0.5'; 6 x 10^5:1 - 6 μM Pho4, 10 pM Pho80-Pho85, 5'; 6 x 10^6:1 - 6 μM Pho4, 1 pM Pho80-Pho85, 50'. The total amount of phosphorylation detected in each reaction was the same. Approximately 0.6 % of the sites are phosphorylated under these conditions. Error bars are the standard deviation from three independent experiments.

Fig. 3 - Tryptic phosphopeptide mapping of Pho4 phosphoforms to determine site preference. ***a***, Schematic illustrating migration of the tryptic phosphopeptides containing the SP phosphorylation sites (O'Neill et al., 1996). ***b***, Phosphoform 1. ***c***, Phosphoform 2. ***d***, Phosphoform 3. ***e***, Phosphoform 4. ***f***, Phosphoform 5. ***g***, Quantitation of the site preference. The amount of each phosphopeptide as a percentage of the total phosphorylation was calculated. Phosphopeptides phosphorylated on SP2 or SP3 alone or SP2 and SP3 together are inseparable so we averaged the radioactive signal in those phosphopeptides. We cannot detect phosphopeptides containing SP1 in this assay. Error bars represent the standard deviation from three independent experiments.

Fig. 4 - Computer Modeling. ***a***, Diagram of the kinetic equation showing the rate of change of the concentration of Pho80-Pho85 bound to Pho4 that is

phosphorylated on SP3 and SP6. "K" is Pho80-Pho85. Superscript ones and zeroes represent the individual phosphorylation sites (SP1SP2SP3SP4SP6) in a species , where a zero is unphosphorylated and a one is phosphorylated. ***b,*** Definitions of constants in ***a***, ***c***, and ***d***. ***c,*** Differential equation that describes the diagram in ***a*** in the computer modeling. ***d,*** Specific definitions of the constants in the different models that were tested. In the Synergistic and Additive models the effect of phosphorylation on the kinetic constants is calculated relative to the kinetic constants for unphosphorylated Pho4.

Fig. 5 – Fit of the computer model to the experimental data. ***a,*** Quantitation of the time course of phosphoform production in Fig. 2b and fit of the best model – the Synergistic k_{off} and Decreasing k_{cat} model. Points on the graph represent 3 experimental time courses of phosphoform production, two of which were run twice on IEF gels for a total of 5 data sets. Error bars indicate the standard deviation and are within 10-20% of the average. The lines through the points are the predicted values from the model. ***b,*** Prediction of the apparent k_{cat}/K_M data by the best-fitting model, the Synergistic k_{off} and Decreasing k_{cat} model. The points represent the experimentally determined concentration of phosphate transferred at different times and with different concentrations of Pho4. Error bars represent standard deviation from 4 independent experiments and are within 10-20% of the average. The lines through the points are the predicted values from the model. ***c,*** Comparison of the experimentally determined site preference and the predicted site preference from the Synergistic k_{off} and

Decreasing k_{cat} model. Note that the predicted data is normalized to make SP2-6 equal to 100 percent to match the experimental data where SP1 cannot be detected.

Table 1 - [1]Numbers indicate the times out of 100 the model will be statistically indistinguishable from the experimental data. [2]Site preference in phosphoform 1 only. [3]Site preference in phosphoforms 2, 3, and 4, and phosphoform 1 in low ATP.

Table 2 – [1]From the Synergistic k_{off} and Decreasing k_{cat} model. [2]Average for all the different species present in phosphoform 1, 2, 3, and 4. [3]Calculated from k_{on} and k_{off}.

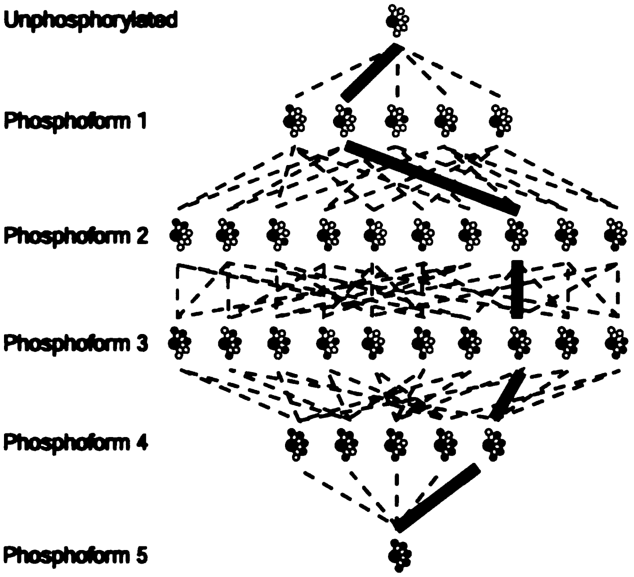
Unphosphorylated
Phosphoform 1
Phosphoform 2
Phosphoform 3
Phosphoform 4
Phosphoform 5

Figure 1a

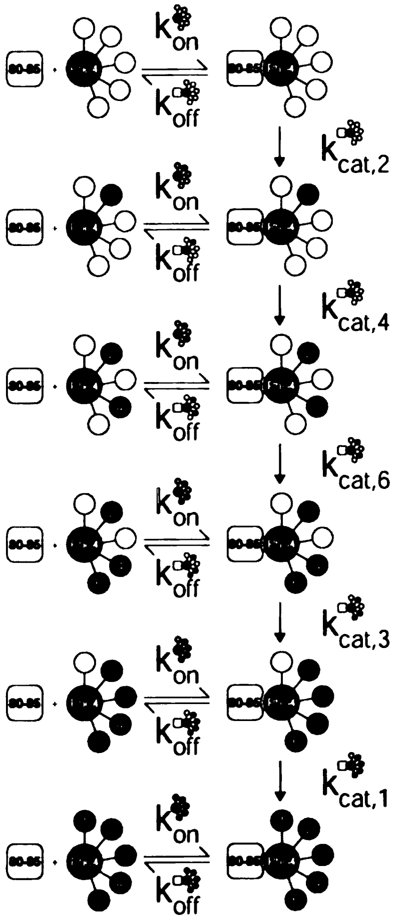
k_on
k_off
k_cat,2
k_cat,4
k_cat,6
k_cat,3
k_cat,1
80-85

Figure 1b

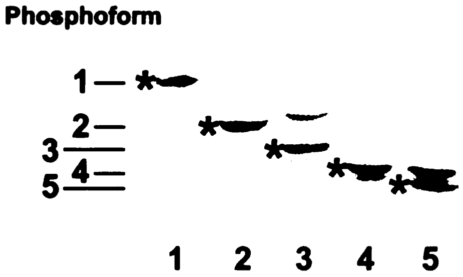
Phosphoform
1
2
3
4
5
*
1
2
3
4
5

Figure 2a

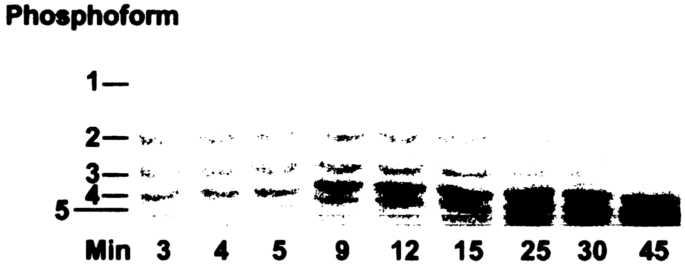
Phosphoform
1
2
3
4
5
Min
3
4
5
9
12
15
25
30
45

Figure 2b

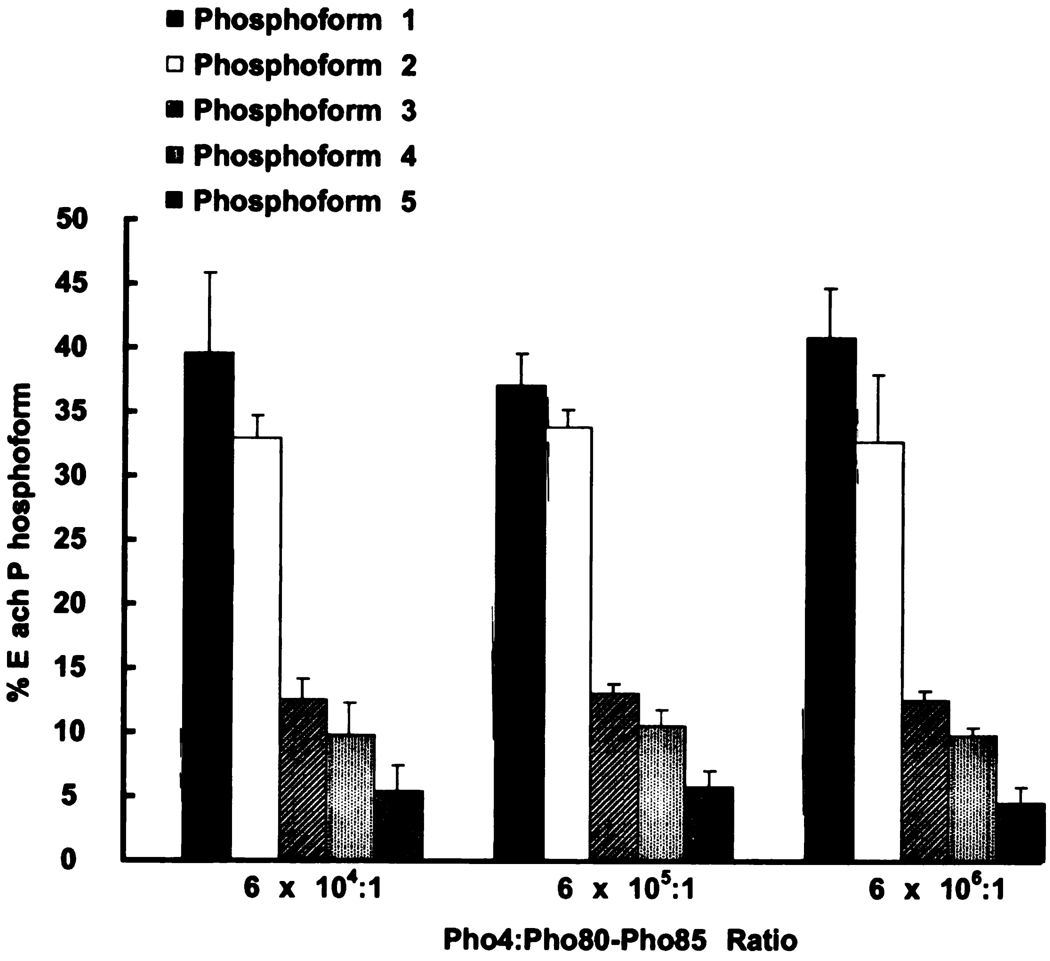
■ Phosphoform 1
□ Phosphoform 2
■ Phosphoform 3
■ Phosphoform 4
■ Phosphoform 5
50
45
40
35
30
25
20
15
10
5
0
% E ach P hosphoform
6 x 10⁴:1
6 x 10⁵:1
6 x 10⁶:1
Pho4:Pho80-Pho85 Ratio

Figure 2c

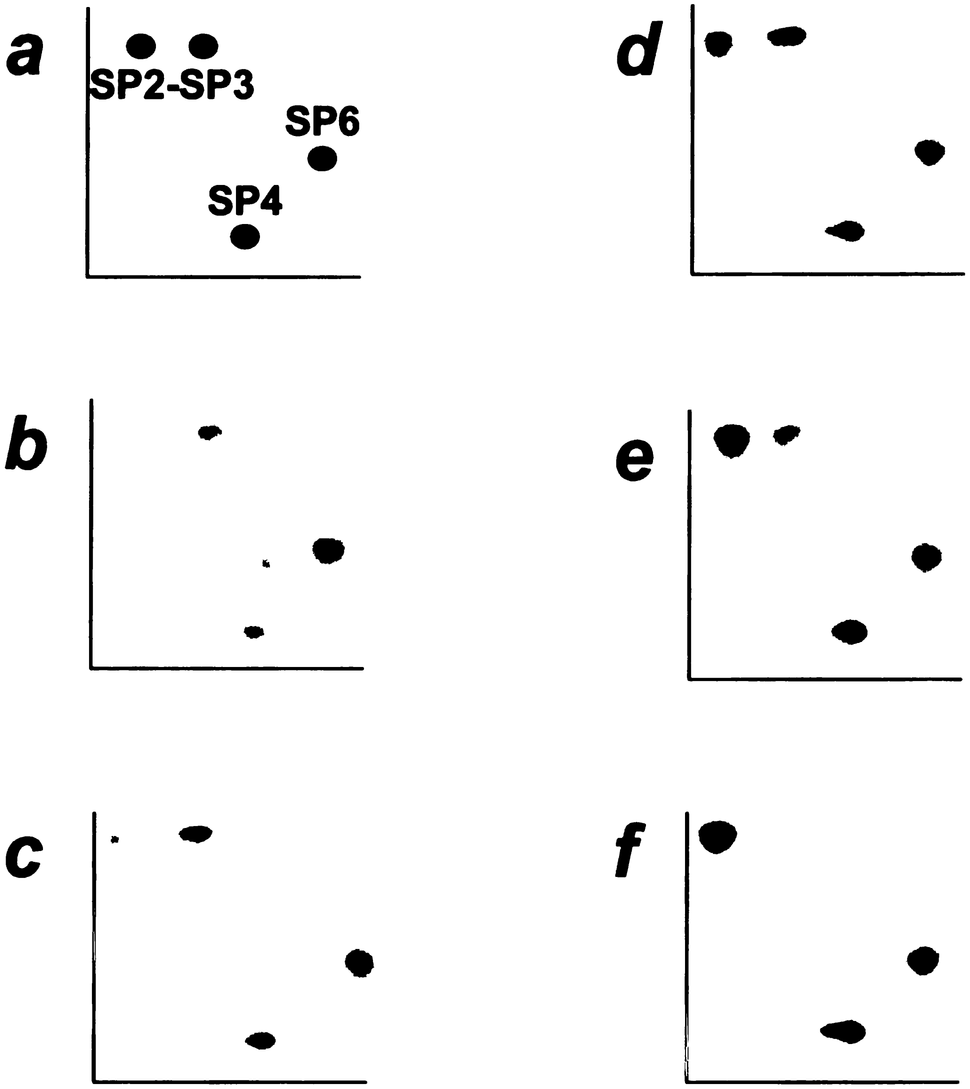
a
SP2-SP3
SP6
SP4
b
c
d
e
f

Figure 3 ***a-f***

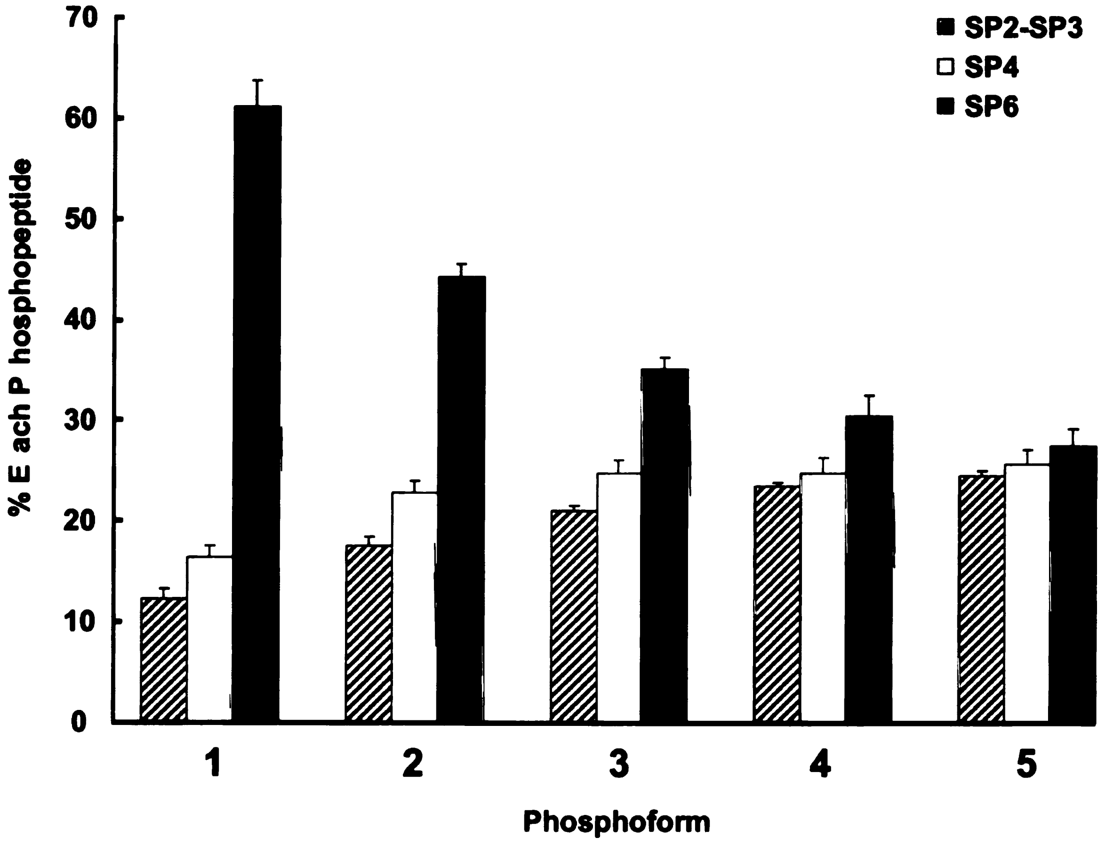
70
60
50
40
30
20
10
0
% E ach P hosphopeptide
▨ SP2-SP3
☐ SP4
■ SP6
1
2
3
4
5
Phosphoform

Figure 3g

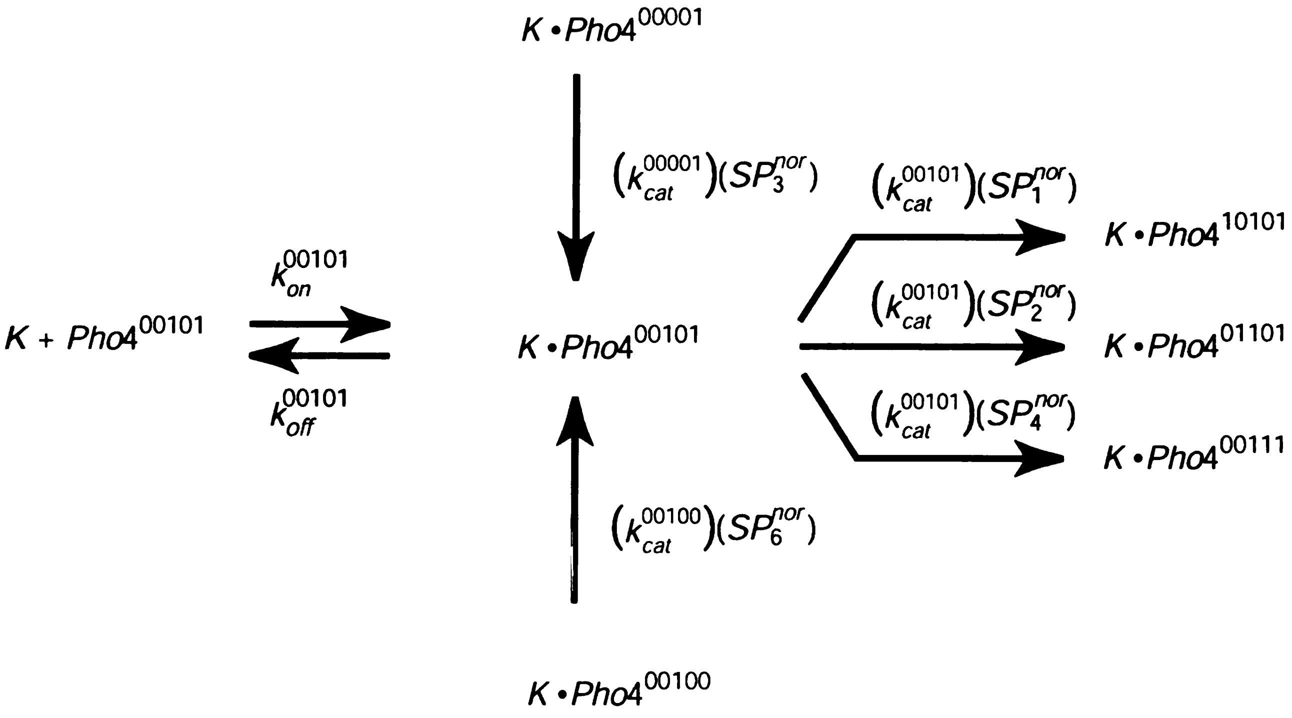
K • Pho4^00001
(k_cat^00001)(SP_3^nor)
k_on^00101
K + Pho4^00101
k_off^00101
K • Pho4^00101
(k_cat^00101)(SP_1^nor)
K • Pho4^10101
(k_cat^00101)(SP_2^nor)
K • Pho4^01101
(k_cat^00101)(SP_4^nor)
K • Pho4^00111
(k_cat^00100)(SP_6^nor)
K • Pho4^00100

Figure 4a

k_{on}^{x}, k_{off}^{x} = Association and dissociation rate constants for the interaction between species x and Pho80 - Pho85

k_{cat}^{x} = Rate constant for phosphorylation of species x on a single site when it is stably bound to Pho80 - Pho85

SP_x = Probability of phosphorylating site x

SP_x^{nor} = Normalized probability of phosphorylating site x

$k_{cat-Tot}^{00101}$ = $\left(SP_1^{nor} + SP_2^{nor} + SP_4^{nor}\right)\left(k_{cat}^{00101}\right)$

Figure 4b

$$
\begin{aligned}
\frac{d[K \bullet Pho4^{00101}]}{dt} &= \left(k_{on}^{00101}[K][Pho4^{00101}]\right) - \left(k_{off}^{00101}[K \bullet Pho4^{00101}]\right) \\
&+ \left(\left(SP_3^{nor}\right)\left(k_{cat}^{00001}\right)[K \bullet Pho4^{00001}]\right) + \left(\left(SP_6^{nor}\right)\left(k_{cat}^{00100}\right)[K \bullet Pho4^{00100}]\right) \\
&- \left(\left(SP_1^{nor}\right)\left(k_{cat}^{00101}\right)[K \bullet Pho4^{00101}]\right) - \left(\left(SP_2^{nor}\right)\left(k_{cat}^{00101}\right)[K \bullet Pho4^{00101}]\right) \\
&- \left(\left(SP_4^{nor}\right)\left(k_{cat}^{00101}\right)[K \bullet Pho4^{00101}]\right)
\end{aligned}
$$

Figure 4c

Synergistic Model $$k_{any}^{00101} = \left(k_{any}^{00000}\right)\left(\frac{k_{any}^{00100}}{k_{any}^{00000}}\right)\left(\frac{k_{any}^{00001}}{k_{any}^{00000}}\right)$$

Additive Model $$k_{any}^{00101} = \left(k_{any}^{00000}\right) + \left(k_{any}^{00100} - k_{any}^{00000}\right) + \left(k_{any}^{00001} - k_{any}^{00000}\right)$$

Decreasing k_{cat} Model $$SP_x^{nor} = \frac{SP_x}{SP_1 + SP_2 + SP_3 + SP_4 + SP_6}$$

Constant k_{cat} Model $$SP_x^{nor} = \frac{1}{\text{\# of unphosphorylated sites remaining}}$$

Figure 4d

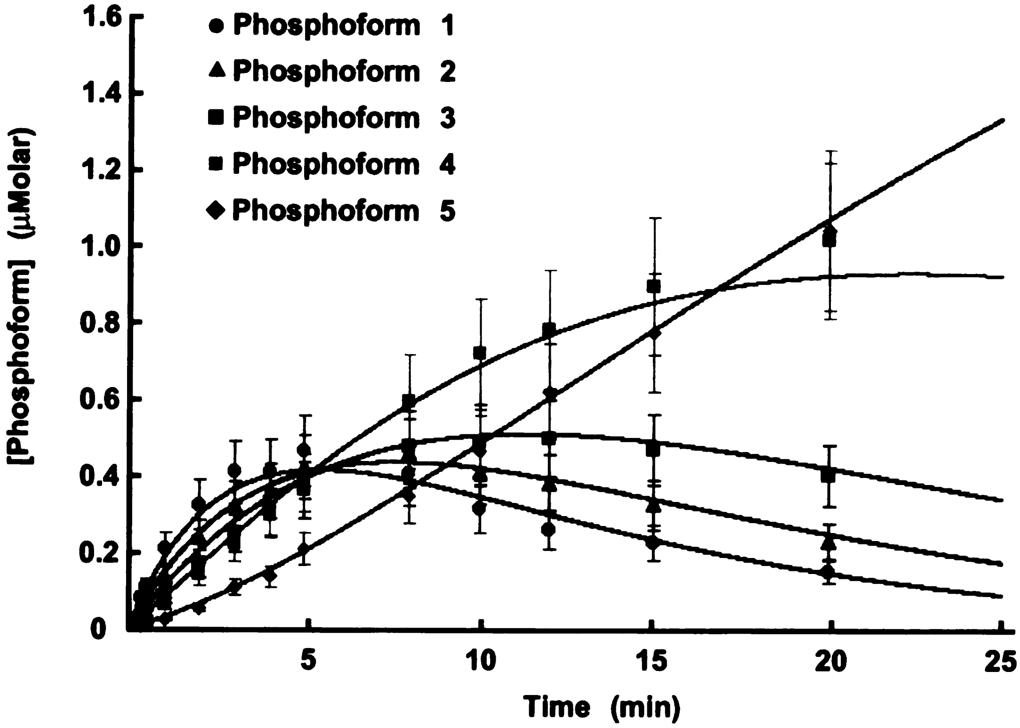

1.6
1.4
1.2
1.0
0.8
0.6
0.4
0.2
0
[Phosphoform] (μMolar)
● Phosphoform 1
▲ Phosphoform 2
■ Phosphoform 3
■ Phosphoform 4
◆ Phosphoform 5
5
10
15
20
25
Time (min)

Figure 5a

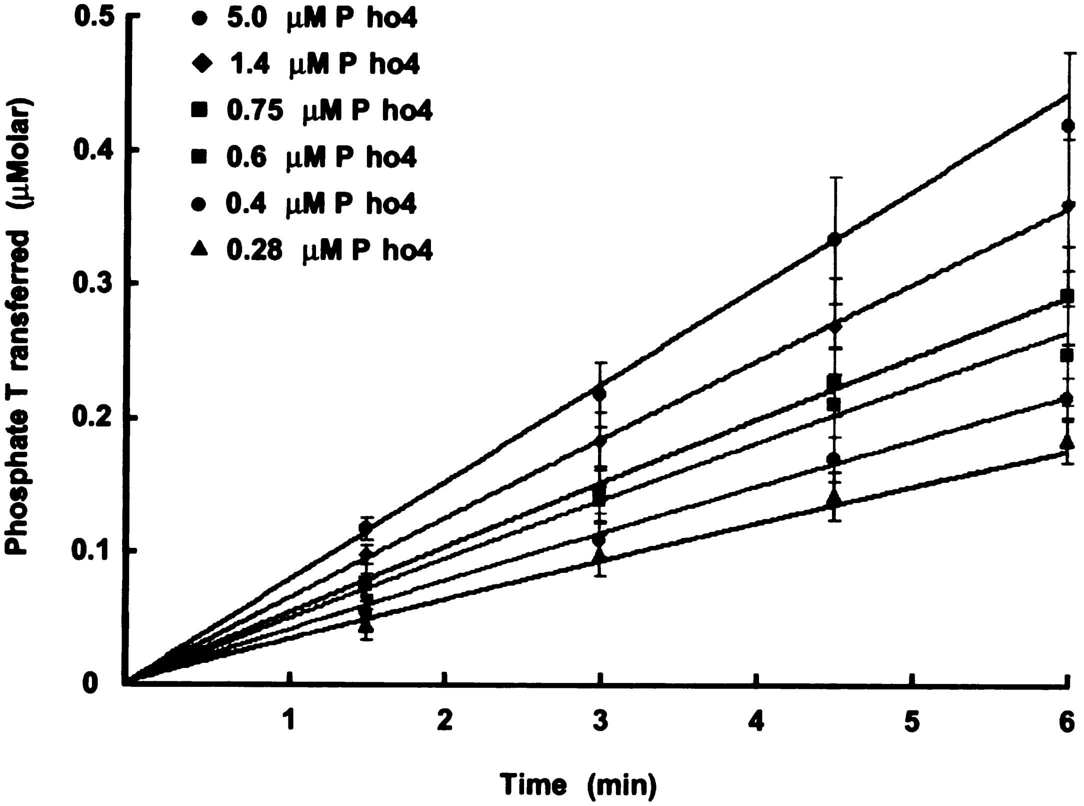

0.5
0.4
0.3
0.2
0.1
0
● 5.0 μM P ho4
◆ 1.4 μM P ho4
■ 0.75 μM P ho4
■ 0.6 μM P ho4
● 0.4 μM P ho4
▲ 0.28 μM P ho4
Phosphate T ransferred (μMolar)
1
2
3
4
5
6
Time (min)

Figure 5b

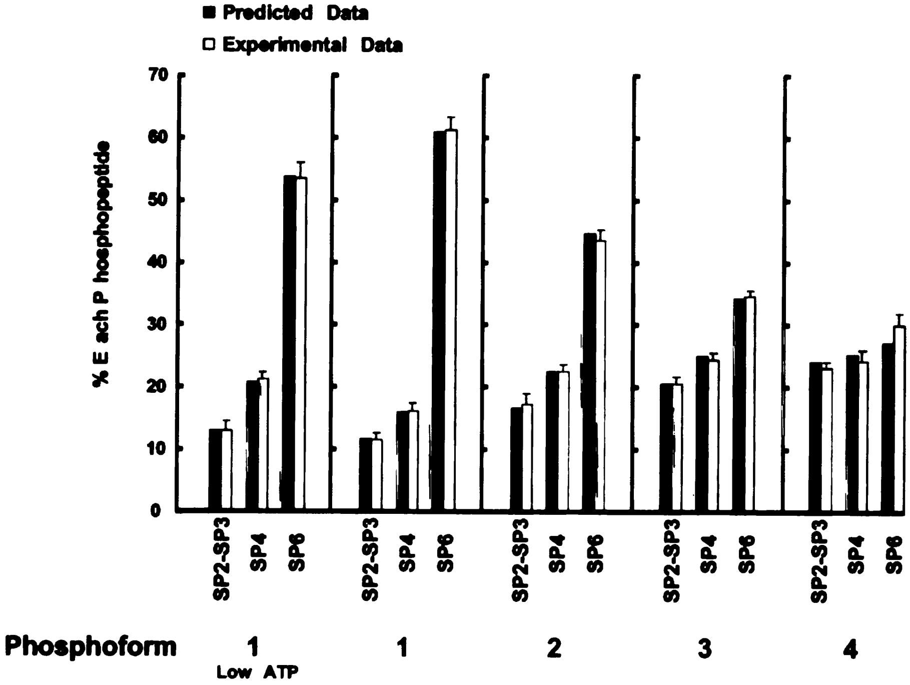
■ Predicted Data
□ Experimental Data
70
60
50
40
30
20
10
0
% E ach P hosphopeptide
SP2-SP3
SP4
SP6
SP2-SP3
SP4
SP6
SP2-SP3
SP4
SP6
SP2-SP3
SP4
SP6
SP2-SP3
SP4
SP6
Phosphoform
1
Low ATP
1
2
3
4

Figure 5c

Table 1 Statistical Analysis of Computer Modeling[1]

Model	Fit of phosphoform and site preference data[2]	Prediction of apparent k_{cat}/K_M data	Prediction of site preference data[3]
Additive k_{all} + Constant k_{cat}	>99	2	<1
Synergistic k_{all} + Constant k_{cat}	<1	<1	<1
Additive k_{all} + Decreasing k_{cat}	>99	2	2
Synergistic k_{all} + Decreasing k_{cat}	>99	>99	>99
Synergistic k_{off} + Decreasing k_{cat}	>99	>99	90
Synergistic k_{cat} + Decreasing k_{cat}	>99	>99	40
Synergistic k_{on} + Decreasing k_{cat}	2	< 1	2

Table 2 Kinetic Constants for the Kinase Reaction[1]

	k_{on} (M^{-1} s^{-1})	k_{off} (s^{-1})	$k_{cat\text{-}Tot}$ (s^{-1})[2]	K_D (nM)[3]
Unphosphorlylated	1.7 - 2.2 x 10^7	10.1 - 13.3	24.7 - 26.5	460 - 780
Phosphoform 1	1.7 - 2.2 x 10^7	9.5 - 12.2	15.6 - 17.2	430 - 720
Phosphoform 2	1.7 - 2.2 x 10^7	8.2 - 10.7	9.6 - 10.7	370 - 630
Phosphoform 3	1.7 - 2.2 x 10^7	7.1 - 9.6	5.1 - 5.8	320 - 560
Phosphoform 4	1.7 - 2.2 x 10^7	5.9 - 7.5	1.8 - 2.1	270 - 440
Phosphoform 5	1.7 - 2.2 x 10^7	6.1 - 8.7	0	280 - 510

Chapter 2

Partially Phosphorylated Pho4 Activates Transcription of a Subset of Phosphate-Responsive Genes

Credits

Michael Springer was responsible for the work involved in figures 2, 4a, 5, and 6.

Dennis Wykoff was responsible for the work involved in figures 3, and 4b.

Nicole Rank was responsible for the work involved in figure 1.

Background: A cell's ability to generate different responses to different levels of a stimulus is an important component of an adaptive environmental response. Transcriptional responses are frequently controlled by transcription factors regulated by phosphorylation.

Methodology/Principal Findings: We demonstrate that differential phosphorylation of the budding yeast transcription factor Pho4 contributes to differential gene expression. When yeast cells are grown in high phosphate growth medium, Pho4 is phosphorylated on four critical residues by the cyclin-CDK complex Pho80-Pho85 and is inactivated. When yeast cells are starved for phosphate, Pho4 is dephosphorylated and fully active. In intermediate phosphate conditions, a form of Pho4 preferentially phosphorylated on one of the four sites accumulates and activates transcription of a subset of phosphate-responsive genes. This Pho4 phosphoform binds differentially to phosphate-responsive promoters and helps to trigger differential gene expression.

Conclusions/Significance: Our results demonstrate that three transcriptional outputs can be generated by a pathway whose regulation is controlled by one kinase, Pho80-Pho85, and one transcription factor, Pho4. Differential phosphorylation of Pho4 by Pho80-Pho85 produces phosphorylated forms of Pho4 which differ in their ability to activate transcription, contributing to multiple outputs.

en

of

pro

ph

loc

per

als

sw

pro

nu

inc

ro

ec

to

Ap

99

va

ma

99

as

ha

UIC
Franc
BRAR

A cell's survival depends on its ability to respond appropriately to its extracellular environment. An appropriate response often depends not only on the presence or absence of a signal, but also on its magnitude and duration. Many signaling pathways utilize protein kinases, which commonly regulate downstream transcription factors through phosphorylation. Phosphorylation can affect the activity, stability, or subcellular localization of transcription factors (Cohen 2000). Multisite phosphorylation of a protein permits not only the binary combination of the effects of each phosphorylation event, but also the emergence of more complex properties such as signal integration (Cohen 2000), switch-like behavior (Ferrell and Machleder 1998; Nash et al. 2001), and kinetic proofreading (McKeithan 1995). Although many proteins are phosphorylated on multiple sites, the biological significance of such phosphorylation is in most cases unclear.

When starved for inorganic phosphate, *Saccharomyces cerevisiae* induces a program of gene expression that includes a phosphate permease, Pho84 (NP_013583); a secreted acid phosphatase, Pho5 (NP_009651); and proteins involved in phosphate storage (Ogawa et al. 2000; Oshima 1982). Induction of the phosphate-responsive gene expression program is controlled by the transcription factor Pho4 (NP_116692) (Oshima 1997). Activity and localization of Pho4 are regulated in response to phosphate availability through phosphorylation by the nuclear cyclin-CDK (cyclin-dependent kinase) complex, Pho80-Pho85 (NP_014642 and NP_015294) (Komeili and O'Shea 1999; O'Neill et al. 1996). Pho4 is unphosphorylated, nuclear-localized and active when yeast cells are starved for phosphate, but is phosphorylated, cytoplasmic and inactive when cells are grown in phosphate-rich medium (Kaffman et al. 1994; O'Neill et al.

1996). Pho4 is phosphorylated by Pho80-Pho85 on four functionally important serine residues (O'Neill et al. 1996) (Fig 1A). Together, phosphorylation of sites 2 and 3 results in export of Pho4 from the nucleus by promoting its interaction with the export receptor Msn5 (NP_010622) (Kaffman et al. 1998a). Phosphorylation of site 4 inhibits nuclear import of Pho4 by impairing its binding to the import receptor Pse1 (NP_014039) (Kaffman et al. 1998b). Phosphorylation of Pho4 also regulates its transcriptional activity within the nucleus; phosphorylation of site 6 inhibits the binding of Pho4 to Pho2 (NP_010177), a transcription factor essential for the induction of many phosphate-responsive genes (Komeili and O'Shea 1999).

The kinetics by which Pho80-Pho85 phosphorylates Pho4 could lead to the accumulation of different Pho4 phosphoforms *in vivo*. *In vitro*, on average only two of the four functionally relevant phosphorylatable serine residues are phosphorylated on a single molecule of Pho4 during one binding interaction between Pho80-Pho85 and an unphosphorylated Pho4 dimer (Jeffery et al. 2001). Additionally, *in vitro* Pho80-Pho85 shows dramatic site preference; site 6 on Pho4 is phosphorylated ~50% of the time during any single phosphorylation event (Jeffery et al. 2001). Together, this leads to phosphorylation of site 6 before phosphorylation of both sites 2 and 3 ~90% of the time (Jeffery et al. 2001). These *in vitro* characteristics of Pho4 phosphorylation by Pho80-Pho85 suggest a partially phosphorylated form of Pho4 predominately phosphorylated on site 6 may accumulate *in vivo* when Pho80-Pho85 is partially active.

We wished to determine if partially phosphorylated forms of Pho4 accumulated under physiological conditions and whether such forms of Pho4 have activity that is different from Pho4 that is either completely phosphorylated or unphosphorylated. We

demonstrated a mutant form of Pho4 that is partially phosphorylated efficiently activates transcription of a subset of phosphate-responsive genes. We also uncovered a physiological growth condition where only a subset of the phosphate-responsive genes are induced significantly. The differential gene expression observed under this growth condition correlates with the appearance of a partially phosphorylated form of Pho4 that is phosphorylated predominately on site 6.

Results

Regulation of either the activity or nuclear localization of Pho4 is sufficient to prevent induction of *PHO5*, but not *PHO84*, in high phosphate medium. Motivated by our *in vitro* observations that Pho80-Pho85 preferentially phosphorylates Pho4 on site 6, we wished to systematically explore the transcriptional properties of Pho4 phosphorylated only on site 6. Our previous studies had demonstrated that this form of Pho4 was localized to the nucleus but could not efficiently activate transcription of *PHO5* (Komeili and O'Shea 1999). We wished to determine if Pho4 phosphorylated only on site 6 could activate transcription of any phosphate-responsive genes.

To address this question we made use of a mutant form of Pho4 which can only be phosphorylated on site 6 - this mutant contains serine to alanine substitutions at phosphorylation sites 1, 2, 3, and 4 (referred to as SA1234). Pho4^{SA1234WT6} is localized to the nucleus and phosphorylated on site 6 in high phosphate conditions, but it cannot efficiently activate transcription of *PHO5* (Komeili and O'Shea 1999). We compared the transcriptional properties of Pho4^{SA1234WT6} to those of a second mutant form of Pho4 which is refractory to phosphorylation because it has serine to alanine substitutions at sites 1,2, 3, and 4 of Pho4 and a proline to alanine substitution at site 6 (referred to as SA1234PA6 – it is necessary to mutate the proline because the serine at site 6 is required for the full induction of phosphate-responsive genes) (Komeili and O'Shea 1999). Pho4^{SA1234PA6} is localized to the nucleus and unphosphorylated on site 6 in high phosphate conditions and efficiently activates transcription of *PHO5* (Komeili and O'Shea 1999). Strains expressed both Pho4^{SA1234PA6} and Pho4^{SA1234WT6} at levels which were indistinguishable from wild-type Pho4 expression as determined by FACS and fluorescence microscopy (see supplementary microscopy section).

Yeast strains expressing Pho4^{SA1234PA6} and Pho4^{SA1234WT6} were analyzed by whole genome expression profiling using cDNA microarrays. The gene expression profile of the *PHO4*^{SA1234PA6} strain grown in high phosphate medium was very similar to the profile observed for a wild-type strain grown in no phosphate medium where Pho4 is completely unphosphorylated - all phosphate-responsive genes, including *PHO5*, are induced (Fig. 1C) (Ogawa et al. 2000). In contrast, the *PHO4*^{SA1234WT6} strain grown in high phosphate medium expressed only a subset of genes normally induced in no phosphate medium (Fig. 1C). The twenty phosphate-responsive genes examined largely fell into two classes when we compared the percent induction of each phosphate-responsive gene in the *PHO4*^{SA1234WT6} strain to its maximal induction in the *PHO4*^{SA1234PA6} strain. Four genes were induced less than 11%, whereas fifteen genes were induced more than 40% (Fig. 1C). The class induced less than 11% was comprised mainly of phosphate-responsive phosphatases whereas the class induced more than 40% consisted mainly of genes involved in phosphate storage, mobilization, and transport. From the first category, we chose to analyze *PHO5* (encoding a secreted acid phosphatase) further because it was both highly induced in no phosphate medium and well characterized. From the second category, we chose to analyze *PHO84* (encoding a high affinity phosphate transporter) because it was induced over 100-fold in both the $PHO4^{SA1234WT6}$ and $PHO4^{SA1234PA6}$ strains.

Physiological conditions that cause differential phosphorylation of Pho4. Our observations with the Pho4 mutants led us to ask if there exist physiologically relevant conditions where partially phosphorylated Pho4 accumulates in the nucleus and causes differential gene expression. We predicted that as the extracellular phosphate concentration drops, Pho80-Pho85 would become partially inactivated, and because of the kinetic properties of Pho80-Pho85, a nuclear pool of Pho4 phosphorylated on site 6 (but not on sites 2 and 3) would accumulate. We anticipated that only at much lower concentrations of phosphate would a nuclear pool of completely unphosphorylated Pho4 build up and activate transcription of all phosphate-responsive genes.

To test these predictions, we grew cells in medium containing different levels of phosphate (0, 50, 100, 300, 10000 μM) and monitored localization of a Pho4-GFP (green fluorescent protein) fusion protein and transcription of *PHO5* and *PHO84*. We observed three different responses to different phosphate conditions. First, the high phosphate response occurs at extracellular phosphate concentrations greater than 300 μM phosphate. Pho4 is cytoplasmic and *PHO5* and *PHO84* are expressed at only basal levels under these conditions (Fig. 2A and Fig. 2B). Second, the no phosphate response occurs when there is no phosphate in the medium. Pho4 is nuclear and *PHO5* and *PHO84* are expressed maximally under these conditions (Fig. 2A and Fig. 2B). Third, the intermediate phosphate response occurs at extracellular phosphate concentrations less than 100 μM phosphate and greater than no phosphate. Pho4 is nuclear and but there is only ~10% of maximal expression of *PHO5* while there is ~50% of maximal expression of *PHO84* under these conditions (Fig. 2A and Fig. 2B).

To further characterize the properties of the intermediate phosphate response we examined the time and concentration dependence of *PHO5* and *PHO84* expression. Differential gene induction was observed in medium containing less than ~150 µM phosphate and more than 1 µM phosphate medium (data not shown). To confirm that the differential transcriptional response of *PHO5* and *PHO84* observed in intermediate phosphate medium is not a kinetic artifact, we monitored the amount of *PHO5* and *PHO84* mRNA over several hours (Fig. 2C). The expression pattern of *PHO5* and *PHO84* was stable over a range of both time and external phosphate concentration indicating that the intermediate phosphate response is robust. After four to six hours, cells adapted to intermediate phosphate medium and Pho4 was relocalized to the cytoplasm (data not shown).

Whole genome expression profiling of cells grown in intermediate phosphate was used to assess the number of phosphate-responsive genes that behave like *PHO5* or *PHO84*. Genes fell into two classes when we compared the induction of each phosphate-responsive gene in intermediate phosphate to its induction in no phosphate medium (Fig. 2D). The two classes were similar to the two classes observed when we compared the strain expressing Pho4$^{\mathrm{SA1234WT6}}$ to the strain expressing Pho4$^{\mathrm{SA1234PA6}}$ (Fig. 2D). This was anticipated because both a wild-type strain grown in intermediate phosphate and a *PHO4*^{SA1234WT6} strain grown in high phosphate have nuclear Pho4 which is predominately phosphorylated on site 6.

To determine if Pho4 is preferentially phosphorylated on site 6 in intermediate phosphate medium, we generated phosphopeptide-specific antibodies that recognize phosphorylation on sites 2, 3, and 6 of Pho4. Cells were grown for two hours in no, intermediate, and high phosphate medium and analyzed by Western blotting, indicating that there is more unphosphorylated Pho4 present in intermediate phosphate conditions than in high phosphate conditions (Fig. 2E). In high phosphate medium, when Pho80-Pho85 kinase activity is high, sites 2, 3, and 6 were phosphorylated. In no phosphate medium, when Pho80-Pho85 kinase activity is low, there was no detectable phosphorylation on sites 2, 3, and 6. In intermediate phosphate medium, as predicted by *in vitro* Pho80-Pho85 kinetics, site 6 was phosphorylated but there was only minimal phosphorylation on sites 2 and 3. Thus, differential phosphorylation of Pho4 occurs in physiologically relevant conditions *in vivo* and site 6 phosphorylation *in vivo* correlates with differential gene expression.

Site 6 phosphorylation is lower in intermediate phosphate medium than high phosphate medium (Fig. 2E). Differential expression of *PHO5* and *PHO84* could be the result of differential sensitivity of these two promoters to the amount of unphosphorylated Pho4 in the nucleus. To assess this possibility we created a Pho4 mutant that behaves as if it is phosphorylated on site 6 constitutively. This was achieved by substitution of the serine at site 6 with aspartate, which hinders its interaction with Pho2 (Komeili and O'Shea 1999). Gene expression in a yeast strain expressing Pho4^{WT1234SD6} was monitored by Northern blotting (Fig. 2F) and microarray analysis (data not shown). Even when grown in no phosphate medium, the strain expressing Pho4^{WT1234SD6} exhibited differential expression of *PHO5* and *PHO84*. Therefore,

differential expression of *PHO5* and *PHO84* in intermediate phosphate conditions is not likely to be due to a subset of Pho4 molecules that are unphosphorylated in the nucleus.

Differential promoter binding of Pho4. To determine if differential gene expression results from differential occupancy of Pho4 at *PHO5* and *PHO84*, we examined the binding of Pho4 to these promoters using chromatin immunoprecipitation. There was little enrichment of Pho4 at the *PHO5* or *PHO84* promoters when cells were grown in high phosphate medium, whereas in no phosphate medium, Pho4 was significantly enriched at both the *PHO5* and *PHO84* promoters (Fig. 3 left). When cells were grown in intermediate phosphate medium, Pho4 was enriched at the *PHO84* promoter, but was not significantly enriched at the *PHO5* promoter. Furthermore, chromatin immunoprecipitation experiments carried out with *PHO4*^{SA1234WT6} and *PHO4*^{SA1234PA6} strains grown in high phosphate medium resembled immunoprecipitations carried out with wild-type cells grown in intermediate and no phosphate medium, respectively (Fig. 3, right). Thus, differential expression of *PHO5* and *PHO84* correlates with differential Pho4 binding to these promoters.

Because site 6 phosphorylation inhibits the Pho4-Pho2 interaction *in vitro* (Komeili and O'Shea 1999), the preferential induction of genes in intermediate phosphate medium could be explained if their transcription does not require Pho2. To determine if the expression of *PHO84* is dependent on Pho2, we deleted *PHO2* in a Pho4 wild-type strain and in strains expressing Pho4^{SA1234WT6} and Pho4^{SA1234PA6}. Northern blotting (Fig. 4A and data not shown) and microarray analysis (data not shown) of these *pho2*Δ strains demonstrated that both *PHO5* and *PHO84* (and the majority of the phosphate-responsive genes) required Pho2 for induction. To determine if the transcriptional defect in *pho2*Δ strains was due to a defect in binding of Pho4, we examined Pho4 occupancy at the *PHO5* and *PHO84* promoters in *pho2*Δ strains by chromatin immunoprecipitation. Surprisingly, in a *pho2*Δ strain little Pho4 was bound to the *PHO5* or *PHO84* promoter in either wild-type or mutant Pho4 strain backgrounds (Fig. 4B) (Barbaric et al. 1996). Therefore, Pho2 must directly or indirectly facilitate Pho4 binding to the *PHO84* promoter even when Pho4 is phosphorylated on site 6.

Physiological role of site 6 phosphorylation. Site 6 phosphorylation correlates with differential gene expression in wild-type cells and is sufficient to cause differential gene expression in strains expressing Pho4 mutants, but this does not mean site 6 phosphorylation is necessary for differential gene induction. If site 6 phosphorylation is the sole mechanism to inhibit *PHO5* expression in intermediate phosphate conditions, a strain grown in intermediate phosphate medium (where Pho4 is nuclear) expressing a mutant Pho4 that cannot be phosphorylated on site 6 should significantly induce *PHO5*. We therefore created a strain expressing a Pho4 mutant, $\text{Pho4}^{\text{WT1234PA6}}$, which cannot be phosphorylated on site 6 but is able to bind Pho2. Fluorescence microscopy was used to confirm proper localization of this mutant (data not shown). In contrast to expectations, the mutant that prevents site 6 phosphorylation did not strongly influence the expression of *PHO5* or *PHO84* in intermediate phosphate medium (Fig. 5A). This suggests that a second mechanism that contributes to differential expression of *PHO5* and *PHO84* expression exists in intermediate phosphate conditions. Because a Pho4 mutant that is refractory to phosphorylation, $PHO4^{SA1234PA6}$ (Fig. 1C), induces all phosphate responsive genes, we conclude that this second mechanism is likely to work through Pho4 and Pho80-Pho85.

Although site 6 phosphorylation is not necessary to inhibit *PHO5* expression, it is necessary to keep cells from inducing transcription of *PHO84* in high phosphate medium. A strain expressing Pho4$^{\text{WT1234PA6}}$ grown in high phosphate medium had levels of *PHO5* and *PHO84* expression that were similar to those of a wild-type strain grown in intermediate phosphate medium (Fig. 5A). Site 6 phosphorylation was necessary to inhibit binding of Pho4 to the *PHO84* promoter in high phosphate medium but was not required to inhibit binding of Pho4 to the *PHO5* promoter in intermediate phosphate medium (Fig. 5B).

It is possible that phosphorylation on site 1 or 4 could be contributing to differential expression of *PHO5* and *PHO84*. To assess this possibility we made a plasmid-expressed version of Pho4, Pho4$^{\text{SA14PA6}}$, which can only be phosphorylated on sites 2 and 3. We used fluorescence microscopy to confirm that in intermediate phosphate this mutant is localized to the nucleus (Fig. 5A) (see supplementary microscopy section). Because this mutant is localized to the cytoplasm in high phosphate conditions, we infer that this mutant can be phosphorylated on sites 2 and 3 (Fig. 5A). Pho4$^{\text{SA14PA6}}$ expressing strains grown in intermediate phosphate medium still induce *PHO5* and *PHO84* differentially (Fig. 5B). This suggests that the second mechanism of inhibition at the *PHO5* promoter does not involve phosphorylation of sites 1 or 4. Because a *PHO4*^{SA1234PA6} strain in high phosphate mimics a wild-type strain grown in no phosphate medium (Fig. 2F), it is likely that the second mechanism for differential regulation of *PHO5* and *PHO84* works through sites 2 and 3.

Supplementary Microscopy Section

To assess whether variations in the nuclear concentration of Pho4 in different mutant backgrounds might affect the expression of *PHO5* and *PHO84*, the levels of Pho4-GFP were quantified by fluorescence microscopy. Nuclear Pho4^{SA1234WT6} was present at 242±5 arbitrary units and nuclear Pho4^{SA1234PA6} was present at 242±6 arbitrary units. Strains expressing either of these two mutants had FACS profiles indistinguishable from that of a wild-type *PHO4-GFP* strain.

Pho4^{SA14PA6} expressed from a low copy plasmid had a nuclear concentration of 359±13 arbitrary units when grown in intermediate phosphate medium. Pho4-GFP had a nuclear concentration of 293±7 arbitrary units when grown in no phosphate medium.

All strains that were directly compared by FACS or microscopy were grown on the same day, to the same cell density, in the same batch of medium (with only phosphate levels varied when appropriate).

Discussion

Our results demonstrate that three transcriptional outputs can be generated by a pathway whose regulation is controlled by one kinase, Pho80-Pho85, and one transcription factor, Pho4. Whereas fully phosphorylated Pho4 cannot activate transcription of any of the phosphate-responsive genes and unphosphorylated Pho4 can efficiently activate transcription of all phosphate-responsive genes, partially phosphorylated Pho4 contributes to the activation of some phosphate responsive genes, but not others. When Pho4 is localized to the nucleus and phosphorylated on site 6 it can efficiently bind to the promoter of *PHO84* and activate its transcription, but it does not efficiently bind to or activate *PHO5*. Our *in vitro* studies of Pho4 phosphorylation

suggested that when Pho80-Pho85 was partially active, Pho4 would accumulate in the nucleus phosphorylated on site 6. *In vivo*, Pho4 accumulates in the nucleus phosphorylated on site 6 in growth medium containing a range of intermediate phosphate concentrations – conditions which we anticipate result in partial activity of Pho80-Pho85. Nuclear accumulation of this Pho4 phosphoform correlates with both differential expression of *PHO5* and *PHO84*, as well as differential binding to the *PHO5* and *PHO84* promoters.

Although nuclear Pho4 phosphorylated on site 6 differentially binds to the *PHO84* and *PHO5* promoters and differentially activates transcription, site 6 phosphorylation is not the only mechanism contributing to differential expression of phosphate-responsive genes in intermediate phosphate conditions. When we prevent site 6 phosphorylation, we still observe differential expression of *PHO84* and *PHO5* in intermediate phosphate conditions. We have not yet identified the second mechanism contributing to differential expression but this mechanism works through Pho80-Pho85 dependent phosphorylation of site 2 and 3 of Pho4. It is possible that this additional mechanism functions redundantly with site 6 phosphorylation to cause differential expression of phosphate-responsive genes.

We propose that differences in the regulation of *PHO5* and *PHO84* are caused by affinity differences and kinetic mechanisms. If the *PHO84* promoter has higher affinity for Pho4 than does the *PHO5* promoter, differential occupancy of these promoters in intermediate phosphate conditions may lead to differences in transcription (Fig. 6A). For example, the concentration of Pho4 and its affinity for DNA may be such that in no phosphate conditions Pho4 binding at the *PHO84* promoter is saturated, but binding at

the *PHO5* promoter is not. When Pho4 is phosphorylated on site 6, as in intermediate phosphate conditions, we expect its affinity for DNA is reduced. This reduced affinity would have a more significant impact on the *PHO5* promoter than on the *PHO84* promoter because the *PHO5* promoter was not saturated for binding. This differential occupancy could account for differences in transcription of these genes in intermediate phosphate conditions.

It is also possible that differences in the kinetic mechanisms leading to transcription of these two genes contribute to differential expression (Fig. 6B). For example, if Pho4 can be phosphorylated while bound to DNA and this phosphorylation can compete with formation of an active transcription complex, the amount of transcription of a gene will be determined by the ratio of the rate of phosphorylation of Pho4 to the rate of formation of an active transcription complex. If formation of an active transcription complex is slower for *PHO5* than for *PHO84*, in intermediate phosphate conditions phosphorylation of Pho4 may compete with formation of an active transcription complex at the *PHO5* gene but not at *PHO84*. This model is plausible given what is known about the *PHO5* promoter - the promoter is regulated by positioned nucleosomes that need to be "remodeled" in order for the gene to be transcribed (Almer et al. 1986). Chromatin remodeling may represent a slow step in the pathway to transcription that could compete with Pho4 inactivation by phosphorylation on DNA. This mechanism is conceptually similar to kinetic proofreading mechanisms proposed for DNA replication and translation (Hopfield 1974).

Differential gene induction should allow a more finely tuned response to changes in external phosphate concentrations. In high phosphate conditions, cells can uptake

ample phosphate from their environment without inducing any phosphate-dependent genes, so the pathway is not induced. In no phosphate conditions, regardless of the amount of phosphate transporter at the plasma membrane, it is essential to also scavenge phosphate from the environment. Extracellular phosphatases can liberate inorganic phosphate which the phosphate transporter can uptake with high affinity. In no phosphate conditions it is therefore necessary to induce all the phosphate-responsive genes. In intermediate phosphate conditions, the concentration of phosphate is near the K_m of the Pho84 permease (Bun-Ya et al. 1991; Wykoff and O'Shea 2001). Therefore, it is likely the amount of phosphate that a cell can take up is proportional to the level of permease at the plasma membrane. Induction of *PHO84* transcription could help to maintain levels of intracellular phosphate as external levels drop. It is not necessary to secrete extracellular phosphatases at high levels because there is ample inorganic phosphate in the growth medium. An intermediate phosphate response may thereby allow cells to take up appropriate amounts of phosphate over a wide extracellular concentration range at a minimal energetic cost. Induction of genes involved in phosphate storage and mobilization may also help to buffer the cells from rapid changes in extracellular phosphate and allow the cells time to adjust the level of phosphate permeases at the plasma membrane.

Even though the phosphate regulon involves a single kinase and a single regulated transcription factor, yeast cells can generate multiple programs of gene expression in response to different phosphate levels. Many transcription factors contain multiple phosphorylation sites, and may also use differential phosphorylation to respond to different levels of extracellular stimuli with different programs of gene expression.

Differential phosphorylation of transcriptional regulators may help generate complex programs of gene expression with only a small set of proteins.

Materials and Methods

Strains and Media. The following pRS306 based plasmids were used in this paper: *PHO4*^{WT1234PA6}*-GFP* (EB1377), *PHO4*^{SA1234WT6}*-GFP* (EB1264),and *PHO4*^{SA1234PA6}*-GFP* (EB1265). These plasmids were integrated into the *PHO4* locus to create EY1471, EY1022, and EY1023 respectively. EY1022 and EY1023 were also crossed to an isogenic *pho2*Δ (EY0337) to make EY0778 and EY0779. The following pRS316 based plasmids were used in this paper *PHO4*^{SA14PA6}*-GFP* (EB1487), *PHO4*^{WT1234SD6}*-GFP* (EB842),and *PHO4*^{WT1234PA6}*-GFP* (EB0843). These plasmids were transformed into a *pho4Δ* strain (EY0130). *PHO4-GFP* EY0693 was used as the wild-type strain. The concentration of phosphate in the growth medium was controlled by adding phosphate in the form of KH_2PO_4 to synthetic medium with dextrose (SD) but lacking phosphate (Huang et al. 2001).

cDNA microarrays. *PHO4*^{SA1234WT6}, *PHO4*^{SA1234PA6}, and wild-type (K699) strains were grown in high phosphate medium (SD with 10 mM phosphate), intermediate phosphate medium (SD with 100μM phosphate), or no phosphate medium (SD with no phosphate) and were harvested in mid-logarithmic growth. Microarray analysis was performed as described (Carroll et al. 2001). Monofunctional reactive Cy5 (Amersham) was used to label reverse-transcribed RNA from the mutant cells and monofunctional reactive Cy3 was used to label reverse-transcribed RNA from the wild-type cells.

Microarray Analysis. Phosphate-responsive genes were analyzed as described previously (Carroll et al. 2001). The percent of maximal induction for each transcript was determined from at least two independent microarray data sets. All error bars are standard error. Genes that were reported met the following criteria: (i) induction was at least 2-fold in an experiment; and (ii) there was less than a two-fold difference between the values calculated from two independent microarray experiments. Microarrays can be accessed at GEO on NCBI as platform number GPL423-425 and sample numbers GSM9157-9162.

Fluorescence Microscopy. Images were captured with a TE300 inverted Nikon microscope using Metamorph software (Universal Imaging) and a Roper Q57 CCD camera. Cells were washed quickly in no phosphate medium and then grown for two hours in media of different phosphate concentrations before visualization.

Northern Analysis. RNA was extracted by standard phenol-chloroform techniques (Steger et al. 2003). Probes to *PHO84*, *PHO5*, and *ACT1* (NP_116614) (the gene encoding actin) were made by random priming from a PCR product of each full length gene. *PHO84* and *PHO5* signal was normalized to signal from *ACT1*. All experiments were performed at least in triplicate. The reported error is the standard error of the mean. Several phosphate responsive genes (*PHO5*, *PHO8* (NP_010769), *PHO11* (NP_009434), and *PHO12* (NP_012087)) share large regions of homology. Cross-hybridization leads to similar response profiles even though the genes probably respond differently.

Quantitation of extracellular phosphate. Phosphate in the medium was measured with an acidified ammonium molybdate/malachite green G solution (Sigma). No more than 50% of the phosphate was depleted in any experiment.

Phosphopeptide generation. Rabbit polyclonal phosphopeptide antibodies were generated (Bethyl Labs) that recognize the following phosphorylated peptides derived from the Pho4 sequence (phosphorylated residues are denoted by square brackets): (1) the peptide containing site 2 is CPRLLY[S]PLIHT; (2) site 3 is VPVTI[S]PNLVACG; and (3) site 6 is VVASE[S]PVIAPCG (Bethyl Labs). Antibodies were affinity-purified using the synthetic phosphopeptides. In all cases, there was minimal cross-reactivity with the unphosphorylated peptide.

Western Analysis. Western blotting was performed with standard techniques using enhanced chemiluminescence (Pierce) for detection.

Quantitation of Pho4 Levels. The level of expression of different versions of Pho4 was quantitated by FACS (Fluorescence Activated Cell Sorting) (Becton Dickinson LSR II). The percent nuclear fluorescence of Pho4 grown in different phosphate conditions was determined by quantitating fluorescent pictures of over a hundred cells grown in each phosphate condition.

Chromatin Immunoprecipitation. The chromatin immunoprecipitation protocol was similar to that previously described (Strahl-Bolsinger et al. 1997). After two hours of growth, cells were fixed with 1% formaldehyde for 15 minutes at room temperature and harvested. To obtain DNA the cell pellet was processed, immunoprecipitated with a polyclonal anti-Pho4 antibody, and co-purifying DNA was purified by phenol-chloroform and chloroform extraction. The DNA was then quantified using an Opticon real-time PCR machine (MJ Research) as described previously (Steger et al. 2003). At least three independent extracts were analyzed for each strain and growth condition.

Acknowledgements

We thank Hiten Madhani, Barbara Panning, Dave Wang, Andrew Uhl, Adam Carroll, Charles Holst and the O'Shea laboratory members for careful reading of the manuscript and David Steger for advice with the chromatin immunoprecipitation. This work was supported by the NIH (GM51377) and the Howard Hughes Medical Institute (E. K. O.). M. S. was supported by the NSF and a fellowship from the Burroughs Wellcome Fund and D. D. W. and N. M. were supported by postdoctoral fellowships from the NIH (GM20762 and GM19734, respectively).

Fig. 1. Whole genome expression DNA microarrays of *PHO4*^{SA1234WT6} and *PHO4*^{SA1234PA6} strains. (**A**) Schematic showing phosphorylation sites (O'Neill et al. 1996), transcriptional activation domain (McAndrew et al. 1998), nuclear localization sequence (NLS) (Kaffman et al. 1998b), Pho2 binding domain (Hirst et al. 1994), and DNA binding domain of Pho4 (Ogawa and Oshima 1990). Pho4 is phosphorylated on five sites (referred to as sites 1, 2, 3, 4, and 6) by Pho80-Pho85 (O'Neill et al. 1996). Site 1 is phosphorylated inefficiently *in vivo* and *in vitro* and no functional consequence has been attributed to its phosphorylation (Komeili and O'Shea 1999; O'Neill et al. 1996). (**B**) Color scheme denoting the fold induction/repression for all of the microarray experiments. (**C**) Expression of phosphate-responsive genes in strains containing Pho4^{SA1234WT6} and Pho4^{SA1234PA6} grown in high phosphate medium. Cy5-labeled samples are colored red and Cy3-labeled samples are colored green. The percent of induction of each gene in the Pho4^{SA1234WT6} strain compared to its maximal induction in the Pho4^{SA1234PA6} strain is presented on the right. Several phosphate responsive genes (*PHO5*, *PHO8*, *PHO11*, and *PHO12*) share large regions of homology. Cross-hybridization leads to similar response profiles even though the genes probably respond differently.

Fig. 2. Growth of yeast cells in intermediate phosphate medium leads to differential phosphorylation of Pho4 and differential expression of *PHO5* and *PHO84*. (**A**) Fluorescence microscopy of yeast cells containing Pho4-GFP grown in no, 50 μM, 100 μM (intermediate or int), 300 μM, or 10000 μM (high) phosphate medium. (**B**) Quantitation of RNA levels by Northern analysis of *PHO84*, *PHO5*, and *ACT1* in wild-

type cells grown in medium containing different concentrations of phosphate. **(C)** Quantitation of RNA levels by Northern analysis of *PHO84*, *PHO5*, and *ACT1*, in wild-type cells grown for 1, 2, or 5 hours in intermediate phosphate medium. **(D)** Expression of genes in the phosphate-responsive cluster (Carroll et al. 2001) for a wild-type strain grown in intermediate or no phosphate medium compared to wild-type cells grown in high phosphate medium. Cy5 and Cy3 samples are colored red and green, respectively. The percent of induction of each gene in intermediate phosphate medium compared to its maximal induction in no phosphate medium is presented on the right. **(E)** Analysis of Pho4 protein and phosphorylation by Western blotting for wild-type cells grown in no, intermediate, and high phosphate medium. Samples were probed with phosphopeptide antibodies specific to sites 2, 3, and 6 of Pho4 and a polyclonal antibody that recognizes Pho4. **(F)** Quantitation of RNA levels by Northern analysis of *PHO84*, *PHO5*, and *ACT1*, in a $PHO4^{WT1234SD6}$ strain.

Fig. 3. Deletion of *PHO2* abrogates expression of *PHO5* and *PHO84* and binding of Pho4 to these promoters. **(A)** Quantitation of RNA levels by Northern analysis in *pho2Δ* strains grown in no, intermediate, or high phosphate medium. **(B)** Chromatin immunoprecipitation analysis of Pho4. Pho4 was immunoprecipitated from extracts of wild-type cells grown in high, intermediate, or no phosphate medium, from a strain lacking Pho4, and from the two mutant Pho4 strains grown in high phosphate medium. Experiments using the $Pho4^{SA1234WT6}$ and $Pho4^{SA1234PA6}$ expressing strains are normalized to the maximal amount of enrichment in a strain expressing $Pho4^{SA1234PA6}$ in high phosphate medium. The fold enrichment of *PHO5* over *ACT1* was 1.03, 0.99, 1.26, 2.84,

2.41, and 5.04 in lanes one through six respectively (*pho4Δ*, wt high, wt int, wt no, *PHO4*^{SA1234WT6}, and *PHO4*^{SA1234PA6}). The fold enrichment of *PHO84* over *ACT1* was 0.99, 1.75, 4.27, 6.28, 10.8, and 11.6 in lanes one through six respectively. (C) Chromatin immunoprecipitation analysis of Pho4. Pho4 was immunoprecipitated from extracts of wild-type cells grown in no phosphate medium, a mutant lacking Pho2 in no phosphate medium, Pho4^{SA1234WT6} and Pho4^{SA1234PA6} strains grown in high phosphate medium, and *pho2Δ* Pho4^{SA1234WT6} and *pho2Δ* Pho4^{SA1234PA6} strains grown in high phosphate medium. The fold enrichment of *PHO5* over *ACT1* was 2.84, 1.19, 2.41, 1.49, 5.04, and 2.06 in lanes one through six respectively (wt no, *pho2Δ* no, *PHO4*^{SA1234WT6}, *pho2Δ PHO4*^{SA1234WT6}, *PHO4*^{SA1234PA6}, and *pho2Δ PHO4*^{SA1234PA6}). The fold enrichment of *PHO84* over *ACT1* was 6.28, 2.0, 10.8, 2.4, 11.6, and 2.63 in lanes one through six respectively.

Fig. 4. A strain expressing Pho4 that cannot be phosphorylated on site 6 does not induce *PHO5* in intermediate phosphate medium. A strain expressing Pho4^{WT1234PA6} grown for two hours in no, intermediate, and high phosphate medium was analysed by (A) Northern and (B) chromatin immunoprecipitation. The fold enrichment of *PHO5* over *ACT1* was 1.71, 2.42, 10.49, 0.99, 1.26, and 2.84 in lanes one through six respectively (*PHO4*^{WT1234WT6} high, *PHO4*^{WT1234WT6} int, *PHO4*^{WT1234WT6} no, wt high, wt int, wt no). The fold enrichment of *PHO84* over *ACT1* was 24.64, 27.44, 43.74, 1.75, 4.27, and 6.28 in lanes one through six respectively.

Fig. 5. A strain expressing Pho4^{SA14PA6} from a low copy plasmid differentially expresses *PHO5* and *PHO84* in intermediate phosphate medium. (A) Fluorescence microscopy of yeast cells containing Pho4 ^{SA14PA6}-GFP grown in no, 100 µM, or 10 mM phosphate medium. (B) Quantitation of RNA levels by Northern analysis of *PHO84*, *PHO5*, and *ACT1* from strains expressing Pho4 ^{SA14PA6} or Pho4^{WT1234PA6} from a low copy plasmid grown in no, 100 µM, or 10000 µM phosphate medium.

Fig. 6. Models for differential gene regulation. (A) Differential affinity of Pho4 for the *PHO84* and *PHO5* promoters can cause differential gene expression. Simulated curves of the percent occupancy of Pho4 at the *PHO84* and *PHO5* promoters, assuming Michaelian binding. Pho4 was modeled as having a K_d of 10 at the *PHO84* promoter and 100 at the *PHO5* promoter. Phosphorylation of Pho4 was simulated as raising the K_d of Pho4 to 40 at the *PHO84* promoter and 400 at the *PHO5* promoter. The nuclear concentration of Pho4 was assumed to be 7.5-fold higher in intermediate phosphate medium than in high phosphate medium and 10-fold higher in no phosphate medium than in high phosphate medium. (B) Kinetic diagram of the steps leading to active transcription at the *PHO84* and *PHO5* promoters. Differences in the kinetic mechanisms of activation of *PHO84* and *PHO5* can lead to differential gene expression. Even if promoter occupancy is high at the *PHO5* promoter, if the transcriptional activation step is slow compared to the rate of Pho4 phosphorylation and inactivation, *PHO5* will not be induced.

ALMER A, RUDOLPH H, HINNEN A,HORZ W (1986) Removal of positioned nucleosomes from the yeast PHO5 promoter upon PHO5 induction releases additional upstream activating DNA elements. *Embo J* 5: 2689-2696.

BARBARIC S, MUNSTERKOTTER M, SVAREN J,HORZ W (1996) The homeodomain protein Pho2 and the basic-helix-loop-helix protein Pho4 bind DNA cooperatively at the yeast PHO5 promoter. *Nucleic Acids Res* 24: 4479-4486.

BUN-YA M, NISHIMURA M, HARASHIMA S,OSHIMA Y (1991) The PHO84 gene of Saccharomyces cerevisiae encodes an inorganic phosphate transporter. *Mol Cell Biol* 11: 3229-3238.

CARROLL AS, BISHOP AC, DERISI JL, SHOKAT KM,O'SHEA EK (2001) Chemical inhibition of the Pho85 cyclin-dependent kinase reveals a role in the environmental stress response. *Proc Natl Acad Sci U S A* 98: 12578-12583.

COHEN P (2000) The regulation of protein function by multisite phosphorylation--a 25 year update. *Trends Biochem Sci* 25: 596-601.

FERRELL JE, JR.,MACHLEDER EM (1998) The biochemical basis of an all-or-none cell fate switch in Xenopus oocytes. *Science* 280: 895-898.

HIRST K, FISHER F, MCANDREW PC,GODING CR (1994) The transcription factor, the Cdk, its cyclin and their regulator: directing the transcriptional response to a nutritional signal. *Embo J* 13: 5410-5420.

HOPFIELD JJ (1974) Kinetic proofreading: a new mechanism for reducing errors in biosynthetic processes requiring high specificity. *Proc Natl Acad Sci U S A* 71: 4135-4139.

HUANG S, JEFFERY DA, ANTHONY MD,O'SHEA EK (2001) Functional analysis of the cyclin-dependent kinase inhibitor Pho81 identifies a novel inhibitory domain. *Mol Cell Biol* 21: 6695-6705.

JEFFERY DA, SPRINGER M, KING DS,O'SHEA EK (2001) Multi-site phosphorylation of Pho4 by the cyclin-CDK Pho80-Pho85 is semi-processive with site preference. *J Mol Biol* 306: 997-1010.

KAFFMAN A, HERSKOWITZ I, TJIAN R,O'SHEA EK (1994) Phosphorylation of the transcription factor PHO4 by a cyclin-CDK complex, PHO80-PHO85. *Science* 263: 1153-1156.

KAFFMAN A, RANK NM, O'NEILL EM, HUANG LS,O'SHEA EK (1998a) The receptor Msn5 exports the phosphorylated transcription factor Pho4 out of the nucleus. *Nature* 396: 482-486.

KAFFMAN A, RANK NM,O'SHEA EK (1998b) Phosphorylation regulates association of the transcription factor Pho4 with its import receptor Pse1/Kap121. *Genes Dev* 12: 2673-2683.

KOMEILI A,O'SHEA EK (1999) Roles of phosphorylation sites in regulating activity of the transcription factor Pho4. *Science* 284: 977-980.

MCANDREW PC, SVAREN J, MARTIN SR, HORZ W,GODING CR (1998) Requirements for chromatin modulation and transcription activation by the Pho4 acidic activation domain. *Mol Cell Biol* 18: 5818-5827.

MCKEITHAN TW (1995) Kinetic proofreading in T-cell receptor signal transduction. *Proc Natl Acad Sci U S A* 92: 5042-5046.

NASH P, TANG X, ORLICKY S, CHEN Q, GERTLER FB, MENDENHALL MD, SICHERI F, PAWSON T,TYERS M (2001) Multisite phosphorylation of a CDK inhibitor sets a threshold for the onset of DNA replication. *Nature* 414: 514-521.

NASMYTH K, ADOLF G, LYDALL D,SEDDON A (1990) The identification of a second cell cycle control on the HO promoter in yeast: cell cycle regulation of SW15 nuclear entry. *Cell* 62: 631-647.

OGAWA N, DERISI J,BROWN PO (2000) New components of a system for phosphate accumulation and polyphosphate metabolism in Saccharomyces cerevisiae revealed by genomic expression analysis. *Mol Biol Cell* 11: 4309-4321.

OGAWA N,OSHIMA Y (1990) Functional domains of a positive regulatory protein, PHO4, for transcriptional control of the phosphatase regulon in Saccharomyces cerevisiae. *Mol Cell Biol* 10: 2224-2236.

O'NEILL EM, KAFFMAN A, JOLLY ER,O'SHEA EK (1996) Regulation of PHO4 nuclear localization by the PHO80-PHO85 cyclin-CDK complex. *Science* 271: 209-212.

OSHIMA Y (1982) Saccharomyces: Metabolism and Gene Expression. New York: Cold Spring Harbor Laboratory. 159-180.

OSHIMA Y (1997) The phosphatase system in Saccharomyces cerevisiae. *Genes Genet Syst* 72: 323-334.

STEGER DJ, HASWELL ES, MILLER AL, WENTE SR,O'SHEA EK (2003) Regulation of chromatin remodeling by inositol polyphosphates. *Science* 299: 114-116.

STRAHL-BOLSINGER S, HECHT A, LUO K,GRUNSTEIN M (1997) SIR2 and SIR4 interactions differ in core and extended telomeric heterochromatin in yeast. *Genes Dev* 11: 83-93.

Fig 1

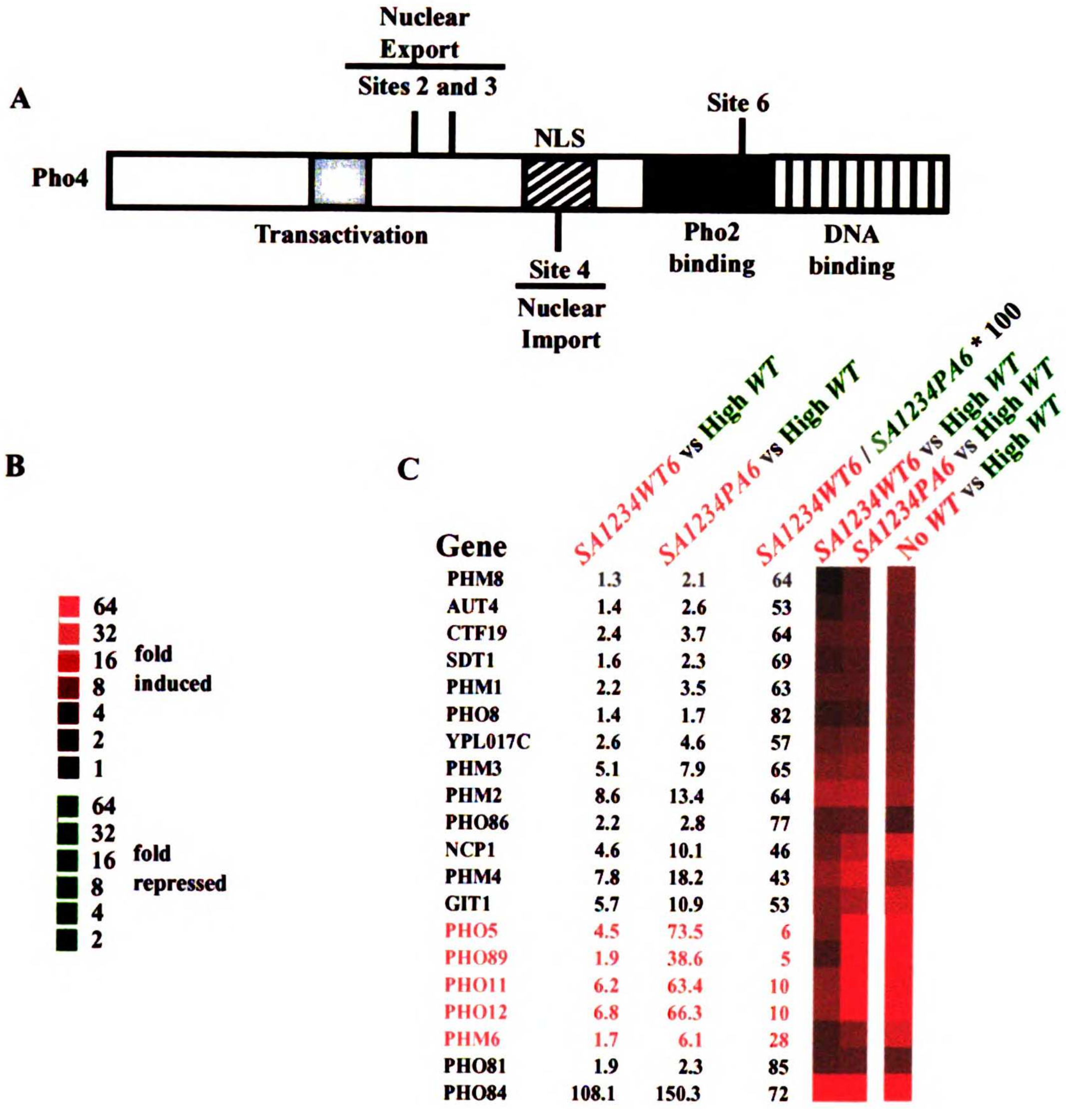

Gene	SA1234WT6 vs High WT	SA1234PA6 vs High WT	SA1234WT6 / SA1234PA6 * 100
PHM8	1.3	2.1	64
AUT4	1.4	2.6	53
CTF19	2.4	3.7	64
SDT1	1.6	2.3	69
PHM1	2.2	3.5	63
PHO8	1.4	1.7	82
YPL017C	2.6	4.6	57
PHM3	5.1	7.9	65
PHM2	8.6	13.4	64
PHO86	2.2	2.8	77
NCP1	4.6	10.1	46
PHM4	7.8	18.2	43
GIT1	5.7	10.9	53
PHO5	4.5	73.5	6
PHO89	1.9	38.6	5
PHO11	6.2	63.4	10
PHO12	6.8	66.3	10
PHM6	1.7	6.1	28
PHO81	1.9	2.3	85
PHO84	108.1	150.3	72

Fig 2

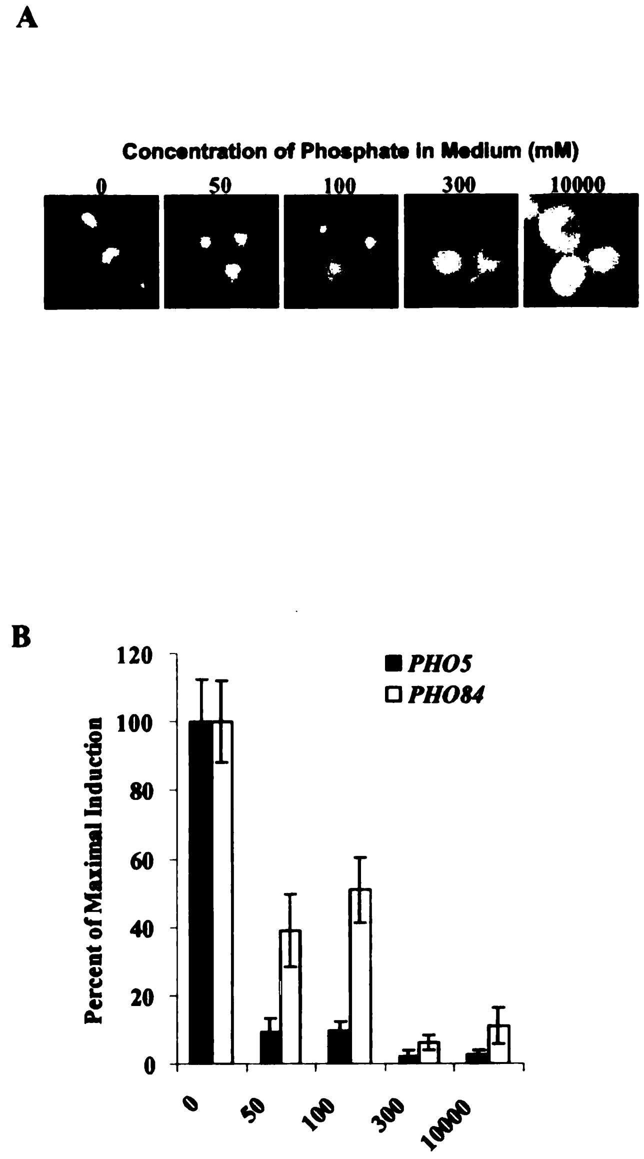
A
Concentration of Phosphate in Medium (mM)
0
50
100
300
10000
B
120
100
80
60
40
20
0
Percent of Maximal Induction
■ PHO5
□ PHO84
0
50
100
300
10000

Fig 2

C

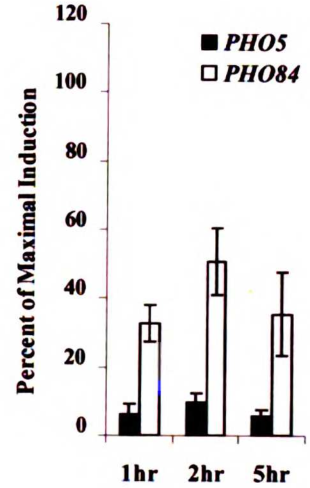

D

Gene	Int WT vs High WT	No WT vs High WT	Int / No * 100
PHM8	2.5	6.0	42
AUT4	2.6	4.0	65
CTF19	2.6	4.0	65
SDT1	2.2	3.3	67
PHM1	2.0	3.5	57
PHO8	2.6	4.1	63
YPL017C	2.8	4.7	60
PHM3	2.6	6.9	38
PHM2	4.3	8.2	52
PHO86	1.2	1.8	67
NCP1	5.9	17.7	33
PHM4	4.0	9.6	42
GIT1	4.6	22.7	20
PHO5	5.1	70.3	7
PHO89	6.7	79.8	8
PHO11	8.8	41.3	21
PHO12	8.5	50.5	17
PHM6	4.8	17.1	28
PHO81	1.4	2.8	50
PHO84	18.9	34.7	54

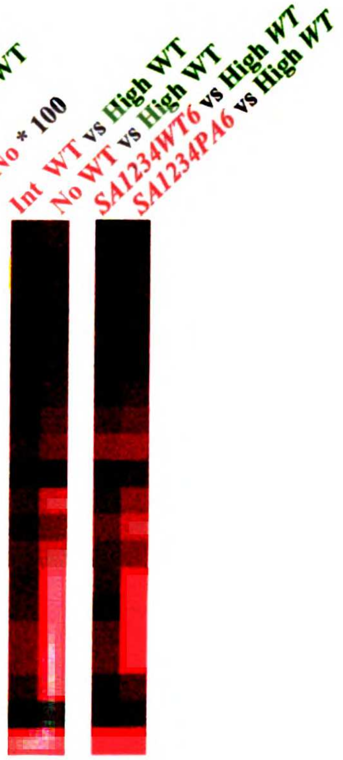

Fig 2

E

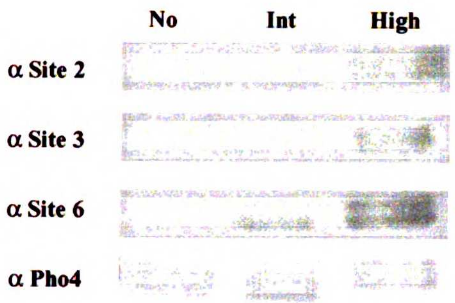
No
Int
High
α Site 2
α Site 3
α Site 6
α Pho4

F

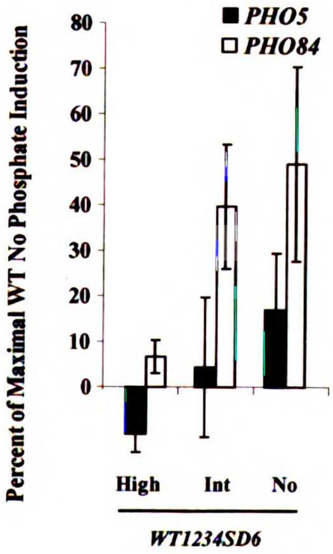
PHO5
PHO84
Percent of Maximal WT No Phosphate Induction
80
70
60
50
40
30
20
10
0
High
Int
No
WT1234SD6

Fig 3

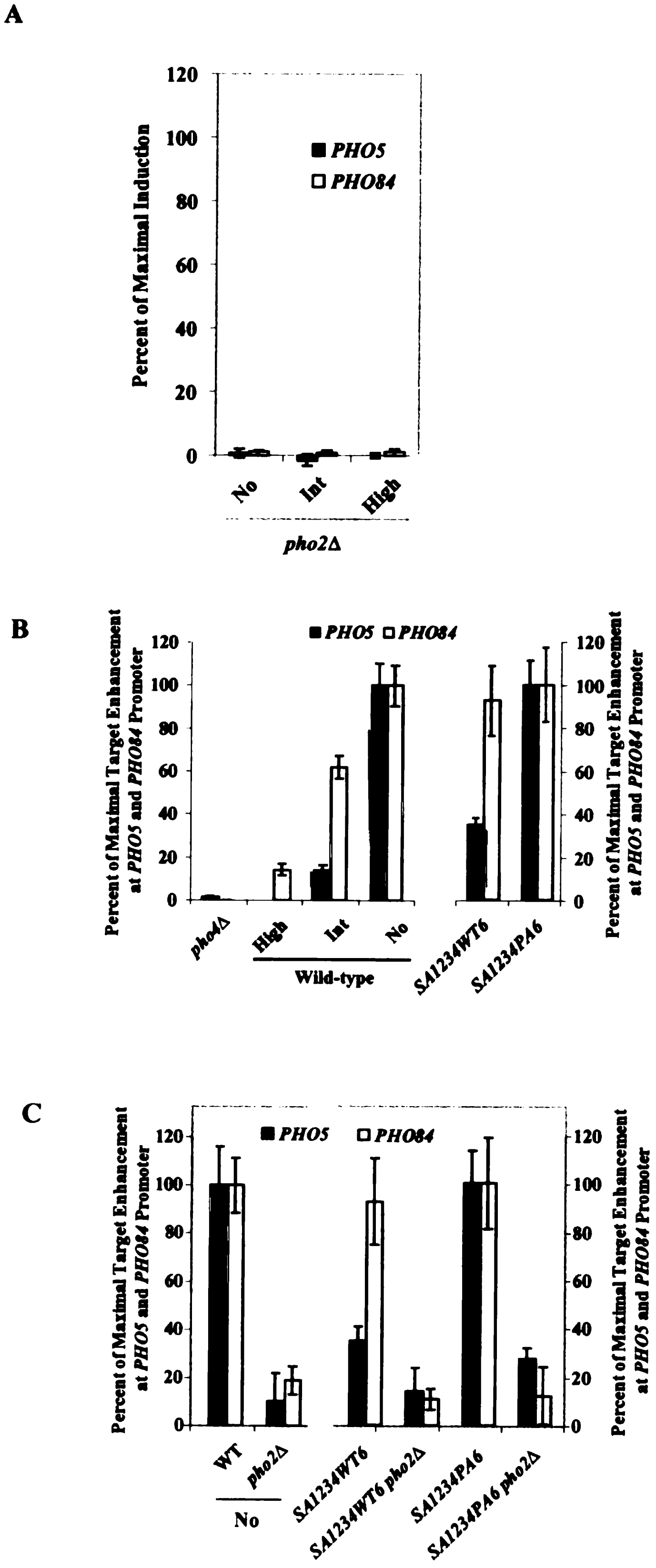

A
Percent of Maximal Induction
120
100
80
60
40
20
0
PHO5
PHO84
No
Int
High
pho2Δ
B
Percent of Maximal Target Enhancement at PHO5 and PHO84 Promoter
PHO5
PHO84
pho4Δ
High
Int
No
Wild-type
SA1234WT6
SA1234PA6
C
WT
pho2Δ
No
SA1234WT6
SA1234WT6 pho2Δ
SA1234PA6
SA1234PA6 pho2Δ

Fig 4

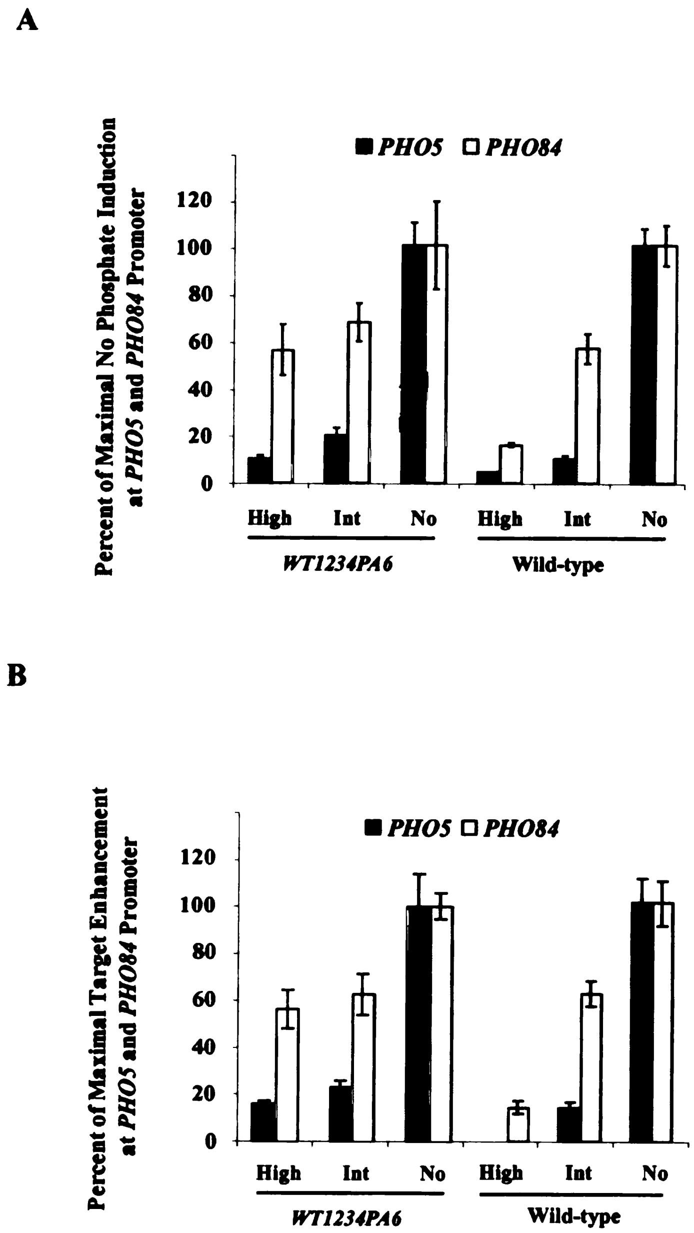
A
■ PHO5 □ PHO84
Percent of Maximal No Phosphate Induction at PHO5 and PHO84 Promoter
0
20
40
60
80
100
120
High
Int
No
High
Int
No
WT1234PA6
Wild-type
B
■ PHO5 □ PHO84
Percent of Maximal Target Enhancement at PHO5 and PHO84 Promoter
0
20
40
60
80
100
120
High
Int
No
High
Int
No
WT1234PA6
Wild-type

Fig 5

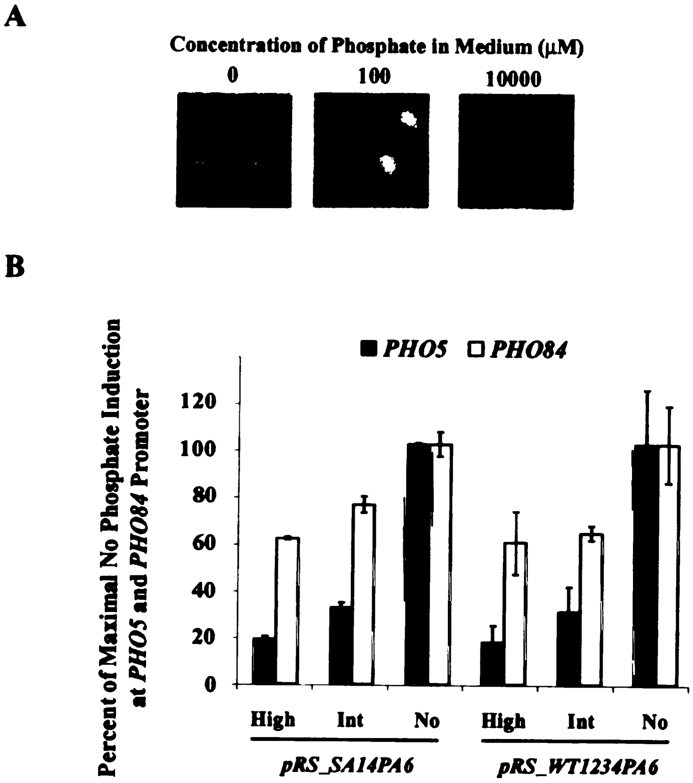
A
Concentration of Phosphate in Medium (μM)
0
100
10000
B
Percent of Maximal No Phosphate Induction at PHO5 and PHO84 Promoter
■ PHO5 □ PHO84
0
20
40
60
80
100
120
High
Int
No
High
Int
No
pRS_SA14PA6
pRS_WT1234PA6

Fig 6

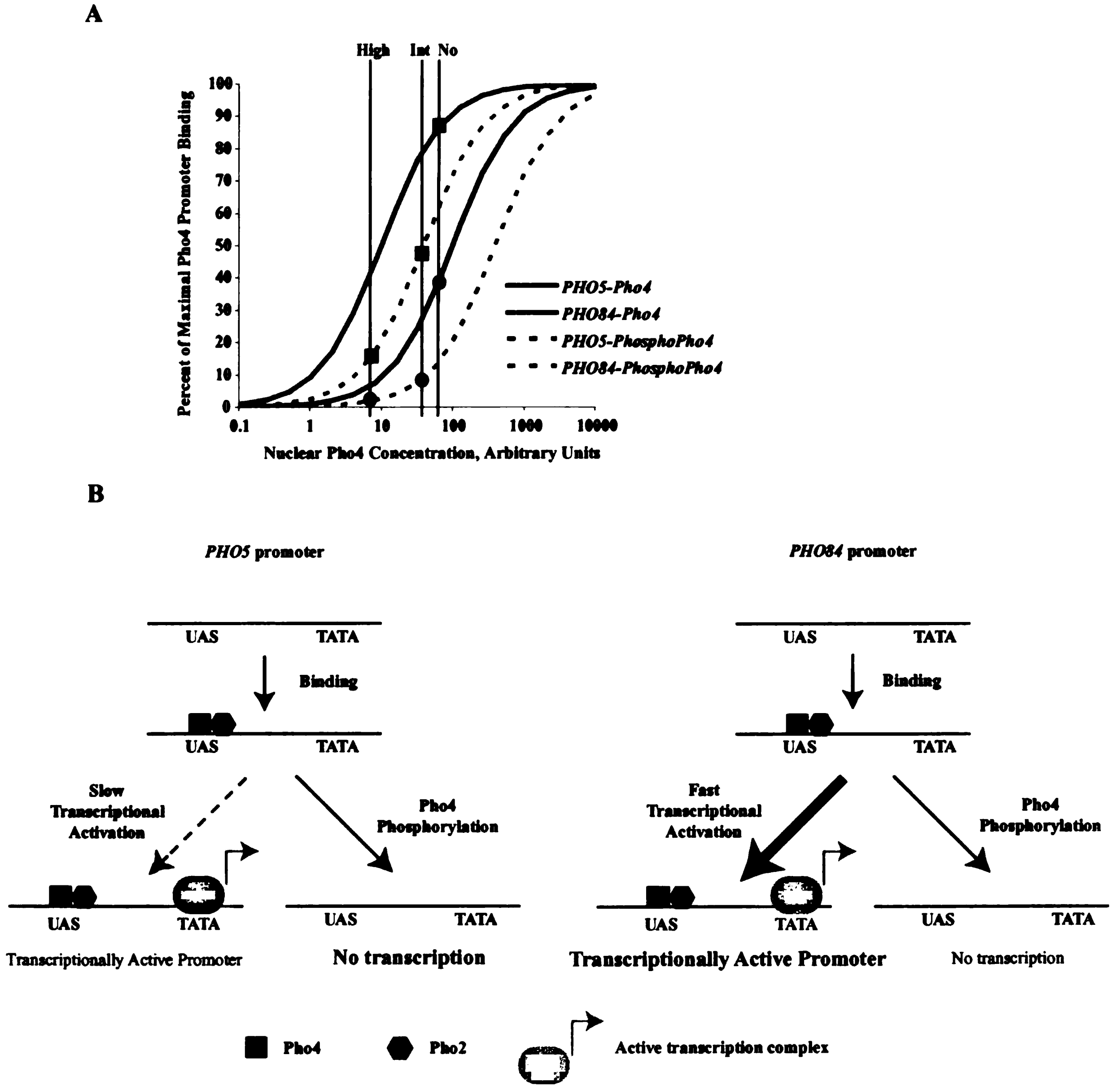
A
High
Int
No
Percent of Maximal Pho4 Promoter Binding
100
90
80
70
60
50
40
30
20
10
0
0.1
1
10
100
1000
10000
Nuclear Pho4 Concentration, Arbitrary Units
PHO5-Pho4
PHO84-Pho4
PHO5-PhosphoPho4
PHO84-PhosphoPho4
B
PHO5 promoter
PHO84 promoter
UAS
TATA
Binding
Slow Transcriptional Activation
Pho4 Phosphorylation
Transcriptionally Active Promoter
No transcription
Fast Transcriptional Activation
Pho4 Phosphorylation
Transcriptionally Active Promoter
No transcription
Pho4
Pho2
Active transcription complex

Chapter 3

Model of Conserved Network Design Allows for Robust Homeostatic Response

Homeostasis is an essential and ubiquitous theme in biology. Biological molecules often need to be maintained in narrow concentration ranges. Multiple different homeostatic networks share a similar basic design including an internal sensor and a regulated high affinity transporter. This network wiring can be described by two coupled differential equations. The solution to this equation is the same as the solution to a damped harmonic oscillator (from physics) or proportional integral control system (from electrical engineering). This design allows maintenance of a constant internal concentration of nutrient even if external nutrient levels, uptake, or other kinetic parameters vary. While maintaining homeostasis, this simple system can be energetically costly and kinetically slow. As seen in many of the systems, additions such as constitutive low affinity transporters, nutrient dependent usage rates and buffering can work to decrease the energy and time required to reach and maintain steady-state levels of nutrient. While robust to many parameters, this system is evolvable and noise in the system allows for individuals to have different thresholds of response in an isogenic population.

Homeostasis is a challenging cellular problem. Many nutrients such as phosphate, glucose, nitrogen, uracil, and metals need to be maintained in a narrow range within cells. Low levels are rate limiting to growth but high levels range from being energetically wasteful to toxic (1). Furthermore, cells have to maintain homeostasis in a dynamic environment. Not only can the external concentration of nutrient change, but other factors such as the demand and uptake ability may change. Also, the ability of a cell to respond to nutrients is constrained. For instance, there are limits to the

concentrations and activities of proteins. Finally, homeostasis is constrained by energetics and evolution.

We were interested in whether cells have developed any common strategies with which to solve the problem of homeostasis. Surprisingly, iron, uracil, copper, magnesium, sulphate, zinc, phosphate, ammonia, glucose, inositol and other homoestatic networks share the same underlying network design. When nutrient levels are high, synthesis of the nutrient transporter is inhibited; when nutrient levels are low, synthesis of the nutrient transporter is induced(2-12). In the cases where it has been determined directly (iron(13), glucose(14), and copper(15)) or inferred (phosphate(16), uracil(6), and ammonia(17)), nutrient is sensed internally, either partially or completely. Furthermore, each nutrient transporter is downregulated through endocytosis(18) or degradation(19). Increasing the external concentration of nutrient increases the downregulation rate of all transporters that have been examined (more cites). We will refer to this shared process of nutrient controlled synthesis and downregulation of transporters as the core homeostatic network.

In at least some of the cases this core network is probably the result of convergent evolution instead of duplicated design because the means of implementation are extremely different. In phosphate homeostasis in *Saccharomyces cervisiae*, changes in the level of transporter mRNA are mediated by a transcription factor whose ability to promote transporter mRNA production is dependent on internal phosphate levels. In iron homeostasis in humans, changes in the level of transporter mRNA are mediated by iron binding proteins stabilizing the transporter mRNA. If the same network design is

achieved through convergent evolution it is likely this network wiring has important properties for maintaining homeostasis.

We found that this core homeostatic network is sufficient to maintain homeostasis regardless of external concentration of nutrients. Surprisingly, this result is dependent upon the nutrient transporter being downregulated only if it is active (bound to nutrient). Depending on the exact nature by which nutrient is sensed (e. g. Michaelian or ultrasensitive) the system is also insensitive to changes in usage, uptake rate, and degradation rate. Additional features observed to work in conjunction with this core homeostatic network improve the properties of the network. Internal buffers and internal nutrient dependent usage rates improve the kinetics of the response by allowing the system to achieve steady-state more quickly with a minimal energy cost. Low affinity transporters improve the energetics of the system by allowing the system to synthesize and downregulate less transporter at steady-state. Noise in low affinity transporter levels can lead to non-genetic individuality (different responses in the same environment for isogenic cells (20)).

Methods

Simulations The set of coupled differential equation were solved numerically using Mathlab 6.1. The code is available in the supplementary materials. While the modeling does not dependent strongly on the choice of constants, whenever possible constants for modeling were based on experimental results for phosphate homeostasis. The usage rate of phosphate has been measured to be 1e6 phosphate molecules per cell per second. We assumed Setpoint for internal nutrient concentration would be about 20% of the total

amount of phosphate in a cell or 1e9 molecules per cell. The half-time of phosphate transporter on the plasma membrane is around 15 minutes. The time it takes for a transporter to go from the ribosome to the plasma membrane was assumed to be around fifteen minutes. On a genome wide scale the ratio between mRNA level and protein level is approximately 1000 proteins per message. The level of induction of PHO84 mRNA is approximately 100-fold over basal expression. The rate of uptake of a single transporter is assumed to be about 1 per second based on measurements of a glucose transporter. The external concentration of nutrient is arbitrarily set to 10 times the Km of the high affinity transporter.

The internal concentration of nutrient and transporter was not allowed to drop below zero. This was achieved by dropping the usage rate to equal the total internal concentration of nutrient for any time period in which nutrient concentration would otherwise become negative. Buffering was simulated assuming rapid uptake by a buffer when the internal nutrient concentration was over the buffering threshold and slower release of nutrient (saturated release) from the buffer when the internal nutrient concentration was under the buffering threshold. The setpoint of the buffer (BufferSetpoint) was arbitrarily chosen to be two times the setpoint of the cell. The rate of release of nutrient from the buffer was arbitrarily chosen to be one tenth the usage rate. This mimics the experimental behavior where the phosphate buffer can fill quickly but drains more slowly (NMR data).

Results and Discussion

Temporal Behavior of Network. We wished to test the ability of this core homeostatic network to adapt to changes in external nutrient concentration and cellular usage rates. This was achieved by writing differential equations that describe this system and solving for the internal concentration of nutrient versus time. The responses to different external nutrient concentrations and usage rates were tested by varying their initial values at time zero and then holding these values constant over the time course of the response. For our initial analysis, we made several assumptions to simplify the math. For this initial analysis we have included extensive details in the text. In addition to this core homeostatic network, many systems contain additional features such as an intracellular buffer and both high and low affinity transporters. We will later introduce the additional complexity to our model required to simulate these common additional biological features. For this further complexity we will present the solutions in the text with the details described in supplementary methods.

Setting up the system. To model this system, we start by defining N as the concentration of nutrient inside the cell. $\frac{dN}{dt}$ is the rate of change of nutrient with respect to time. Therefore in this system:

i. $$\frac{dN}{dt} = \text{UptakeRate} - \text{UsageRate}$$

We will assume the UsageRate is constant during the course of this simulation.

ii. $\text{UptakeRate} = k_{\max} K_{act}[\text{Transporter}]$

$k_{\max}$ = maximal rate of a single transporter

$$K_{act} = \frac{\text{NutrientExternal}}{(\text{NutrientExternal} + \text{KmTransporter})}$$

Or in words, K_{act} is the chance that the transporter is bound by nutrient. This equation results from assuming Michaelian kinetics for transporter binding to nutrient. Because the external concentration of nutrient is held constant over the course of the each simulation, K_{act} will be a constant.

iii. $$\frac{d[\text{Transporter}]}{dt} = \text{Synthesis Rate} - \text{DownRegulation Rate}$$

iv. $\text{SynthesisRate} = \alpha(\text{Setpoint} - N)$

α = proportionality (scaling) factor for synthesis

Setpoint = The internal nutrient concentration at which the system begins to responsd with increased transporter synthesis.

Equation iv roughly mimics experimental behavior: when N is high, synthesis rates are low, and when N is low, synthesis rates are high. There are many potential relationships between internal nutrient level and synthesis. For simplicity, we will first solve this system using a linear proportionality between synthesis rate and the difference between the setpoint and the internal nutrient concentration. In equation iv it is possible to have negative synthesis, which is not possible biologically. We have shown analytically and will show numerically that the form of the solution does not change significantly if we instead assume that when the internal nutrient concentration is greater than the setpoint, the synthesis rate is either zero or a basal value.

Later in the text we will solve analytically and numerically for internal nutrient concentration over time assuming different relationships between synthesis rate and internal nutrient concentration. For example,. we could also assume the system behaved in an ultrasensitive (threshold) or Michaelian (graded) manner or even could have different responses in different internal concentration ranges (cite Ferrell and Leibler for input output profiles). The form of the solution also does not change significantly if mRNA synthesis, protein synthesis, and protein translocation to the plasma membrane with appropriate time constants are included in this model.

v. $\text{DownRegulation Rate} = \beta\{K_{act}\}[\text{Transporter}]$

β=Chance of Downregulation $(0 \leq \beta \leq 1)$

Downregulation as written is dependent not just on the concentration of transporter but also on the chance that the transporter is active (which is dependent of the external level of nutrient). In other words, only active transporters have a chance of being downregulated. We have included activity dependent downregulation because, in the one case where it has been examined, endocytosis is most likely controlled by whether or not the transporter is bound to nutrient(6). Also, cadium can trigger downregulation of zinc transporter and both cobalt and manganese can trigger endocytosis of magnesium transporter. This suggests activity dependent endocytosis may also be operating in these systems. This $\{K_{act}\}$ term is the same as that in equation ii but we have bracketed it so we can follow it throughout our analysis and determine if it plays a role in the ability of this network to maintain homeostasis.

Equations i-v can be combined to make two coupled differential equations which completely describe this system.

Solving the system. To determine the behavior of this system over time we solved for the internal nutrient concentration in terms of constants. We started by taking the derivative of equations i and ii:

vi. $$\frac{d^2N}{dt^2} = \frac{d\text{UptakeRate}}{dt}$$

vii. $$\frac{d\text{UptakeRate}}{dt} = k_{\max} K_{act} \frac{d[\text{Transporter}]}{dt}$$

Substituting equation v and iv into equation iii and the resulting equation into equation vii we get:

viii. $$\frac{d^2N}{dt^2} = k_{\max} K_{act} \left[\alpha(\text{Setpoint} - N) - \beta\{K_{act}\}[\text{Transporter}] \right]$$

Rearranging and then substituting equation i into equation ii and the rearranging and then substituting the resulting equation into equation viii results in:

ix. $$\frac{d^2N}{dt^2} = k_{\max} K_{act} \left[\alpha(\text{Setpoint} - N) - \beta\{K_{act}\} \left(\frac{\frac{dN}{dt} + \text{UsageRate}}{k_{\max} K_{act}} \right) \right]$$

This can be rearranged so that all the nutrient dependent terms are on the left and the nutrient independent terms are on the right two obtain the two equivalent equations:

x. $$\frac{d^2N}{dt^2} + \beta\{K_{act}\}\frac{dN}{dt} + k_{\max} K_{act} \alpha N = k_{\max} K_{act} \alpha \text{Setpoint} - \beta\{K_{act}\}(\text{UsageRate})$$

xib.

$$\frac{dN}{dt} = k_{\max} K_{act} \alpha (\text{Setpoint}) t - k_{\max} K_{act} \alpha \int N dt - \left(\beta \{ K_{act} \} N \right) - \left(\beta \{ K_{act} \} \text{UsageRate} \right) t + \text{Constant}$$

Equation x is a common result in physical systems and describes a damped harmonic oscillator. Depending on the values of $\beta\{K_{act}\}$ and $k_{\max} K_{act} \alpha$ this will take one of three forms: a sinusoidal function bounded by an exponential decay (referred to as underdamped), an exponential decay multiplied by time (referred to as a critically damped system), or an exponential decaying system (referred to as overdamped) (Fig 1).

Equation xib is the same as the equation for a circuit having proportional integral control. These circuits are commonly used to make a system reach a stable setpoint regardless of disturbance and have the exact same properties as a damped harmonic oscillator. The advantage of using integral control to regulate homeostasis has been reported (TauMu). The use of proportional and integral control (PI) together has been analyzed as a method for calcium homeostasis in cows (cow paper). As suggested by these authors the properties of PI control are very useful for adaptation and this core homeostatic network may be a functional implementation of PI control in biology.

The solution to equation x (and equation xi) is:

Solution to x.

$$N = A e^{-\left[\frac{\left(\beta\{K_{act}\} \pm \sqrt{\left(\beta\{K_{act}\} \right)^2 - 4 k_{\max} K_{act} \alpha} \right)}{2} \right] t} + C$$

A and C are constants determined by the parameters of the system (e.g. Setpoint) and the initial values for transporter and nutrient levels. As time gets large the first term approaches zero and internal nutrient levels reach a constant value. The behavior of this system is an exponentially bounded decay to steady-state (Fig 2A, left).

Network Properties at Steady-State. Because this system always reaches a stable steady-state we can solve for the steady-state value of nutrient. This is done by setting $\frac{d^2N}{dt^2}=\frac{dN}{dt}=0$. Rearranging equation x we get:

xii. $$N = \text{Setpoint} - \frac{\beta\{K_{act}\}(\text{UsageRate})}{k_{\max}K_{act}\alpha} = \text{Setpoint} - \frac{\beta(\text{UsageRate})}{k_{\max}\alpha}$$

Once again, $\{K_{act}\}$ came from the dependence of endocytosis on activity. Counterintuitively, as long as downregulation depends on the whether a transporter is active, the K_{act} terms cancel and the internal concentration of nutrient is completely independent of external nutrient concentrations. We therefore predict that the endocytosis rate of the vast majority of transporters involved in homeostasis will be regulated by their activity. For our future network description we will continue to include an activity dependent endocytosis term. We will consider it as part of the core homeostatic network design.

While the internal concentration of nutrient does not depend on external nutrient concentration, the transporter concentration does depend on external nutrient concentration (Fig 2B). At steady-state we can determine the rate of synthesis of transporter by substituting the steady-state value of N from equation xii into equation iv to get $\frac{\beta(\text{UsageRate})}{k_{\max}}$. At steady-state the amount of transporter synthesized and downregulated must be equal. Solving equation iii at steady-state by substituting $\frac{\beta(\text{UsageRate})}{k_{\max}}$ for the synthesis rate and equation v for the downregulation rate shows that the steady-state concentration of transporter is $\frac{(\text{UsageRate})}{k_{\max} K_{act}}$. As the external concentration of nutrient drops K_{act} goes down and therefore the steady-state concentration of transporter goes up (Knox and Segel).

Internal nutrient concentration at steady state is largely independent of usage rate (UsageRate), downregulation rate (equation v constants), synthesis rate (equation iv constants), and maximal uptake rate of individual transporters ($k_{\max}$). This can be seen by analyzing equation xii for conditions that cause the internal concentration of nutrient to vary. The parameters defined by the relationship $\frac{\text{Setpoint}}{2} < \frac{\beta(\text{UsageRate})}{k_{\max}\alpha} \leq \text{Setpoint}$ is the only physiological parameter range which will not be able to maintain nutrient levels within a two-fold concentration range. Outside of this range internal nutrient concentrations will deviate less than two-fold from the setpoint or the cells will starve. There is therefore only a two-fold range in which usage rate, downregulation rate, synthesis rate, or maximal uptake rate will not keep the internal nutrient concentration within a two fold range.

Cells need to balance the homeostasis of many nutrients. Changes in growth rate or energy supplies might change the usage rate of a number of nutrients. Because the steady-state internal nutrient concentration is not sensitive to usage rates, each nutrient system will independently adjust. For example, the demand for phosphate fluctuates through the cell cycle. Any time the internal concentration of phosphate begins to fall the phosphate homeostasis system will adjust and increase the level of phosphate transporter on the plasma membrane to bring the internal concentration back to its steady-state value. Each pathway that requires phosphate does not need to directly affect the phosphate signaling pathway.

Effect of Alternative Relationships Between Synthesis and Nutrient. We wished to determine how dependent our results were on our assumption that the relationship between nutrient levels and synthesis rates was linear (equation iv). Many different relationships are possible even with a small number of signaling components. We decided to test some of the most commonly observed relationships: Michaelian (graded), cooperative (switch-like or ultrasensitive), and zero order ultrasensitive (switch-like). We also tested how the time delay caused by mRNA synthesis, protein translation, and transit of the transporter to the plasma membrane might affect the dependence on external nutrient level and usage rate.

In a Michaelian relationship between nutrient and expression:

ivb. $$\text{SynthesisRate} = \alpha\left(\frac{\text{Setpoint}}{\text{Setpoint}+N}\right)$$ **xiib.** $$N = \text{Setpoint}\left(\frac{k_{\max}\alpha - \beta(\text{UsageRate})}{\beta(\text{UsageRate})}\right)$$

In this situation, internal nutrient concentration at steady-state does not depend on external nutrient but does depend on UsageRate (Fig. 3A).

In a cooperative relationship between nutrient and expression (assume fit by Hill function):

ivc. $\text{SynthesisRate} = \alpha(\frac{\text{Setpoint}^{\text{h}}}{\text{Setpoint}^{\text{h}} + N^{h}})$ **xiic.** $N = \text{Setpoint}\left(\sqrt[\frac{1}{h}]{\frac{k_{\max}\alpha - \beta(\text{UsageRate})}{\beta(\text{UsageRate})}}\right).$

Under these conditions, internal nutrient does not depend on external nutrient concentration at steady-state. The amount of cooperativity (h, Hill coefficient) will determine how strongly the internal concentration of nutrient depends on the usage rate. When h=1 we get the Michaelian limit; as h becomes large the system becomes more switch-like and the dependence of the internal nutrient concentration on usage rate goes down (Fig. 3B and 3C). At the limit where the system acts like a perfect switch (h→∞) the internal nutrient concentration is independent of usage rate.

In a zero-order ultrasensitive relationship: **ivd.** $\text{SynthesisRate} = \alpha(\frac{\text{Setpoint}}{N})$

Where $\text{MinimalSythesisRate} \leq \text{SynthesisRate} \leq \text{MaximalSynthesisRate}$

Numerically the internal concentration of the core homeostatic network having a zero-order ultrasensitive relationship between internal nutrient and transporter synthesis does not depend on external concentration but does depend on usage rate (Fig. 3D).

Bounding our initial linear assumption for synthesis in equation iv by the constraint $\text{MinimalSythesisRate} \leq \text{SynthesisRate} \leq \text{MaximalSynthesisRate}$ still results in a system that is independent of both external concentration and usage rate (Fig. 3E).

Threshold behavior or ultrasensitivity is common in biological responses. For example, in the phosphate homeostatic system, induction of phosphate transporter appears ultrasensitive in response to phosphate (unpublished Mike). We predict that threshold responses will be common in homeostatic system because this will make the response only weakly sensitive to changes in kinetic parameters such as usage rate.

Finally, if mRNA synthesis, protein synthesis, and transit of the protein to the plasma membrane are included, for all five different relationships between synthesis rate and internal nutrient concentration, the systems are all still independent of external nutrient concentration but the systems all take longer to reach steady-state (data not shown and Fig. 4A).

Energetics Versus Speed in Homeostasis. While the described circuitry is sufficient to maintain homeostasis, the time to reach homeostasis is dependent on the kinetic parameters of the system. This is important because the growth rate or survivability can be affected while the cell is adapting. The quicker a system reaches steady-state, the less adverse the effect on the cell. For example, having too much iron can lead to increased superoxide formation, while too little iron slows down the growth of the cell (cite iron papers).

For underdamped systems (most of biologically relevant parameter space gives underdamped systems, data not shown), the rate at which the system approaches steady-state is $e^{-\frac{(\beta\{K_{act}\})}{2}t}$ (from solution to equation x). This means that the downregulation rate (βK_{act}, see equation v) must be increased to approach steady-state quicker. If the downregulation rate is doubled the time to steady-state is decreased two-fold.

At steady-state the downregulation and synthesis rate must be equal so the quicker the system reaches steady-state the more energy it will take to maintain nutrient levels at steady-state. In other words the flux of transporters through the system (creation and destruction) is dependent on how quickly the system reaches steady-state. Creation and destruction of plasma membrane transporter is possibly one of the most energetically

costly processes in which a cell engages (do you know a good cite?). It is also worth noting that while the external concentration of nutrient does not affect the energy required to maintain steady-state, the time to reach steady-state will depend on the external concentration of nutrient because the time to steady-state depends on K_{act}. The lower the external concentration of nutrient the longer it will take to reach steady-state.

Buffers, Nutrient Dependent Usage, and Low Affinity Transporter. Most homeostatic networks contain other components in addition to the core network described above. Interestingly, most of these additions can be shown to decrease the time to steady-state or the energy requirements of the system.

When nutrients are supplied in excess of the cellular demands, many nutrient systems store the nutrient in an intracellular buffer (cite phosphate and nitrogen and carbon and iron). Alternatively, enzymes which use nutrients can have a Km above the internal concentration of the nutrient ([phosphate]<km of some phosphate enzymes). This will make the usage rate of the nutrient (and growth rate of the cell) dependent on the internal nutrient concentration. Both these additions affect the rate of change of internal nutrient.

The effect of this change can be solved by replacing equation i with:

$$\frac{dN}{dt} = \text{UptakeRate} - \text{UsageRate} + \text{UsageRateChange}*N - \text{BufferingRate}(\text{BufferSetpoint}-N)$$

Equation x becomes:

$$\frac{d^2N}{dt^2}+\left(\beta\{K_{act}\}+\text{URC+BR}\right)\frac{dN}{dt}+\left(k_{\max}K_{act}\alpha+\beta\{K_{act}\}\left(\text{UsageRate+URC+BR}\right)\right)N$$

$$=k_{\max}K_{act}\alpha\text{Setpoint}-\beta\{K_{act}\}\left(\text{UsageRate+BufferRate*BufferSetpoint}\right)$$

URC $\equiv$ UsageRateChange and BR $\equiv$ BufferingRate.

BufferSetpoint is the internal concentration of nutrient at which the buffer switches from a nutrient sink to a nutrient source.

Buffers and nutrient dependent usage therefore have a similar effect on the core homeostatic network. Both decrease the time required to reach steady-state without affecting the downregulation rate (Fig. 4A-C). Because the downregulation rate is unaffected the decreased time to steady-state can be achieved without requiring more flux of transporter through the system. Without increasing the energetic cost, this allows networks with a buffer or usage dependent uptake to reach steady-state more quickly than a network without a buffer or usage dependent uptake.

Almost every homeostatic network contains both regulated high affinity transporters and low affinity transporters which are often constitutive (cite phosphate, iron, glucose, ammonia, copper, zinc). We modeled the effect of low affinity transporters by expanding the nutrient uptake equation (equation ii) as follows:

iic. $\text{UptakeRate}=k_{\max}K_{act}[\text{Transporter}]+k_{\max}K_{act,\text{LowAffinity}}[\text{LowAffinityTransporter}]$

$k_{\max}$ = maximal rate of a single transporter both high and low affinity

$$K_{act,\text{LowAffinity}}=\frac{\text{NutrientExternal}}{(\text{NutrientExternal}+\text{KmLowAffinityTransporter})}$$

Because $k_{\max}K_{act,\text{LowAffinity}}[\text{LowAffinityTransporter}]$ is a constant (which we will call LA_Rate), equation x becomes:

$$\frac{d^2N}{dt^2}+\beta\{K_{act}\}\frac{dN}{dt}+k_{\max}K_{act}\alpha N=$$

$$k_{\max}K_{act}\alpha\text{Setpoint}-\beta\{K_{act}\}(\text{UsageRate-LA\_Rate})$$

and the steady-state concentration of nutrient is:

xiid. $$N=\text{Setpoint}-\frac{\beta(\text{UsageRate-LA\_Rate})}{k_{\max}\alpha}$$

Once again, by substituting this steady-state value into equation iii then equation ii, the steady-state concentration of high affinity transporter can be calculated as $\frac{(\text{UsageRate-LA\_Rate})}{k_{\max}K_{act}}$. Because transporter cannot be negative when LA is greater than UsageRate the internal concentration will rise uncontrollably. In other words, when the rate of uptake of nutrient through constitutive transporters exceeds nutrient demand, the internal concentration of nutrient will rise. Therefore, systems that contain constitutive transporters will need to have some mechanism, such as a buffer, to stop internal concentrations from rising uncontrollably.

Low affinity transporters make the internal concentration of nutrient weakly dependent on external nutrient concentration. If the low affinity system is constitutive, a cell cannot tell the difference between a decrease in usage and a higher level of low affinity transporter at the plasma membrane. Therefore, if homeostasis is dependent on usage rate, the addition of constitutive low affinity transporter will make the system

dependent on external nutrient concentration. Internal concentration of nutrient follows one of four behaviors in a system with constitutive low affinity transporters. First, uptake can occur primarily through the low affinity system (this will occur at high external nutrient concentration). In this range the internal concentration is independent of the external nutrient concentration and set by the buffer. Second, uptake can occur primarily through the high affinity system (this will occur at low nutrient concentration). In this range the internal concentration is independent of the external nutrient concentration (this internal concentration will be lower than the one set by the low affinity transporters). Third, there is a narrow range in which the cells uptake significant amounts of nutrient through both the low affinity and high affinity systems. The internal concentration of nutrient will vary in this range and be bounded by the internal concentration found when only high or low affinity systems are utilized. Finally, the amount of synthesis of transporter may be too low to balance usage and the internal concentration of nutrient will drop to zero (Fig 4D).

Low affinity transporters can reduce the energy to maintain steady-state. If low affinity transporters are only very slowly downregulated, the amount of low affinity transporters which needs to be synthesized per second is the number of low affinity transporters on the plasma membrane divided by the doubling time (cell growth rate). We can calculate the concentration of nutrient at which a cell would have to make more low affinity transporter than high affinity transporter. This is achieved by changing the rate of down regulation of high affinity transporter to include the doubling time (adding doubling time to equation v) and setting the rate of low affinity synthesis as less than the rate of high affinity synthesis (supplementary text):

xiii. $$\frac{\mathrm{DoublingTime}\left(\beta+\frac{1}{\mathrm{DoublingTime}}\right)(\mathrm{UsageRate})}{k_{\max}} > \frac{\beta_{\mathrm{LowAffinity}}\mathrm{UsageRate}}{k_{\max}K_{act,\mathrm{LowAffinity}}}$$

Solving for nutrient concentration:

xiv. $$N > \frac{\beta_{\mathrm{LowAffinity}}K_{M,\mathrm{LowAffinity}}}{\mathrm{DoublingTime}\beta}$$

At high nutrient concentrations, the most efficient strategy is to use only low affinity transporters. At low nutrient concentration, the most efficient strategy is to use only high affinity transporters. In reality the external concentration will vary between high and low levels. Combining a high affinity and low affinity system will lower the total number of transporters required in an uncertain environment (Table 1).

Because biology is inherently stochastic it is important to consider how robust a network is to noise. While each cell maintains the ability to achieve homeostasis (data not shown), fluctuations in protein levels will cause different cells in an isogenic population to behave distinctly. For example, the amount of low affinity transporters will set the concentration at which high affinity transporter is induced. Fluctuations in the amount of low affinity transporter between cells due to stochastic noise will cause different cells to have different thresholds at which they induce high affinity transporter (Fig 5). A wide variety of behaviors can be maintained in the population without needing to have different responses encoded at the genetic level. Non-genetic variation has the advantage that it will not be eliminated from a population as quickly. Fluctuations in protein level leading to differences in response behavior may make an isogenic population more able to survive in a varied environment.

While robust to external concentrations of nutrient and usage rates, the homeostatic network is highly evolvable. For example, if a system has only a low affinity transporter, overexpression of the transporter will let the cells cope with low levels of nutrient. A common mechanism of overexpression is tandem duplication of the transporter. This increases the chance of getting a mutation that will convert one of the low affinity transporters into a high affinity transporter. The tandem duplication can collapse leaving a low and high affinity transporter. Selection on more advantageous promoter regulation can also proceed in a step-wise manner to achieve the homeostatic wiring described above.

Conclusion. Our model for the apparent core network design for homeostasis is well suited for dealing with changing environments and intracellular needs. This explanation is appealing because it does not require that regulation of different nutrients be intricately co-regulated – every nutrient can maintain itself. By this model, transporter endocytosis should have the property that the downregulation rate of the transporter be dependent on the activity of the transporter. By taking into account energetics this model also provides an explanation for why low affinity transporters and intracellular buffers are so common. The system is robust and evolvable with many paths by with which to reach this simple network design. Stochastic noise in protein levels will lead to phenotypic variation in an isogenic population, a property that can be advantageous to the population.

This model is not an attempt to explain every feature of every homeostatic network. Other features such as multiple high affinity transporters and reverse flux of nutrients can be added to the core homeostatic network. We chose buffering, usage dependent uptake, and constitutive low affinity transport to show that these additions tend to change the dynamic properties of the system and energy requirements of the system without changing the basic ability to maintain homeostasis. We believe this will be true for much of the additional complexity that can exist in nature.

This model suggests that caution needs to be taken when examining homeostatic systems. The rate at which the external concentration is changed, the time after which the system is analyzed, and the assay used as an output for the system can all lead to drastically different results. Also, homeostatic systems have the potential to exhibit hysteresis. For example, the internal buffer can be empty or full so it is important to consider the starting state of the cell.

While determining kinetic constants of all interacting species is important for understanding the details of a system, this model suggests that it may be possible to gain a functional understand of a network with just a limited set of interactions. This could be a very useful principle for analyzing more complicated networks.

This model makes many predictions that can be tested experimentally. It will be important to measure internal concentration of nutrient and nutrient transporter for a homeostatic system in different concentrations of external nutrient and at different growth rates (to change the usage rate). In general, we feel this method of comparative network design will help uncover core functional modules in other, more complicated systems.

1. Walker, J. D., Enache, M. & Dearden, J. C. (2003) *Environ Toxicol Chem* **22,** 1916-35.

2. Yamaguchi-Iwai, Y., Ueta, R., Fukunaka, A. & Sasaki, R. (2002) *J Biol Chem* **277,** 18914-8.

3. Kruckeberg, A. L., Ye, L., Berden, J. A. & van Dam, K. (1999) *Biochem J* **339 (Pt 2),** 299-307.

4. Graschopf, A., Stadler, J. A., Hoellerer, M. K., Eder, S., Sieghardt, M., Kohlwein, S. D. & Schweyen, R. J. (2001) *J Biol Chem* **276,** 16216-22.

5. Guo, B., Phillips, J. D., Yu, Y. & Leibold, E. A. (1995) *J Biol Chem* **270,** 21645-51.

6. Seron, K., Blondel, M. O., Haguenauer-Tsapis, R. & Volland, C. (1999) *J Bacteriol* **181,** 1793-800.

7. Jin, Y. H., Jang, Y. K., Kim, M. J., Rad, M. R., Kirchrath, L., Seong, R. H., Hong, S. H., Hollenberg, C. P. & Park, S. D. (1995) *Biochem Biophys Res Commun* **214,** 709-15.

8. Labbe, S., Zhu, Z. & Thiele, D. J. (1997) *J Biol Chem* **272,** 15951-8.

9. Zhao, H. & Eide, D. J. (1997) *Mol Cell Biol* **17,** 5044-52.

10. Bun-Ya, M., Nishimura, M., Harashima, S. & Oshima, Y. (1991) *Mol Cell Biol* **11,** 3229-38.

11. Marini, A. M., Vissers, S., Urrestarazu, A. & Andre, B. (1994) *Embo J* **13,** 3456-63.

12. Lai, K. & McGraw, P. (1994) *J Biol Chem* **269,** 2245-51.

13. Kang, D. K., Jeong, J., Drake, S. K., Wehr, N. B., Rouault, T. A. & Levine, R. L. (2003) *J Biol Chem* **278,** 14857-64.

14. Rolland, F., Winderickx, J. & Thevelein, J. M. (2002) *FEMS Yeast Res* **2,** 183-201.

15. Graden, J. A. & Winge, D. R. (1997) *Proc Natl Acad Sci U S A* **94,** 5550-5.

16. Wykoff, D. D. & O'Shea, E. K. (2001) *Genetics* **159,** 1491-9.

17. van Riel, N. A., Giuseppin, M. L. & Verrips, C. T. (2000) *Metab Eng* **2,** 49-68.

18. Rotin, D., Staub, O. & Haguenauer-Tsapis, R. (2000) *J Membr Biol* **176,** 1-17.

19. Ooi, C. E., Rabinovich, E., Dancis, A., Bonifacino, J. S. & Klausner, R. D. (1996) *Embo J* **15,** 3515-23.

20. Spudich, J. L. & Koshland, D. E., Jr. (1976) *Nature* **262,** 467-71.

Figure 1. **Properties of a damped harmonic oscillator after perturbation.**

We will use the simplified damped harmonic oscillator $\frac{d^2N}{dt^2} + \beta\frac{dN}{dt} + \alpha N = 0$ to demonstrate the properties of this system. A) β is held at 4 while α is set to 10 (underdamped; red), 1 (critically damped; green), or 0.1 (overdamped; blue). B) α is held at 1 while β is set to 40 (overdamped; blue), 4 (critically damped; green), or 0.4 (underdamped; red). For these simulations N is set to 100 at time zero.

Figure 2. **Temporal Properties of the core homeostatic network.** Values for the external nutrient concentration are varied by four orders of magnitude and the simulated A) internal nutrient concentration and B) transporter level at plasma membrane are graphed versus time. Unvaried constants were chosen as described in the methods.

Figure 3. **Properties of the network with different relationships between synthesis rate and internal nutrient levels.** The dependence of the internal concentration versus external concentration (left) and usage rates (right) were determined for the core network where the relationships between internal nutrient and synthesis rate were A) Michaelian, B) cooperative h=4, C) cooperative h=16 D) zero-order ultrasensitive, and E) linear with bounds.

Figure 4. **Effect of a buffer, nutrient dependent usage, and constitutive low affinity transporter on internal nutrient levels.** The response of the A) network, B) network plus a buffer, C) network plus nutrient dependent usage, and D) network plus a constitutive low affinity transporter to changes in external nutrient concentration. All

networks including mRNA synthesis, transporter synthesis, and transporter transit to the plasma. All networks also assume a linear relationship between synthesis and internal nutrient concentration and have an upper and lower limit on synthesis. Constants were chosen as described in the methods.

Figure 5. **Noise causes distinct outputs from isogenic cells.** Noise was introduced to the system varying the steady-state level of low affinity transporter by a random Gaussian distribution such that one standard deviation corresponds to twice or half as much low affinity transporter. We simulated 1000 different cells at five different concentrations of external nutrient (each having a slightly different level of low affinity transporter due to noise). The total amount of transporter made per cell was simulated and binned. The network was assumed to have a linear relationship between synthesis and internal nutrient concentration and have an upper and lower limit on synthesis. mRNA synthesis, transporter synthesis, transporter translocation, and a buffer were also included in this network.

Figure 1

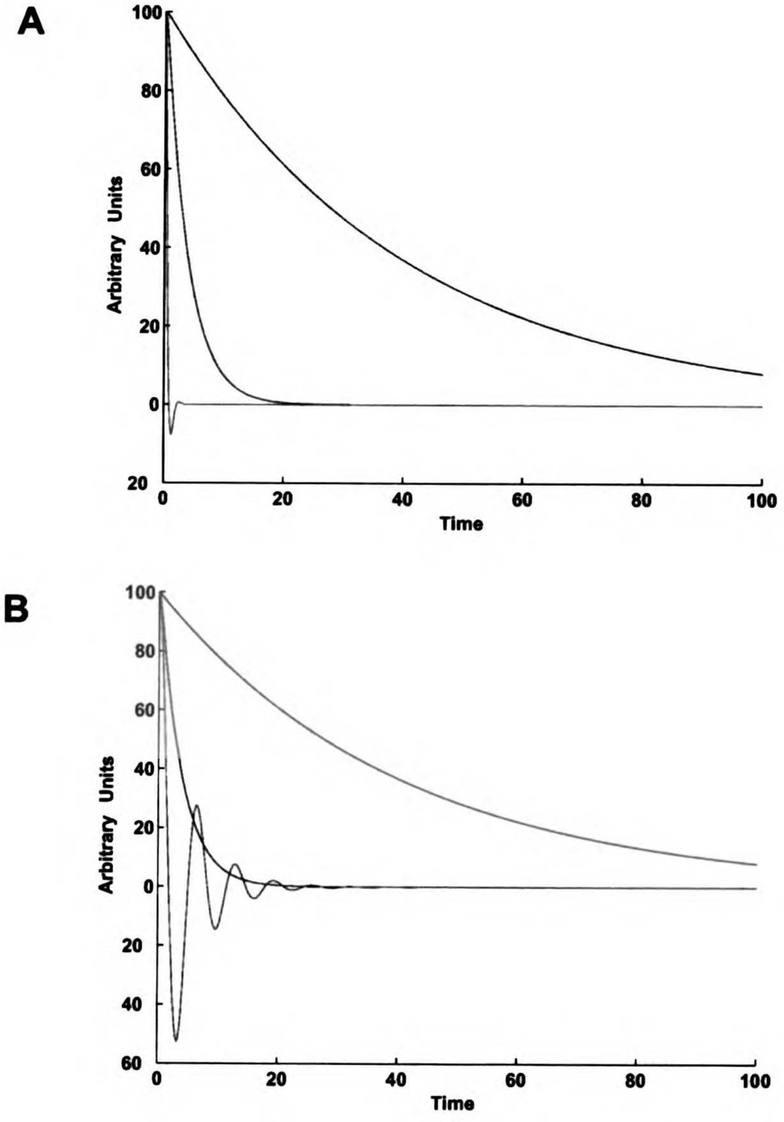
A
100
80
60
40
20
0
20
Arbitrary Units
0
20
40
60
80
100
Time
B
100
80
60
40
20
0
20
40
60
Arbitrary Units
0
20
40
60
80
100
Time

Figure 2

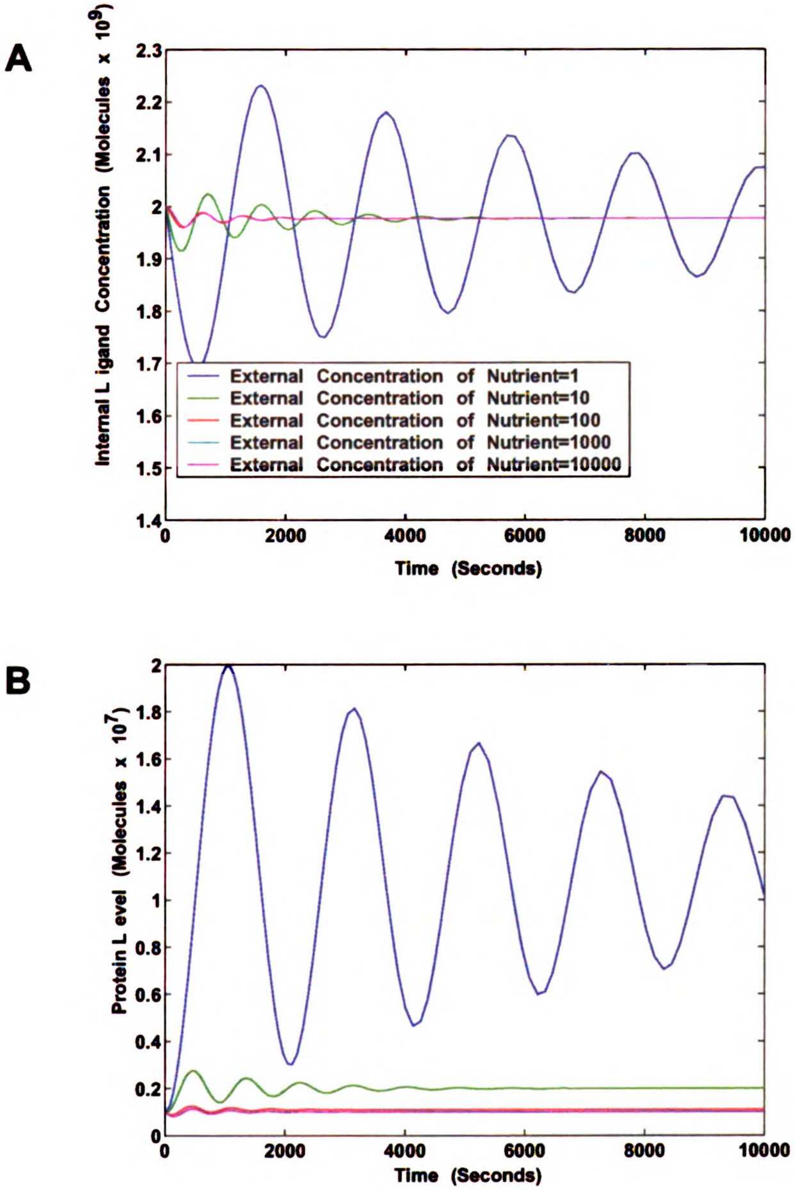
A
Internal Ligand Concentration (Molecules x 10^9)
2.3
2.2
2.1
2
1.9
1.8
1.7
1.6
1.5
1.4
0
2000
4000
6000
8000
10000
Time (Seconds)
External Concentration of Nutrient=1
External Concentration of Nutrient=10
External Concentration of Nutrient=100
External Concentration of Nutrient=1000
External Concentration of Nutrient=10000
B
Protein Level (Molecules x 10^7)
2
1.8
1.6
1.4
1.2
1
0.8
0.6
0.4
0.2
0
0
2000
4000
6000
8000
10000
Time (Seconds)

Figure 3

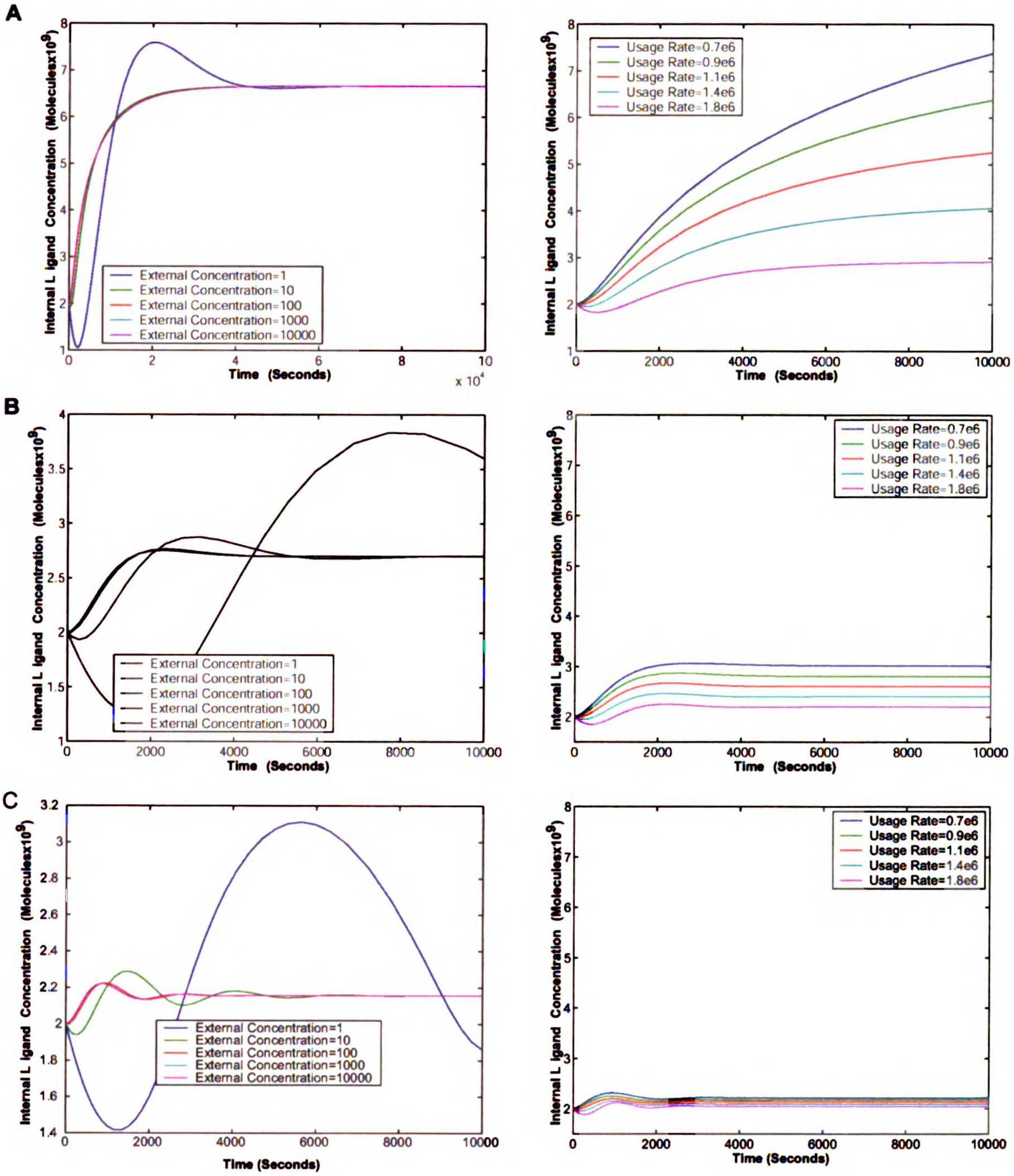
A
Internal L igand Concentration (Moleculesx10^9)
Time (Seconds)
x 10^4
External Concentration=1
External Concentration=10
External Concentration=100
External Concentration=1000
External Concentration=10000
Usage Rate=0.7e6
Usage Rate=0.9e6
Usage Rate=1.1e6
Usage Rate=1.4e6
Usage Rate=1.8e6
B
C
0
2
4
6
8
10
2000
4000
6000
8000
10000

Figure 3

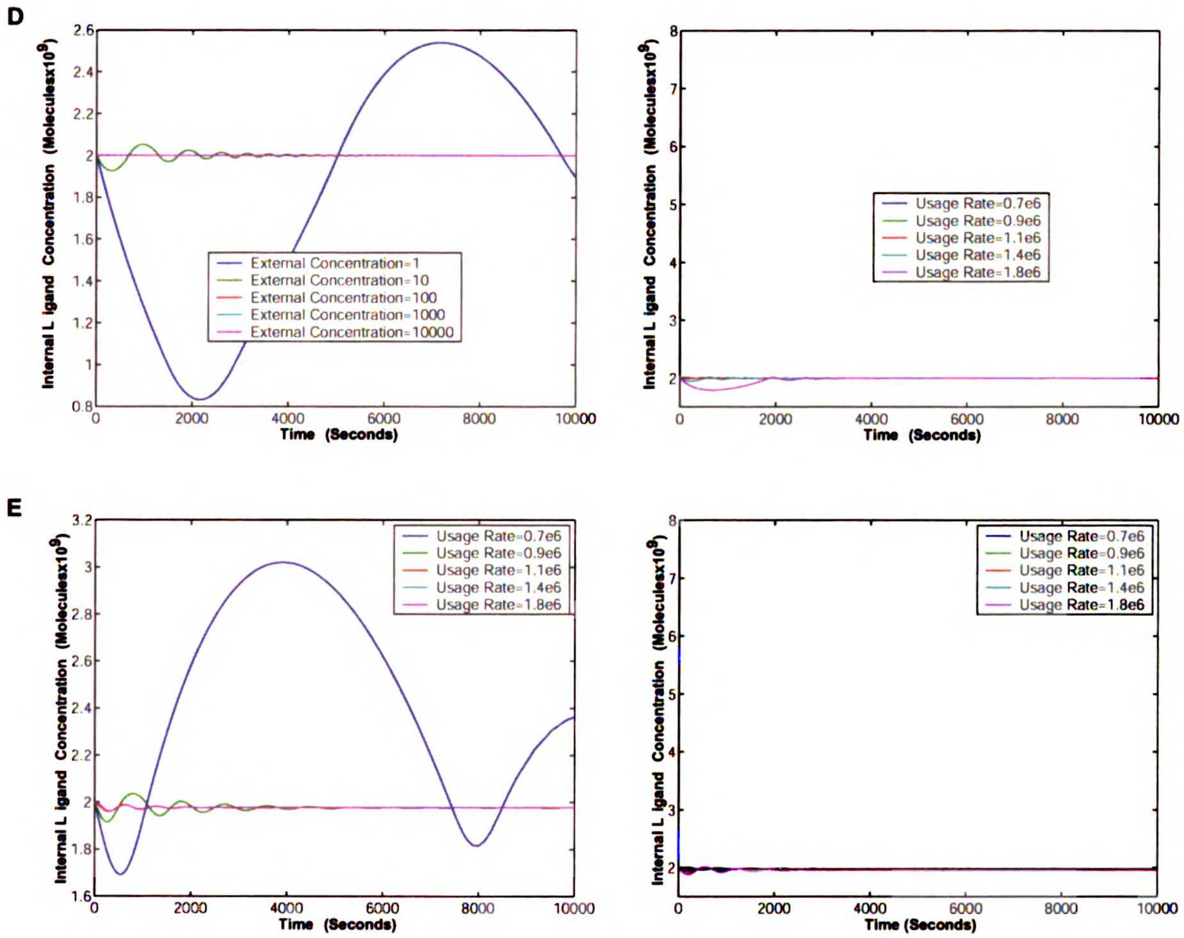
D
E
Internal L igand Concentration (Moleculesx10^9)
Time (Seconds)
0
2000
4000
6000
8000
10000
2.6
2.4
2.2
2
1.8
1.6
1.4
1.2
1
0.8
External Concentration=1
External Concentration=10
External Concentration=100
External Concentration=1000
External Concentration=10000
8
7
6
5
4
3
2
Usage Rate=0.7e6
Usage Rate=0.9e6
Usage Rate=1.1e6
Usage Rate=1.4e6
Usage Rate=1.8e6
3.2
3
2.8
2.6
2.4
2.2
2
1.8
1.6
Time (Seconds)

Figure 4

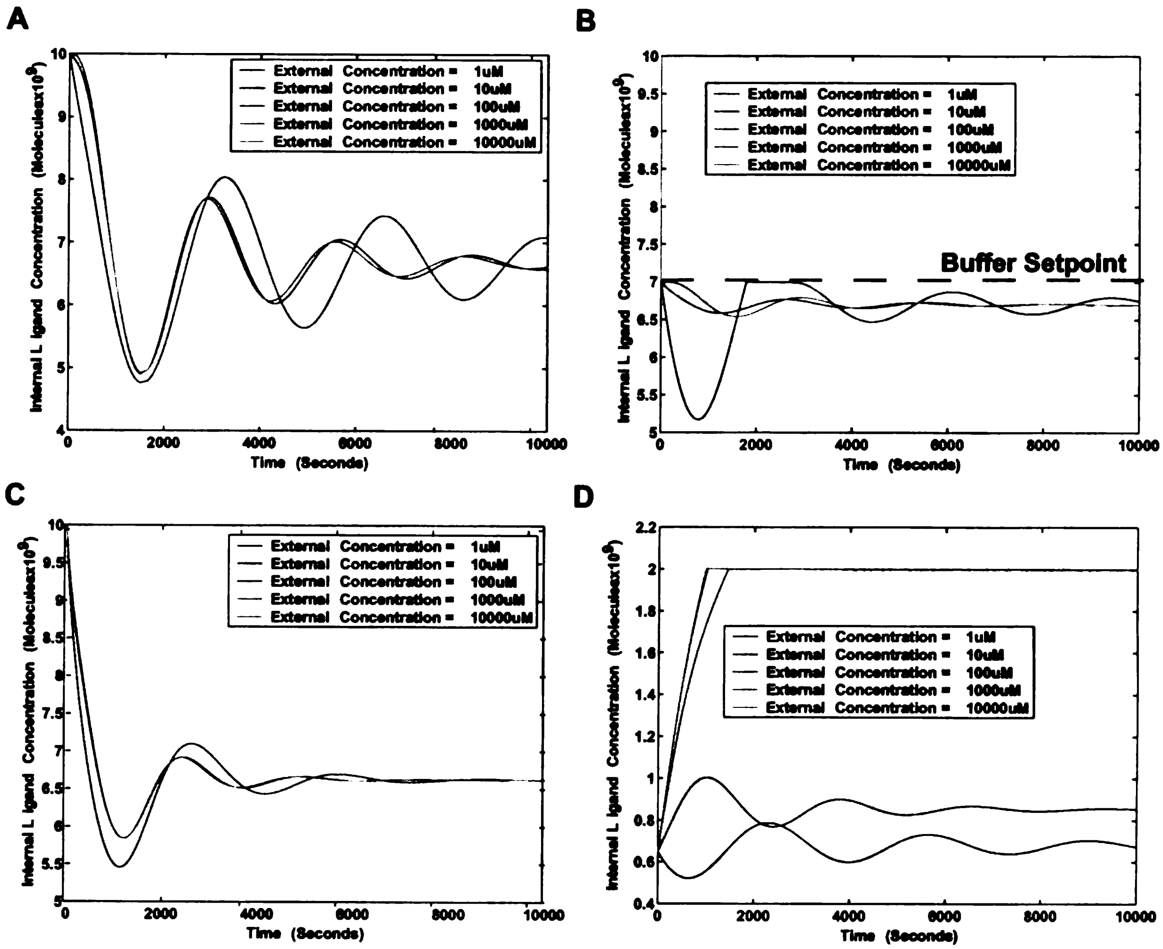
A
B
C
D
External Concentration = 1uM
External Concentration = 10uM
External Concentration = 100uM
External Concentration = 1000uM
External Concentration = 10000uM
Buffer Setpoint
Internal L igand Concentration (Moleculesx10^9)
Time (Seconds)
0
2000
4000
6000
8000
10000
4
5
6
7
8
9
10
5.5
6.5
7.5
8.5
9.5
0.4
0.6
0.8
1
1.2
1.4
1.6
1.8
2
2.2

Figure 5

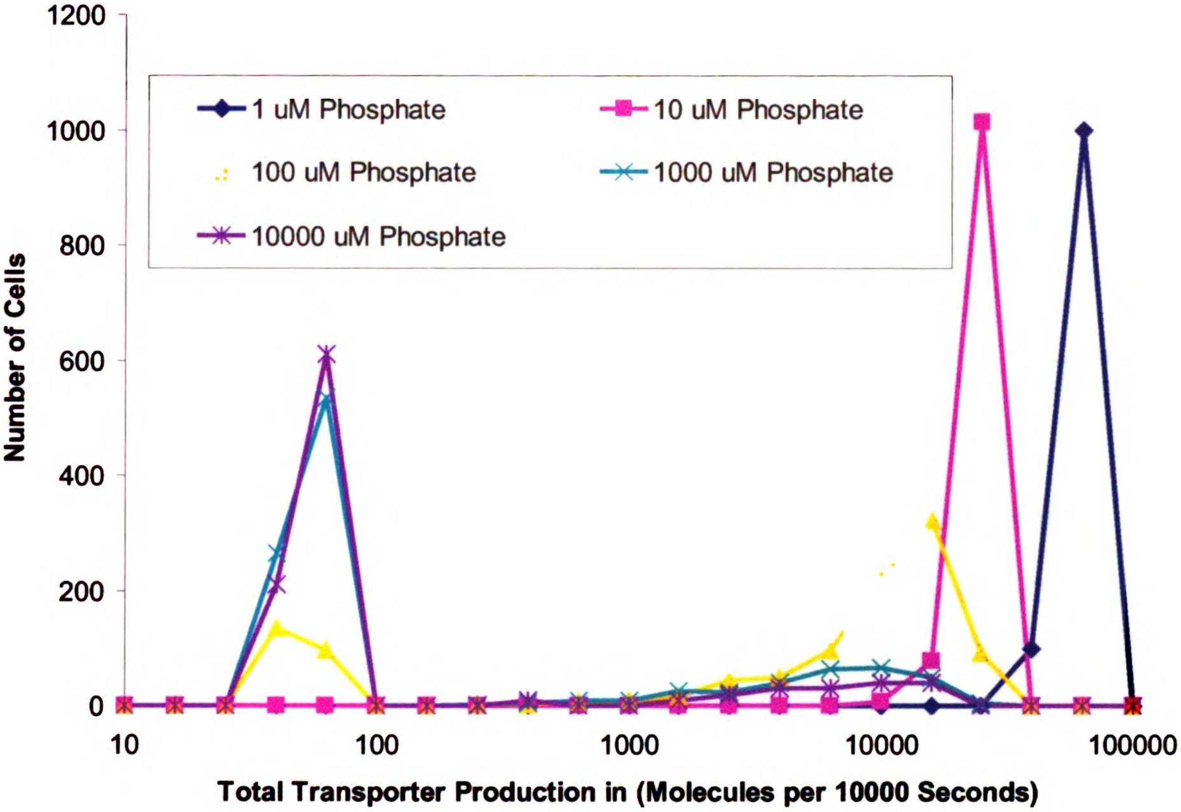
1200
1000
800
600
400
200
0
Number of Cells
10
100
1000
10000
100000
Total Transporter Production in (Molecules per 10000 Seconds)
1 uM Phosphate
10 uM Phosphate
100 uM Phosphate
1000 uM Phosphate
10000 uM Phosphate

	high affinity	low affinity	total transporter (high and low affinity)				
[nutrient]	A	B	C	D	E	F	G
1	**6.00E+06**	2.01E+08	2.01E+08	2.64E+07	8.91E+06	7.16E+06	6.99E+06
10	**6.00E+06**	2.10E+07	2.01E+08	2.10E+07	8.14E+06	6.86E+06	6.73E+06
100	6.00E+06	**3.00E+06**	2.01E+08	2.10E+07	**3.00E+06**	4.80E+06	4.98E+06
1000	6.00E+06	**1.20E+06**	2.01E+08	2.10E+07	3.00E+06	**1.20E+06**	1.92E+06
10000	6.00E+06	**1.02E+06**	2.01E+08	2.10E+07	3.00E+06	1.20E+06	**1.02E+06**

Table 1. Total Amount of Transporter Synthesis Required at Different Nutrient Concentrations at Steady-State. Given a usage rate of 1e6 and a cell cycle time of 5400 seconds, the amount of **A)** high or **B)** low affinity transporter synthesis needed at five different nutrient concentrations (arbitrary units) was calculated. Using the values from B, five different "cells" were simulated that had different levels of low affinity transporter: **C)** 2.01E+08, **D)** 2.10E+07, **E)** 3.00E+06, **F)** 1.20E+06, and **G)** 1.02E+06 and the total number of transporters needed (both high and low affinity together) was calculated for the five different nutrient concentrations. Below the heavy line only low affinity transporter is needed to bring in sufficient nutrient. Above the solid line the cells need to use both low and high affinity transporters to take up sufficient nutrient. In bold is the lowest number of transporters needed for each of the five nutrient contentrations. At each concentration the optimal solution is to have either high or low affinity transporter. The Km of the low affinity transporters is assumed to be 400 units. The concentration below which the low affinity system is more energetically costly than just a high affinity system is ~67 units.

Conclusion:

Through a combination of experimentation, simulation, and cross pathway comparison, I have helped to obtain a much more detailed understanding of how yeast are able to molecularly respond to phosphate starvation. While my analysis has given potential answers to some questions it has raised many new questions. A new line of experiments is now critical. We must in the future measure responses in a well controlled reproducible environment. It is important to monitor the response not only to changes in the external phosphate concentration but also to the rate of change of the external phosphate concentration. We will need to implement new techniques to measure different parameters *in vivo* such as the internal phosphate concentration. Preferably techniques can be developed to allow for measurement of all parameters at the single cell level. We will need to monitor the response in a number of mutant backgrounds and from different starting states.

It will also be important to try to think of biological responses in the framework of physics and electrical engineering principles. While the exact constraints that a biological system will place on a response are different then the constraints that a physical or electrical circuit will place on a response, these other two fields are much more developed so principles and ideas from these fields may help illuminate some of the core principles of cellular circuitry. For example damped harmonic oscillators should strongly oscillate if driven at their resonance frequency. It should be possible to remove the phosphate buffer and then use modulation of extracellular phosphate or kinase inhibitor to drive the system into resonance oscillations. Dissection of the circuit by isolating parts of the response, such as endocytosis or transcription, and examining these behaviors with and without feedback will also further our understanding of the system.

If these types of analysis and models continue to explain the response of yeast to phosphate deprivation it will be important to use these techniques on a more complex system such as carbon or nitrogen regulation. These systems appear to have the same core design as the phosphate response but have extra layers of regulation that the phosphate system does not have. It will be important to understand how transferable the principles we can learn from the phosphate response are to other responses in yeast and other organisms.

UC San Francisco LIBRARY

7270773
3 1378 00727 0773